

CHEMOMECHANICAL POLISHING OF SILICON  
NITRIDE WITH CHROMIUM  
OXIDE ABRASIVE

By  
SEKHAR . R. BHAGAVATULA

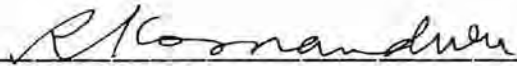
Bachelor of Engineering  
Manipal Institute of Technology  
Manipal, India  
1987

Master of Technology  
Indian Institute of Technology  
Bombay, India  
1991

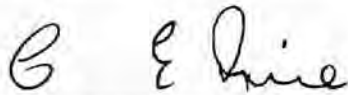
Submitted to the Faculty of the  
Graduate College of the  
Oklahoma State University  
in partial fulfillment of  
the requirements for  
the Degree of  
MASTER OF SCIENCE  
July, 1995

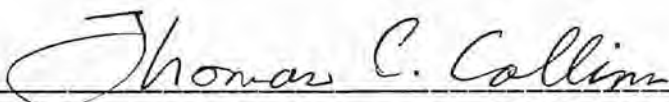
CHEMOMECHANICAL POLISHING OF SILICON  
NITRIDE WITH CHROMIUM  
OXIDE ABRASIVE

Thesis Approved :

  
\_\_\_\_\_  
Thesis Adviser

  
\_\_\_\_\_

  
\_\_\_\_\_

  
\_\_\_\_\_  
Dean of the Graduate College

## PREFACE

Advanced ceramics, such as aluminum oxide, silicon nitride, silicon carbide, and zirconia are difficult to shape and finish, in general, owing to their high hardness and brittleness. With conventional grinding and polishing techniques surface damage is inherently present on the workpiece in the form of pits, and scratches, and subsurface damage in the form of lateral and median cracks. These defects affect the performance and reliability of the products in service. Diamond abrasive is invariably used for grinding as well as for polishing. Consequently, the cost of finishing is high and the time taken for finishing is also significantly long, sometimes taking several weeks.

Conventional material removal using abrasives harder than the work material involves abrasion leaving scratches, pitting, and fine cracks on the surface. In contrast, chemo-mechanical polishing (also called mechano-chemical polishing) depends on the chemical interaction between the abrasive, the workmaterial, and the environment. Oftentimes, the abrasives used are about the same hardness or softer than the workmaterial. Consequently, no groove formation is expected with these abrasives leading to a smooth surface. Hence, for finishing advanced ceramics chemo-mechanical action is rather an attractive proposition especially during the final stages of polishing.

The chemo-mechanical process initiates a chemical reaction between an abrasive and the work material which have high chemical affinity for each other. The process generally produces a weaker reaction product compared to either the abrasive or the workmaterial. The environment used can facilitate this chemical action. The reaction product thus formed is brittle and subsequently removed by the abrasive action. This results in producing a smooth surface. However, the presence of defects such as pits, grooves from an earlier semifinishing operation can still exist in the final operation unless all the defects are removed by this operation.

The present investigation focuses on the chemo-mechanical polishing of hot isostatically pressed  $\text{Si}_3\text{N}_4$  balls and rollers. Magnetic float polishing technique with a water based magnetic fluid was used for finishing balls and magnetic abrasive finishing

technique using magnetic abrasive conglomerate was used for finishing rollers.  $B_4C$ ,  $SiC$ , and  $Cr_2O_3$  were used as abrasives, with the former two being harder than the silicon nitride workmaterial and the later being about the same or slightly softer than the workmaterial. As will be shown, the material removal mechanism in the latter case is by chemo-mechanical polishing.

$Si_3N_4$  oxidizes rapidly in air above 1000 °C. The presence of water enhances oxidation of  $Si_3N_4$ . The surface silica layer formed on  $Si_3N_4$  during oxidation further reacts with water to form  $Si(OH)_4$ . This reaction also produces  $NH_3$  gas as a by product. Thermodynamic analysis confirmed the action of water in enhancing oxidation of  $Si_3N_4$ . Gibb's free energy analysis showed that the reaction proceeds more readily in water up to 500 °C. Flash temperatures developed at the real areas of contact during polishing were determined using a moving disc heat source model and were found to be in the range of 1200-2000 °C.

Wear debris was collected after polishing and analyzed using an ABT 32 scanning electron microscope (SEM) with a Kevex energy dispersive X-ray microanalyzer and a Seimens X-ray diffractometer (XRD). Similarly, the finished balls and rollers were examined in the SEM and TalySurf for surface characterization and surface roughness measurements, respectively. SEM analysis showed that the  $Si_3N_4$  wear particles formed by the abrasive action are coarser in the case of  $B_4C$  and  $SiC$  abrasives compared to  $Cr_2O_3$  abrasive, suggesting that most of the material is removed mechanically in the former case. Particle cleavage has resulted in the dislodgement of grains. Although, the surface finish obtained with  $SiC$  and  $B_4C$  abrasives was inferior to that obtained with  $Cr_2O_3$  abrasives, the material removal rates were higher.

Based on the experimental evidence as well as the theoretical analysis, a new model of chemo-mechanical polishing of silicon nitride with chromium oxide abrasive was developed. XRD analysis of the ball polished with  $Cr_2O_3$  showed the presence of chromium nitride and chromium silicate in detectable amounts suggesting the formation of solid - gaseous reaction at high temperatures. Chromium in its oxidation state of  $3^+$  can react with nitride ions and provide a source for the excess nitride ions to diffuse into the abrasive material. This can have a major effect in enhancing the oxidation of silicon nitride. Due to this reaction, the amount of nitrogen gas molecules generated in the bulk of silicon nitride can be reduced. This facilitates in achieving a surface with almost no porosity even with continuous oxidation during the polishing process. X-ray diffraction analysis also

showed the presence of chromium silicate which can form by reacting silica with chromium oxide, when chromium is in its  $2^+$  state. This brittle reaction product can then be removed during subsequent mechanical action by the abrasive. Chromium oxide, besides participating in the formation of the reaction products also facilitates in further enhancing the oxidation of silicon nitride.

In conclusion, it may be pointed out that polishing of silicon nitride workmaterial with chromium oxide abrasive yields the best surface finish with minimal surface and subsurface defects. Use of carbide abrasives, on the other hand, results in higher material removal rates but at the expense of surface finish.

## ACKNOWLEDGEMENTS

I wish to express my sincere appreciation to my thesis advisor, Dr. Ranga Komanduri for his guidance and support. Sincere thanks are due to my other thesis committee members, Dr. C. E. Price and Dr. D. A. Lucca for agreeing to serve on the committee.

This project is sponsored in part by a grant from the National Science Foundation (CMS-9414610) on "Tribological Interactions in Polishing of Advanced Ceramics and Glasses," and in part by ARPA's Ceramic Bearing Technology Program (F33615-92-5933). Dr. Komanduri is the principle investigator of these projects. I wish to thank the sponsors for their financial support without which this work would not have been possible. I would also like to thank Dr. Larsen Basse of NSF and Dr. K. R. Mecklenburg of WPAFB and Dr. W. Coblenz of ARPA for their interest in this work.

I wish to thank Dr. N. Umehara, formerly a visiting professor at OSU from Tohoku University, Japan, for many valuable suggestions. I would also like to thank Prof. Hou Zhen Bin, currently a visiting professor from China, for valuable inputs to this work. My understanding of the subject grew with their help and support. I would also like to thank Dr. Ali Noori Khajavi for his encouragement. Sincere thanks are due to Dr. T.R.R. Mohan, my former advisor in India, for his interest in this work.

I would like to thank my colleagues, Mr. Michael Fox and Mr. M. Raghunandan for providing me with the samples used in this investigation and for valuable discussions. I would also like to thank all my lab members for their support, in particular, Johnie Hixon and K. Mallika for their assistance with the SEM.

Finally, I would like to take this opportunity to thank my parents, who have been a continuous moral support during the course of this investigation.

## TABLE OF CONTENTS

CHAPTER	TITLE	PAGE
1.	INTRODUCTION	1
1.1	Problems associated with conventional finishing of ceramics	1
1.2	Chemomechanical Polishing	3
2.	LITERATURE REVIEW	11
2.1	Tribochemical Studies	11
2.1.1	Effects of Physical Parameters	12
	Effect of Load	12
	Effect of Speed	14
	Effect of Temperature	14
	Effect of External Conditions	17
2.2	Analysis of Reaction Products	24
	Oxide Ceramics	24
	Non - Oxide Ceramics	25
2.3	Chemomechanical polishing mechanisms	34
3.	PROBLEM STATEMENT	38
4.	EXPERIMENTAL APPARATUS AND CHARACTERIZATION OF THE WORKMATERIAL AND THE ABRASIVES	40
4.1	Magnetic Field assisted Polishing of Si <sub>3</sub> N <sub>4</sub> balls and rollers	40
4.1.1	Magnetic Float Polishing of Si <sub>3</sub> N <sub>4</sub> balls	41
4.1.2	Magnetic Field assisted Polishing of Si <sub>3</sub> N <sub>4</sub> rollers	44
4.2	Silicon Nitride Workmaterial	45

4.3	Abrasives used	46
5.	<b>THERMODYNAMIC AND HEAT TRANSFER ANALYSES</b>	53
5.1	Thermodynamic Analysis	53
5.2	Heat Transfer Analysis	56
5.2.1	Flash Temperature Determination	57
5.3	Phase Diagram Study	58
6.	<b>RESULTS</b>	61
6.1	Magnetic Float Polishing of Silicon Nitride Balls	61
6.1.1	Surface Characterization of the Balls	61
6.1.2	Analysis of Wear Debris	67
	Silicon Carbide	67
	Boron Carbide	72
	Chromium Oxide	72
6.1.3	XRD analysis	81
6.2	Magnetic abrasive finishing of rollers	85
6.2.1	Surface characterization of rollers	85
6.2.2	Analysis of the wear debris	87
6.2.3	XRD analysis	87
7.	<b>DISCUSSION AND PROPOSED CHEMO-MECHANICAL MODEL</b>	93
7.1	Analysis of the chemo-mechanical polishing mechanisms proposed in the literature	93
7.2	Theoretical considerations	95
7.3	Correlation of Results	100
7.4	Proposed chemo-mechanical polishing model	102
7.4.1	Chemo-mechanical action of chromium oxide in air	102
7.4.2	Chemo-mechanical action of chromium oxide in water	106
8	<b>CONCLUSIONS</b>	110
9.	<b>SUGGESTIONS FOR FUTURE WORK</b>	113



REFERENCES

119

APPENDIX

126

## LIST OF FIGURES

FIGURE	TITLE	PAGE
1.1.1	Schematic Showing the network of crack formation in cermics under a sliding indenter [Marshal, 1983]	4
1.1.2	SEM micrograph showing subsurface damage in alumina during surface grinding [Hockin, 1994]	4
1.1.3	SEM micrograph of the ground surface of alumina showing surface defects [Hockin, 1994]	4
1.2.1	Schematic of the chemomechanical polishing process [Uematsu, 1993]	6
1.2.2	Surface profiles of polished surfaces of alumina with various abrasives [Namba, 1977]	6
2.1.1.1	Time evolution of the friction coefficient of silicon nitride in air for various loads [Fischer and Tomizawa, 1985]	13
2.1.1.2	Wear volume versus the number of revolutions at various loads [Akazawa and Kato, 1986]	13
2.1.1.3	Variation of coefficient of friction with speed at two humidity levels [Gee and Butterfield, 1993]	15
2.1.1.4	Variation in wear volume with speed for different humidity levels [Gee and Butterfield, 1993]	15

2.1.1.5	Optical micrographs of wear scars at different speeds [Gee and Butterfield, 1993]	16
2.1.1.6	SEM of a wear scar of silicon nitride in dry argon [Fisher, 1988]	16
2.1.1.7	SEM of a wear scar of silicon nitride after sliding in humid argon [Fisher,1988]	18
2.1.1.8	Wear tracks of silicon nitride in hexadecane [Jahanmir and Fisher, 1988]	18
2.1.1.9	Wear behavior of silicon nitride rubbed in hexadecane and 0.5 % stearic acid [Jahanmir and Fisher, 1988]	20
2.1.1.10	SEM of the wear scar of silicon nitride rubbed in water [Fisher,1988]	20
2.1.1.11	SEM of silicon carbide surfaces before and after rubbing in water [Mizutani et al., 1990]	21
2.1.1.12	SEM of a worn surface of alumina sample after rubbing in water [Gates et al., 1989]	21
2.1.1.13	SEM of the wear scar of zirconia rubbed in water [Fisher,1988]	23
2.2.1	Ion microprobe spectrum of an alumina surface during ribbing in water [Sugita et al., 1979]	26
2.2.2	X-ray diffraction spectrum of alumina wear debris obtained from polishing with silica [Yasunaga et al., 1979]	26
2.2.3	Alumina single crystal polished with various abrasives [Namba and Tsuwa, 1977]	27
2.2.4	TGA scans of gamma-alumina and gamma-alumina-water reaction products [Gates et al., 1989]	27

2.2.5	X-ray microanalysis of a wear particle obtained during dry rolling of silicon nitride [Kato, 1990]	28
2.2.6	Auger-electron spectroscopy analysis conducted on the inside and outside of the wear tracks of silicon nitride after rubbing in water [Xu et al., 1993]	28
2.2.7	Infrared spectra obtained during a dry rolling test [Akazawa et al., 1986]	30
2.2.8	Light element energy dispersive x-ray spectroscopy of the wear tracks of silicon nitride during a dry rolling test [Gee and Butterfield, 1993]	30
2.2.9	TEM micrographs obtained from amorphous and crystalline wear particles and their electron energy loss spectra [Jahanmir and Fischer, 1986]	31
2.2.10	X-ray photoelectron spectroscopy data obtained from the worn surfaces of silicon nitride [Cranmer, 1989]	31
2.2.11	Spectra obtained from an ion microprobe mass spectrometer as a function of the number of scars of the polished surface, fractured surface and baked surface [Sugita et al., 1984]	33
2.2.12	XRD data of the wear debris before and after the baking treatment [Karaki-Doy et al., 1989]	33
4.1.1.1	Diagram of the magnetic float polishing apparatus	43
4.1.2.1	Schematic of the magnetic abrasive finishing process	43
4.2.1	SEM micrograph of a polished and etched silicon nitride showing internal linked columnar beta-silicon nitride grains	48
4.3.1	SEM micrograph of as received silicon carbide abrasives	49

4.3.2	SEM micrograph of as received boron carbide abrasives	50
4.3.3	SEM micrograph of as received chromium oxide abrasives	51
6.1.1.1	SEM micrographs of the silicon nitride ball polished with silicon carbide abrasives	63
6.1.1.2	SEM micrographs of the silicon nitride ball polished with boron carbide abrasives	64
6.1.1.3	SEM micrographs of the silicon nitride ball polished with chromium oxide abrasives	65
6.1.1.4	Talysurf surface roughness plots of the silicon nitride ball polished with silicon carbide, boron carbide and chromium oxide	66
6.1.2.1	SEM micrographs and EDX analysis of the silicon carbide wear debris showing silicon carbide wear particle	68
6.1.2.2	SEM micrographs and EDX analysis of the silicon carbide wear debris showing silicon carbide wear particles	69
6.1.2.3	SEM micrographs and EDX analysis of the silicon carbide wear debris showing silicon nitride wear particles	70
6.1.2.4	SEM micrographs and EDX analysis of the silicon carbide wear debris showing silicon nitride wear particle	71
6.1.2.5	SEM micrographs and EDX analysis of the boron carbide wear debris showing silicon nitride wear particle	73
6.1.2.6	SEM micrographs and EDX analysis of the boron carbide wear debris showing cleaved silicon nitride wear particle	74
6.1.2.7	SEM micrographs and EDX analysis of the boron carbide	75

	wear debris showing silicon nitride wear particle	
6.1.2.8	SEM micrographs and EDX analysis of the boron carbide wear debris showing boron carbide wear particle	76
6.1.2.9	SEM micrographs and EDX analysis of the chromium oxide wear debris showing chromium oxide wear particle	77
6.1.2.10	SEM micrographs and EDX analysis of the chromium oxide wear debris showing particle with viscous deformation	78
6.1.2.11	SEM micrographs and EDX analysis of the chromium oxide wear debris showing silicon nitride particle	79
6.1.2.12	SEM micrographs and EDX analysis of the chromium oxide wear debris showing chromium silicate reaction product	80
6.1.3.1	XRD pattern obtained from silicon carbide wear debris showing various forms of silica	82
6.1.3.2	XRD pattern obtained from boron carbide wear debris showing presence of borosilicate	83
6.1.3.1	XRD pattern obtained from chromium oxide wear debris showing chromium nitride as a result of oxidation and chromium silicate as a result of chemo-mechanical action	84
6.2.1.1	SEM micrograph showing the surface of silicon nitride rod during magnetic abrasive finishing	85
6.2.1.2	Talysurf surface roughness plot obtained during magnetic abrasive finishing of silicon nitride rod using chromium oxide abrasive	86
6.2.2.1	SEM micrographs and EDX analysis of the chromium oxide wear debris obtained during magnetic abrasive finishing of silicon nitride rod	88

6.2.2.2	SEM micrographs and EDX analysis of the chromium oxide wear debris obtained during magnetic abrasive finishing of silicon nitride rod shows chromium silicate reaction product	89
6.2.2.3	SEM micrographs and EDX analysis of the chromium oxide wear debris obtained during magnetic abrasive finishing of silicon nitride rod shows chromium silicate reaction product	90
6.2.3.1	XRD pattern obtained during chemomechanical polishing of silicon nitride using chromium oxide abrasives showing the presence of Chromium nitride and chromium silicate	91
7.2.1	Schematic showing the reaction processes occurring during the oxidation of silicon nitride in air [Singhal, 1976 (a)]	96
7.4.1.1	Schematic of the chemomechanical model for polishing silicon nitride using chromium oxide abrasives in air	103
7.4.2.1	Schematic of the chemomechanical model for polishing silicon nitride using chromium oxide abrasives in water	107

## LIST OF TABLES

TABLE	TITLE	PAGE
1.1	Thermo-mechanical properties of ceramics [Schnieder, 1991]	2
2.1.1.1	Friction and wear coefficients obtained from various ceramics tested under acidic, basic and neutral environments [Loffelbein, 1993]	19
4.2.1	Properties of HIP'ed silicon nitride used in present investigation	47
4.3.1	Hardness values of the abrasives used [Schnieder, 1991]	47
5.1.1	Thermodynamic values of compounds in the oxidation of silicon nitride [Kubashevski and Block, 1979]	55
5.1.2	Values of Gibb's free energy of formation in the oxidation of silicon nitride (From calculations)	55
5.3.1	Reaction data of oxide abrasives with silicon nitride	59
5.3.2	Reaction data of carbide abrasives with silicon nitride	60



## CHAPTER 1

### INTRODUCTION

The development of high performance ceramics (or advanced ceramics) is stimulating major advances in a large spectrum of industries including machine tools, electronics, manufacturing engineering and chemical and metallurgical processing. In contrast to the traditional ceramics, which are natural and complex mixtures of diverse oxides and carbides and silicates, high performance ceramics are processed using relatively pure materials and compacted close to theoretical densities. Alumina, zirconia, silicon carbide and silicon nitride are the most important materials among high performance ceramics. In this category, Silicon nitride is the most widely used material for structural applications.

Table 1.1 lists some of the thermo-mechanical properties of various advanced ceramics [Schnieder, 1991]. It can be seen that silicon nitride has better thermal and mechanical properties than most other advanced ceramics. It has superior thermal shock resistance which makes it useful for applications which require rapid thermal cycles [Katz, 1985, 1989, and 1994]. Its coefficient of thermal expansion is low, making it the ideal material for application which demands high dimensional accuracy. Its fracture toughness is the highest among structural ceramics apart from tetragonal zirconia. It has the least coefficient of friction and its failure mode is by spalling instead of catastrophic brittle fracture as in other advanced ceramics, which makes it to be used as a high speed roller and ball bearing material for aerospace applications.

#### 1.1. PROBLEMS ASSOCIATED WITH CONVENTIONAL FINISHING OF CERAMICS

Structural ceramics are formed into desired shapes generally by the powder metallurgy route. This involves pressing of fine raw powders to the required shape in a die under the application of pressure. This is known as a green compact. The compact is subsequently fired at a high temperature (and hydrostatic pressure) to obtain a dense product. Grinding and polishing are the most important techniques used for finishing

Table 1.1 Thermo-mechanical properties of ceramics [Schnieder, 1991]

Material	Crystal structure	Theoretical density, g/cm <sup>3</sup>	Knoop or Vickers hardness		Transverse rupture strength		Fracture toughness		Young's modulus		Poisson's ratio	Thermal expansion, 10 <sup>-6</sup> /K	Thermal conductivity, W/m·K
			GPa	10 <sup>3</sup> psi	MPa	ksi	MPa√m	ksi√in.	GPa	10 <sup>3</sup> psi			
Glass-ceramics	Variable	2.4-5.9	6-7	0.9-1.0	70-350	10-51	2.4	2.2	83-138	12-20	0.24	5-17	2.0-5.1 2.7-3.1 1.3(a) 1.7(c) 8.8(a)
Pyrex glass	Amorphous	2.52	5	0.7	69	10	0.75	0.7	70	10	0.2	4.6	
TiO <sub>2</sub>	Rutile tetragonal Anatase tetragonal Brookite orthorhombic	4.25 3.84 4.17	7-11 ...	1.0-1.6 ...	69-103 ...	10-15 ...	2.5 ...	2.3 ...	283 ...	41 ...	0.28 ...	9.4 ...	3.3(d)
Al <sub>2</sub> O <sub>3</sub>	Hexagonal	3.97	18-23	2.6-3.3	276-1034	40-150	2.7-4.2	2.5-3.8	380	55	0.26	7.2-8.6	27.2(a) 5.8(d)
Cr <sub>2</sub> O <sub>3</sub>	Hexagonal	5.21	29	4.2	>262	>38	3.9	3.5	>103	>15		7.3	10-33
Mullite	Orthorhombic	2.8	...	...	185	27	2.2	2.0	145	21	0.23	5.7	5.2(a) 3.3(d)
Partially stabilized ZrO <sub>2</sub>	Cubic, monoclinic, tetragonal	5.70-5.75	10-11	1.5-1.6	600-700	87-102	(f)	(f)	205	30	0.23	8.9-10.6	1.8-2.1
Fully stabilized ZrO <sub>2</sub>	Cubic	5.56-6.1	10-15	1.5-2.2	245	36	2.8	2.5	97-207	14-30	0.23-0.32	13.5	1.7(a) 1.9(g)
Plasma-sprayed ZrO <sub>2</sub>	Cubic, monoclinic, tetragonal	5.6-5.7	...	...	6-80	0.9-12	1.3-3.2	1.2-2.9	48(b)	7	0.25	7.6-10.3	0.89-2.1
CeO <sub>2</sub>	Cubic	7.28	...	...	...	...	...	...	172	25	0.27-0.31	13	9.6(a) 1.2(d)
TiB <sub>2</sub>	Hexagonal	4.5-4.54	15-45	1.5-6.5	700-1000	102-145	6-8	5.5-7.3	514-574	75-83	0.09-0.13	8.1	65-120 33-80 54-12 33(a) 43(d) 32(a) 40(d) 19
TiC	Cubic	4.92	28-35	4.0-5.1	241-276	35-40	...	...	430	62	0.19	7.4-8.6	
TaC	Cubic	14.4-14.5	16-24	2.3-3.5	97-290	14-42	...	...	285	41	0.24	6.7	
Cr <sub>3</sub> C <sub>2</sub>	Orthorhombic	6.70	10-18	1.5-2.6	49	7.1	...	...	373	54		9.8	
Cemented carbides	Variable	5.8-15.2	8-20	1.2-2.9	758-3275	110-475	5-18	4.6-16.4	396-654	57-95	0.2-0.29	4.0-8.3	16.3-111
SiC	α, hexagonal	3.21	20-30	2.9-4.4	(l)	(l)	(m)	(m)	207-483	30-70	0.19	4.3-3.6	63-15 21-33
SiC (CVD)	β, cubic	3.21	28-44	4.1-6.4	(n)	(n)	5-7	4.6-6.4	415-441	60-64		5.5	121(a) 34.6(g)
Si <sub>3</sub> N <sub>4</sub>	α, hexagonal β, hexagonal	3.18 3.19	8-19	1.2-2.8	(o)	(o)	(p)	(p)	304	44	0.24	3.0	9-30
TiN	Cubic	5.43-5.44	16-20	2.3-2.9	...	...	...	...	251	36		8.0	24(a) 67.8(q) 56.9(r)

(a) At 400 K. (b) At 1200 K. (c) At 800 K. (d) At 1400 K. (e) At 350 K. (f) 8-9 (7.3-8.2) at 293 K, 6-6.5 (5.5-5.9) at 723 K, and 5 (4.6) at 1073 K, in units of MPa√m (ksi√in.). (g) At 1800 K. (h) 21 (1) at 300 K, GPa (10<sup>3</sup> psi). (i) At 300 K. (j) At 1100 K. (k) At 2300 K. (l) Sintered: 96-320 (14-75) at 300 K, and 250 (36) at 1273 K. Hot pressed: 230-825 (33-120) at 300 K, and 398-745 (58-108) at 1273 K. MPa (m) Sintered: 4.8 (4.4) at 300 K, and 2.6-5.0 (2.4-4.6) at 1273 K. Hot pressed: 4.8-6.1 (4.4-5.6) at 300 K, and 4.1-5.0 (3.7-4.6) at 1273 K. MPa√m (ksi√in.). (n) 1034-1380 (150-200) at 300 K, and 1000 (300-350) at 1473 K. MPa (ksi). (o) Sintered: 414-650 (60-94). Hot pressed: 700-1000 (100-145). Reaction bonded: 250-345 (36-50), MPa (ksi). (p) Sintered: 5.3 (4.8). Hot pressed: 4.1-4.0 (3.7-3.5). Reaction bonded: 3.6 (3.3), MPa√m (ksi√in.). (q) At 1773 K. (r) At 2573 K.

many advanced ceramics. However, these materials are very difficult to finish by conventional grinding and polishing techniques due to their high hardness and brittleness. Diamond grinding wheels and diamond polishing compounds are invariably used to shape and finish ceramics. High precision, rigid machine tools, with high power and speed capabilities are required for this application. The product is finished to the final dimensions before it is put into service.

Because of the hardness and brittleness associated with ceramics, the finished product always suffers the grinding and polishing damage [Marshall, 1983]. Figure 1.1.1 is a schematic showing the network of crack formation in ceramics under a sliding indenter [Marshall, 1983]. Median cracks are formed perpendicular to the direction of polishing and reduce the mechanical properties considerably. Lateral cracks, on the other hand, extend parallel to the direction of polishing and cause groove formation on the surface which ultimately contributes towards failure of the part by acting as a stress concentrator.

Grinding, also, leaves high residual stresses in these materials which can reduce the mechanical properties of the material significantly. Even further heat treatment, in most cases, cannot eliminate these defects. Conventional polishing techniques such as lapping, though using ultrafine abrasives of the order of submicron size, leave a polished surface with occasional pits and scratches on the surface. These act as stress raisers during service and initiate premature failure. As already pointed out, subsurface damage is also present in these materials in terms of lateral and median crack development. These defects could only be minimized when ultrafine abrasives were used in the polishing but could not be eliminated altogether. Figure 1.1.2 is a SEM micrograph showing subsurface damage generated in alumina during surface grinding [Hockin et al., 1994]. Figure 1.1.3 is the SEM micrograph of the ground surface of alumina showing these defects [Hockin, 1994].

## 1.2. CHEMOMECHANICAL POLISHING

To provide a defect free surface with a high rate of polishing and good finish, a new polishing method was developed [Yasunaga et al., 1978; Vora et al., 1982; Sugita et al., 1986; and Kikuchi et al., 1992]. This process is known as chemomechanical polishing and depends on the availability of a certain threshold pressure and temperature at the contact zone of the polishing process, provided a chemical reaction layer can form by the

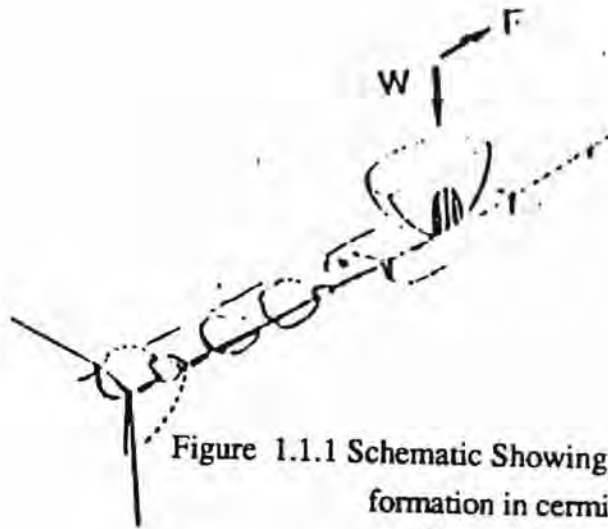


Figure 1.1.1 Schematic Showing the network of crack formation in ceramics under a sliding indenter [Marshall, 1983]

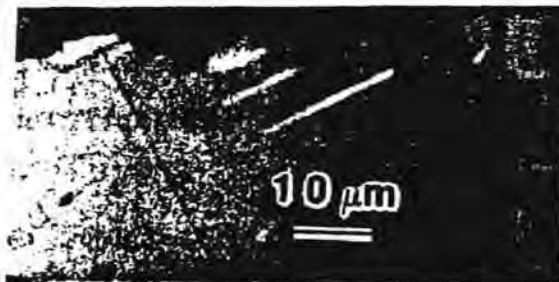


Figure 1.1.2 SEM micrograph showing subsurface damage in alumina during surface grinding [Hockin, 1994]

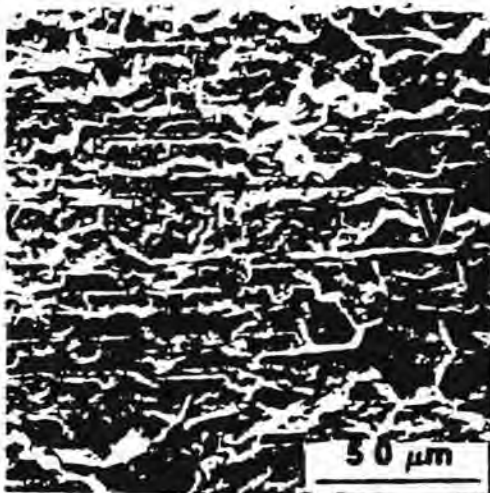


Figure 1.1.3 SEM micrograph of the ground surface of alumina showing surface defects [Hockin, 1994]

interaction of the abrasive and workmaterial, and the environment. The exact values of pressure and temperature determine the type of reaction product that can form for a given pair of workmaterial and abrasive in a given environment.

Figure 1.2.1 is a schematic of the chemo-mechanical polishing process [Uematsu, 1993]. The zone at the vicinity of the contact between the abrasive and work piece is called the micro-reaction zone. Chemical reactions are anticipated to occur in this zone and the reaction product is subsequently removed, due to the subsequent abrasive action. In principle, an abrasive with a high chemical affinity towards the workmaterial (and not necessarily an abrasive harder than the workmaterial) is used as the polishing medium. The environment can also play an important role in the process. During polishing a reaction product, generally, a brittle, intermetallic compound is formed. This product is weaker than either the abrasive or the workmaterial. Since chemical action is the predominant mechanism of material removal in this process, it would facilitate the use of abrasives which are softer compared than the workmaterial. Such a situation would eliminate scratching and other damage to the workmaterial and at the same time enable the removal of material, at reasonable rates. Therefore, this process, under controlled conditions, has the potential to yield high material removal rates and give high surface finish with a scratch free surface and perhaps a surface free of subsurface defects.

Chemomechanical polishing is widely used in the silicon industry [Namba and Tsuwa, 1977, 1979]. Compound semiconductor crystals of groups III and V families such as GaAs, GaP and InP and groups II and VI families such as CdTe and ZnSe require a high quality polished surface which is strain and stress free [Karaaki-Doy, 1989]. The polishing method uses a highly alkaline sodium bromite solution as the polishing medium. Typically, the composition of the medium is 69.0% NaBrO<sub>2</sub>, 1.8% NaBrO<sub>3</sub>, 0.6% NaOH and 27.3% water. The p<sup>H</sup> of the solution is maintained at 12.5. Colloidal silica particles of about 100 Å and 0.5% vol. are used in solution. The solution reacts with the surface and the reaction product is removed by the mechanical action of the abrasives. A surface finish of the order of about 10 Å or less is obtained, with a material removal rate of about 1 μm/minute.

Single crystal silicon substrates used in the electronics application are polished using a KOH solution with 0.1 μm ZrO<sub>2</sub> abrasive [Karaaki-Doy, 1993]. An abrasive concentration of about 20 Wt %, with a 1.5M concentration of KOH, yielded a material removal rate of about 1 μm/min and a surface roughness of about 150 Å.

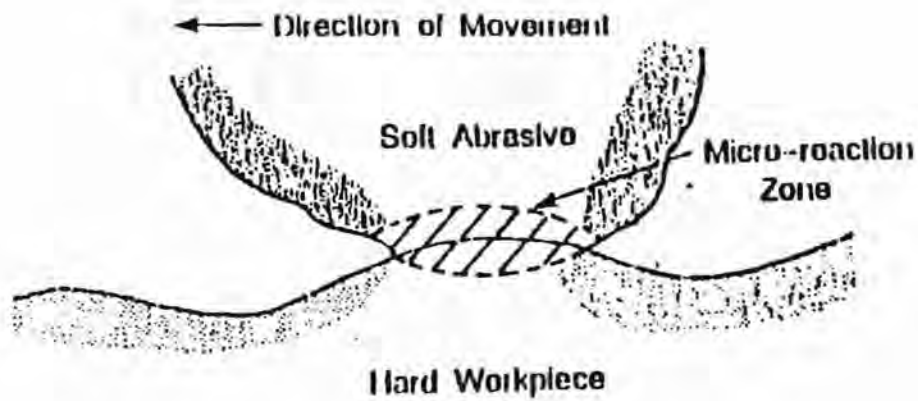


Figure 1.2.1 Schematic of the chemomechanical polishing process [Uematsu, 1993]



(a) Lapped surface with 8µm SiC



(b) Lapped surface with 3µm diamond



(c) Ultra-fine finished surface with 0.02µm SiO<sub>2</sub>

Figure 1.2.2 Surface profiles of polished surfaces of alumina with various abrasives [Namba, 1977]

Mechano-chemical processing was first introduced to the field of ceramics by Yasunaga [Yasunaga, 1977].  $\alpha$   $\text{Al}_2\text{O}_3$  was successfully polished with soft abrasives such as  $\text{SiO}_2$  and  $\text{Fe}_2\text{O}_3$ . Alumina is very stable chemically, but it is reactive with  $\text{SiO}_2$  and  $\text{Fe}_2\text{O}_3$ . Upon reacting with alumina, mullite and spinel are formed respectively, which are subsequently removed due to the abrasive action.

Silicon single crystals were polished using  $\text{BaCO}_3$  and  $\text{CaCO}_3$  and quartz crystals are polished using  $\text{Fe}_3\text{O}_4$  and  $\text{MgO}$  yielding a damage free mirror surface [Yasunaga, et al., 1979; Sugita et al., 1979; Ikeda et al., 1979]. In both cases, the polished surface was so smooth that the wear was believed to proceed fundamentally as a consequence of exfoliation of very small reacted parts at the real contact points.

During the polishing of alumina with silica abrasives, studies were conducted by simulating the actual polishing conditions [Namba and Tsuwa, 1977]. The plastic flow pressure at the contact points would be nearly equal to the hardness of the softer material at that temperature. The pressure generated at a contact point between the sapphire surface and silica powder can therefore be estimated from the hardness of quartz glass. It is found to be about 38 Kbar at 800 °C and 50 Kbar at 600 °C. Alumina powder and silica powder was mixed and heated to about 900 °C at 36 Kbar for about 10 sec.. The reaction product was determined to be Kyanite, which is a stable phase in the alumina-silica system. Figure 1.2.2 is the surface profiles of polished surfaces of alumina with various abrasives; (0.8  $\mu\text{m}$  SiC; 3  $\mu\text{m}$  diamond, and 0.02  $\mu\text{m}$  of  $\text{SiO}_2$ ) showing an  $R_A$  of 0.3  $\mu\text{m}$  with SiC, 350 Å with diamond, and molecular smoothness of less than 10 Å with silica [Namba and Tsuwa, 1977]. Polycrystalline Mn-Zn and Ni-Zn ferrites are polished to crystallographic perfection using chemomechanical polishing technique using  $\text{Fe}_2\text{O}_3$  powder [Namba and Tsuwa, 1979]. Very good flatness, excellent retention of edge geometry and very small surface roughness of about 20 Å are obtained.

Silicon carbide was chemomechanically polished using  $\text{SrCO}_3$ , and boron carbide was polished using NiO and silica [Wang, 1994]. Chromium oxide was found to be an important abrasive used in the chemomechanical polishing of SiC [Kikuchi, 1992]. SiC single crystals were polished using 0.5  $\mu\text{m}$  chromium oxide abrasives against a polishing pressure of 5 MPa. Two oxides of iron  $\text{Fe}_2\text{O}_3$  and  $\text{Fe}_3\text{O}_4$  were identified as suitable abrasives for chemomechanical polishing of silicon nitride to obtain a scratch free

surface finish [Vora et al., 1982]. Removal rates upto 1.6  $\mu\text{m/hr}$  were obtained when HIPped silicon nitride samples were mechano-chemically polished using these abrasives on a linen plastic lap. Polished surfaces were flat and scratch free with a peak to valley roughness less than 20 nm. Silicon nitride round bars have been chemo-mechanically polished using chromium oxide polishing film [Suzuki et al., 1992]. The surface roughness of the bars was improved from 1.2  $\mu\text{m}$  to 45 nm by polishing it for 1 hour. A polymer film, coated with chromium oxide abrasive, was rubbed against the rotating roller and the above polishing characteristics were obtained.

Although, the Chemomechanical polishing technique is widely used, the nature of the process is not well understood. This is particularly so with a silicon nitride workmaterial. The conditions under which the actual reaction takes place is rather complex and the reaction products vary in their composition and amount. depending on the conditions of pressure and temperature at the contacting points

The present work is an attempt to understand the mechanism(s) involved in the chemomechanical polishing of silicon nitride ceramics. The mechanism postulated from the tribological and tribochemical studies conducted earlier by earlier researchers [Vora et al., 1982; Sugita et al., 1984; and Xu et al., 1994] do not completely explain the action of the abrasive -workmaterial-environment in the case of silicon nitride. Moreover, the temperatures developed due to the presence of friction at the contact points vary constantly and render the process more complex. The present study concentrates on determining the action of the abrasive and its role in the mechanism of polishing. Silicon nitride was polished with different abrasives including silicon carbide, boron carbide and chromium oxide. The emphasis of this investigation is to understand the mechanism of polishing of silicon nitride workmaterial with chromium oxide.

The precursor to chemo-mechanical polishing is the tribochemical action experienced in tribology. Hence, the tribochemical behaviour of ceramics in general and silicon nitride in particular is reviewed in chapter 2. This review can facilitate determination of the nature of chemical reactions between the abrasive and the workmaterial in a particular environment during polishing. Possible reaction products resulting from the above tribochemical studies were also reviewed. Various mechanisms proposed for chemomechanical polishing of ceramics are also discussed in chapter 2.



Chapter 3 provides the problem statement. It includes an experimental study of the wear debris generated during polishing of silicon nitride with different abrasives as well as the polished silicon nitride samples; examination of the wear debris and finished balls and rollers in a scanning electron microscope with an energy dispersive X-ray microanalyzer and X-ray diffraction studies; analytical determination of the flash temperatures generated at the actual points of contact during polishing; identification of possible compound formation using Gibb's free energy analysis; and finally development of a model for the chemo-mechanical polishing of silicon nitride with chromium oxide abrasive (in air as well as water).

Chapter 4 provides the details of the two techniques used in the magnetic field assisted polishing of silicon nitride balls and rollers as well as the characterization of the workmaterial and the abrasives used. The experimental part of finishing ceramic balls and rollers is not within the scope of this investigation. Instead, the polished samples were provided to the author by his colleagues (Mr. M. Raghunandan and Mr. M. Fox). The characterization and analysis of the wear debris collected with different abrasives as well as polished balls and rollers are central to this investigation.

Chapter 5 focuses on the theoretical (thermodynamic and heat transfer) studies made in the present investigation. A Gibb's free energy analysis was performed to identify appropriate compounds that may form during polishing and to suggest suitable environments conducive to polishing. A heat transfer analysis was conducted using a moving disc heat source model developed by Hou and Komanduri [1994] to estimate the flash temperatures developed at the contact points during chemo-mechanical polishing. Various compounds (and their phases) which can form during polishing of silicon nitride were identified using the phase diagrams. This information was used as the basis for the X-ray diffraction analysis of the wear debris as well as polished silicon nitride samples.

Chapter 6 presents the results of this investigation. It includes examination of the polished surfaces of silicon nitride balls and rollers as well as the wear debris generated by different abrasives during polishing. This was accomplished using an ABT-32 scanning electron microscope (SEM) with a Kevex energy dispersive X-ray analyser (EDXA) and Siemens low angle X-ray diffractometer. In chapter 7, various mechanisms of chemo-mechanical polishing presented by earlier researchers are discussed and a model of the chemo-mechanical polishing of silicon nitride workmaterial with chromium oxide abrasive

(in air and in water) is presented. Chapter 8 presents conclusions of this investigation and chapter 9 provides suggestions for future work.

## CHAPTER 2

### LITERATURE REVIEW

This chapter reviews the literature on tribochemical characteristics of some advanced ceramics in different environments. Since chemo-mechanical polishing is closely related to these characteristics, such a study enables an understanding of the nature and mechanism of chemo-mechanical polishing. Also, a study of the friction and wear behavior of an abrasive-workmaterial combination in a given environment can provide insights into ways of increasing the material removal rates and the finish obtainable in polishing. The frictional characteristics, also, determine the flash temperatures that can develop in the vicinity of the contact zone between an abrasive and the workmaterial. The chemistry of the abrasive-workmaterial combination under the conditions of polishing would determine the reaction products that could form during chemo-mechanical polishing. In the following, the tribochemical aspects, including the effect of physical parameters, such as load, speed, temperature, relative humidity, and the environment on the tribochemical behavior of ceramics are reviewed. Various characterization studies undertaken by previous researchers of the reaction products for both oxide and non-oxide ceramics are then reviewed. This is followed by a review of the mechanisms of chemo-mechanical polishing in general, and that of silicon nitride work material in particular.

#### 2.1. TRIBOCHEMICAL STUDIES

Chemical interactions between the ceramic work material and abrasive in a given environment are quite active during friction, even at nominal room temperature. These reactions influence not only the dissolution of the materials or the growth of surface films, such as oxides but also the mechanical response of the materials to the contact stresses [Fischer, 1988; and Akazawa and Kato, 1988].

Tribochemical reactions can alter the wear behavior of ceramics by modifying the stress distribution and by influencing the material's response to stress. Pure, mechanical wear usually produces rough contact surfaces that increase stress concentrations.

Tribochemical wear on the other hand, produces a smooth, undamaged wear surface [Fischer, 1988 and Fischer et al., 1989]. In pure mechanical wear, the stress distribution is unaltered and the resulting wear surface is rough, where as in tribochemical wear, stresses are distributed by the surface layers of the ceramic material. These surface layers are usually softer than the substrate. As a result, the value of the maximum contact stress decreases under a constant load, thus reducing the mechanical wear. Often, the contact area in the case of tribochemical wear is larger than that of mechanical wear keeping the frictional force unchanged. This modification of stresses can take several forms depending on the material, the environment, and the processing parameters. It may result in the formation of surface coatings that decrease the wear by dissolution in the liquid environment [Fischer and Tomizawa, 1985]. Alternately, it may provide boundary lubrication by chemisorption in the presence of hydrocarbons and other molecules [Jahanmir and Fischer, 1988]. It may even provide chemically induced fracture that can increase the wear rates [Fischer and Tomizawa, 1985]. The rates of these chemical reactions are very much influenced by the simultaneous action of friction and chemical reactions. Usually, such reactions can proceed even at nominal room temperature which would otherwise proceed only above 800 °K in the absence of friction. This is because of the flash temperatures generated at the frictional sliding contacts. The effect of physical parameters, such as load, speed, temperature, relative humidity, and the environment on the tribochemical behavior of ceramics will be discussed in the following.

### 2.1.1 EFFECT OF PHYSICAL PARAMETERS

#### EFFECT OF LOAD

The effect of load on the friction and wear coefficients has been studied under conditions of high contact pressure and low sliding velocity [Fischer and Tomizawa, 1985; Akazawa and Kato, 1988]. These conditions were chosen to avoid hydrodynamic or mixed lubrication between the surfaces and to isolate the effect of temperature. Loads were varied between 0.5 and 30 N (which resulted in a mean Hertzian pressures of 3 to 12 GPa). Sliding velocity was kept constant at 1 mm/sec. Figure 2.1.1.1 shows the time evolution of the friction coefficient of silicon nitride in air for various loads. It usually starts at a relatively low value and reaches a stable value of  $f = 0.7$  to  $0.8$  after a certain distance of sliding. This effect could be attributed to the initial contamination of the surface which subsequently gets removed during sliding. The higher the load the faster the removal of contamination.

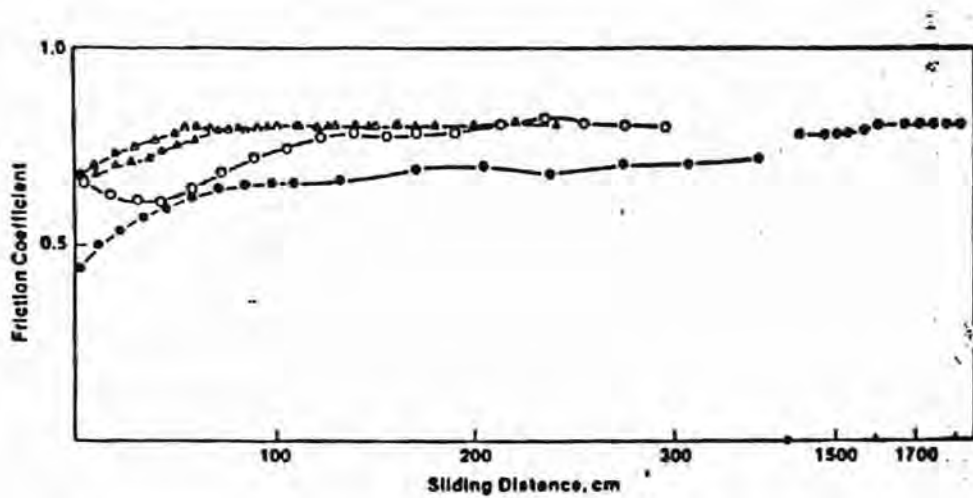


Figure 2.1.1.1 Time evolution of the friction coefficient of silicon nitride in air for various loads [Fischer and Tomizawa, 1985]

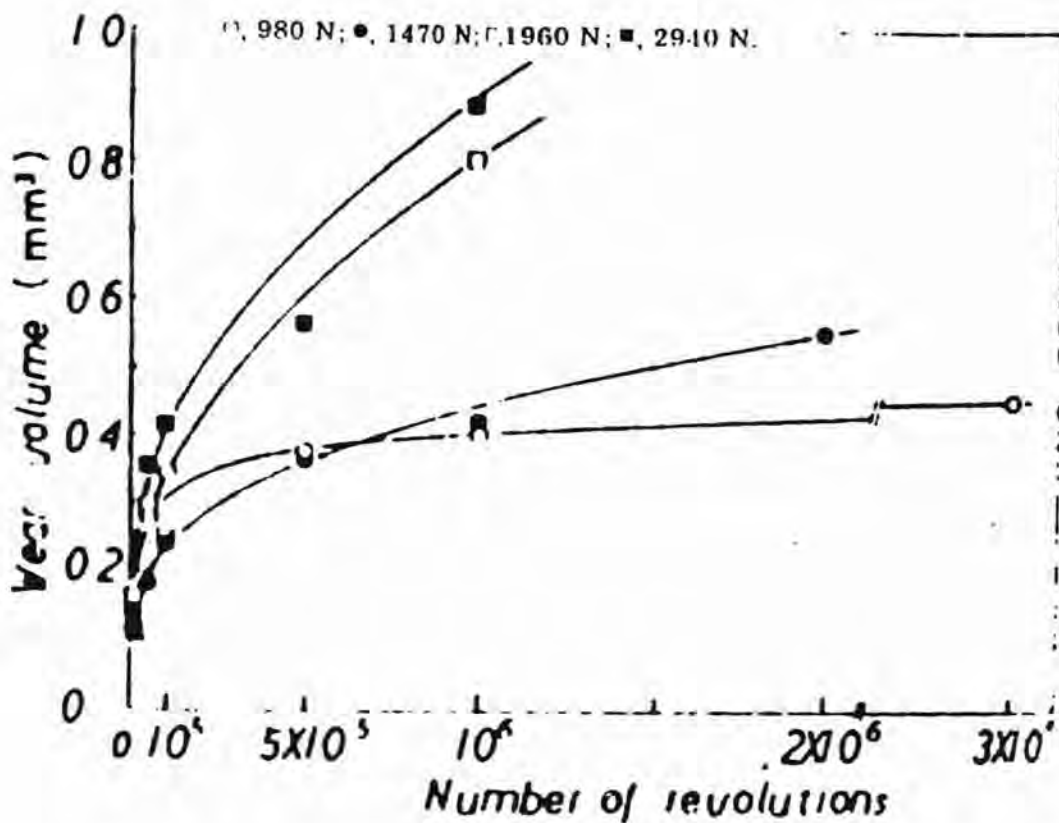


Figure 2.1.1.2 Wear volume versus the number of revolutions at various loads [Akazawa and Kato, 1986]

The effect of load on wear of silicon nitride was studied in a ring-on-ring configuration under loads of 980 N, 1470 N, 1960 N and 2940 N. Hertzian pressures ranged from 1 GPa to 1.83 GPa. Figure 2.1.1.2 shows the wear volume versus the number of revolutions at various loads [Akazawa and Kato, 1986]. The figure shows two distinctive wear stages in each case, initial severe wear and secondary steady state wear. Initial wear ends before  $10^5$  cycles.

#### EFFECT OF SPEED

The change in the relative speed between mating members effects the amount of heat generated at the contact interface, which in turn changes the temperature at the interface. The formation of reaction products is accelerated at higher temperatures which may lead to an entirely different wear behavior of the ceramic material. Figure 2.1.1.3 shows the variation of coefficient of friction with speed at two humidity levels [Gee and Butterfield, 1993]. It may be noted that the scatter in the friction coefficient is quite large. Figure 2.1.1.4 shows the variation in the wear volume with speed for different humidity levels. At low humidity levels, the scar diameter drops with increasing speed to a minimum at a speed of 0.05 m/sec and then increases to a maximum at a speed of 0.5 m/sec. At intermediate speeds and high humidity levels, the scar diameter increases slowly with increasing speed and reaches a maximum at 0.1 m/sec and then drops as the speed increases.

Figure 2.1.1.5 shows optical micrographs of wear scars at different speeds [Gee and Butterfield, 1993]. Some of the wear scars have polished appearance while others have a rough, dull appearance. At 0.3 m/sec, the scars had a mixed behavior with a central band which is rough and the outer region which is polished.

#### EFFECT OF TEMPERATURE

Temperature is the most crucial parameter in determining the tribochemical behavior of a ceramic material. It affects the rate of reactions occurring at the wear interface and brings additional reaction routes into play. There are two components to the interface temperature. First, the bulk temperature which is the average temperature of the surface layers of the specimen. The second is the flash temperature which is the temperature reached by the individual contact points between the surfaces [Gee and Butterfield, 1993].

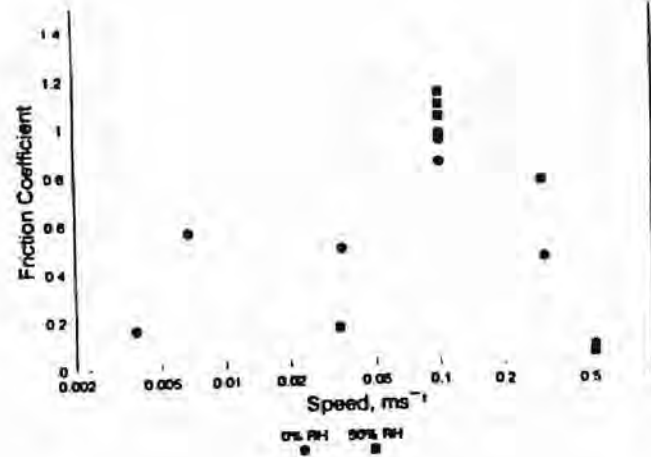


Figure 2.1.1.3 Variation of coefficient of friction with speed at two humidity levels [Gee and Butterfield, 1993]

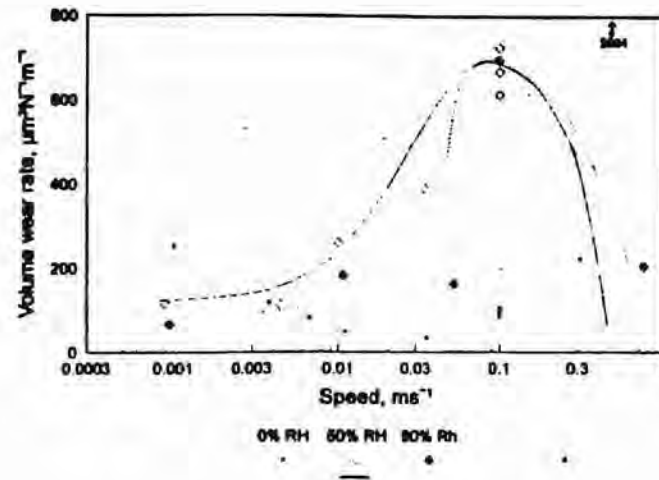


Figure 2.1.1.4 Variation in wear volume with speed for different humidity levels [Gee and Butterfield, 1993]

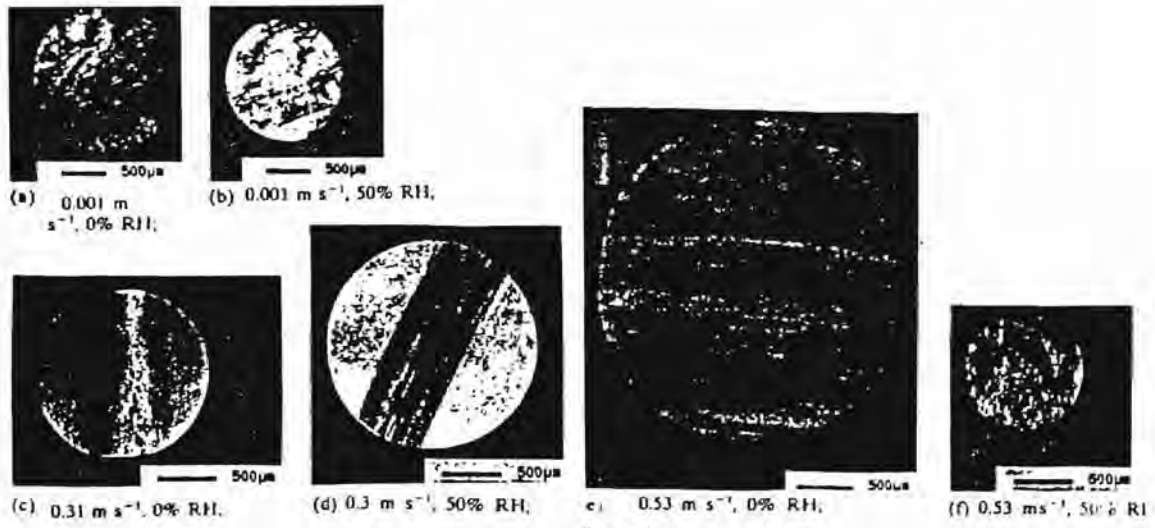


Figure 2.1.1.5 Optical micrographs of wear scars at different speeds  
[Gee and Butterfield, 1993]

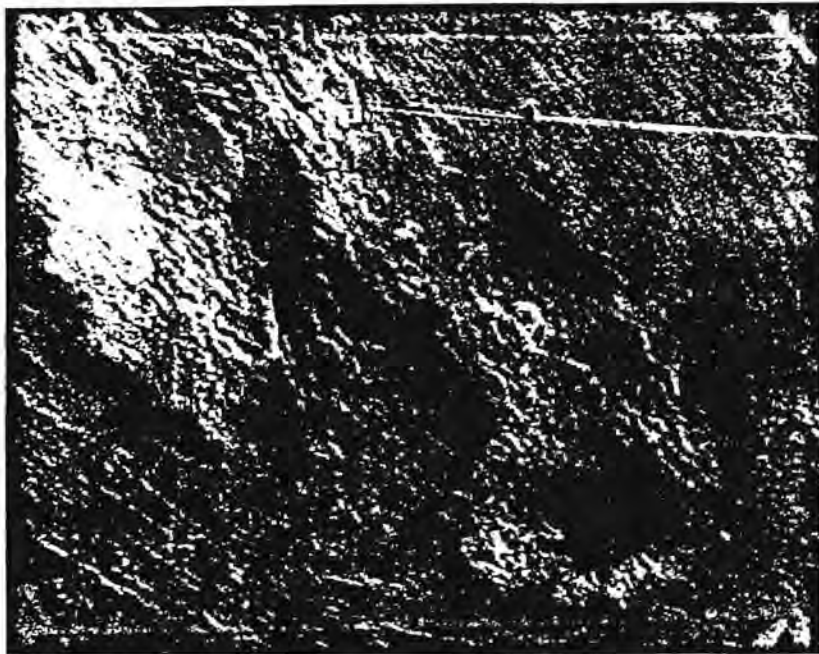


Figure 2.1.1.6 SEM of a wear scar of silicon nitride in dry argon [Fisher, 1988]



These asperities are typically about 10  $\mu\text{m}$  across for a nominal engineering surface. So, the heat generated is concentrated in a very small area.

## EFFECT OF EXTERNAL CONDITIONS

Apart from the physical conditions, humidity and the medium in which the relative movement takes place also play an important role in determining the tribochemical characteristics of ceramics. Figure 2.1.1.6 shows a SEM micrograph of a wear scar of silicon nitride sliding in dry argon. It consists of purely mechanical wear that shows microfractures at the surface [Fischer, 1988]. A few micrometers below where the contact stresses are diffused, cracks follow grain boundaries that are surfaces of mechanical weakness. Wear debris is ground to fine powder after repeated passes of the slider. In dry argon, the grains do not adhere to each other, and the wear debris does not influence the contact stresses at the temperature.

When sliding occurs in humid argon, the wear track has a completely different appearance. Figure 2.1.1.7 shows the SEM micrograph of a wear scar of silicon nitride after sliding in humid argon [Fisher, 1988]. It is smooth and the surface is covered with a coherent material that differs from the original material. Wear debris was predominantly amorphous with dispersed fine crystallites.

Figure 2.1.1.8 shows the wear tracks of silicon nitride in hexadecane [Jahanmir and Fischer, 1988]. The coefficient of friction in this case was the least, of the order of 0.2 when compared to 0.8 in air and water. Higher magnification (Figure 2.2.1.10c) shows that a film of material has covered these surfaces. The composition of the film was found to be different from the parent material. A similar behavior was observed when silicon nitride is rubbed in hexadecane + 0.5 % stearic acid, which is shown in Figure 2.1.1.9 [Jahanmir and Fischer, 1988].

Self mating sliding couples of silicon nitride, silicon carbide, zirconia, and alumina were tested in different aqueous solutions of varying pH from 3 to 13 [Loffelbein, 1993]. Table 2.1.1.1 gives the friction and wear coefficients obtained from the above tests [Loffelbein, 1993]. In comparison with dry conditions, the friction coefficients of all couples were reduced in the presence of different aqueous solutions. The lowest frictional coefficients were measured for the silicon nitride couples and silicon carbide couples.

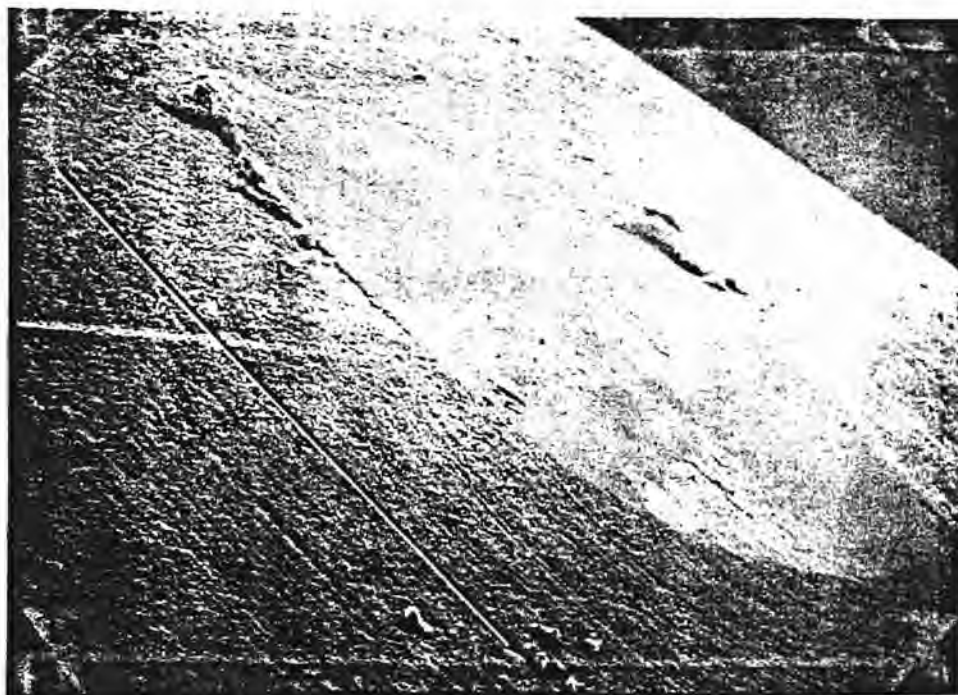


Figure 2.1.1.7 SEM of a wear scar of silicon nitride after sliding in humid argon [Fisher,1988]

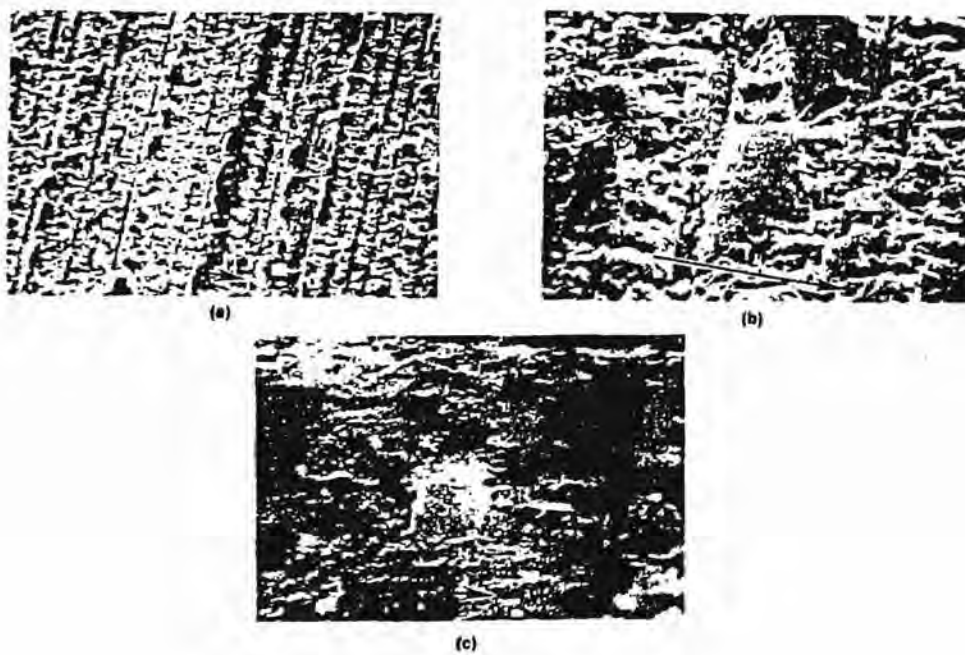


Figure 2.1.1.8 Wear tracks of silicon nitride in hexadecane [Jahanmir and Fisher, 1988]

Table 2.1.1.2 Friction and wear coefficients of ceramics in acid, basic and neutral environments[Loffelbein, 1993]

friction coefficients  $f$  (a) and wear coefficients  $k_w$  of stationary specimen ( $10^{-6} \text{ mm}^3 \text{ Nm}^{-1}$ ) (b) for all sliding couples tested (pin on disc,  $T=23 \text{ }^\circ\text{C}$ ,  $F_N=44 \text{ N}$ ,  $v=0.1 \text{ m s}^{-1}$ ,  $s=2000 \text{ m}$ )

Self-mated sliding couple	Interfacial medium										Dry friction
	H <sub>2</sub> O	NaOH	KOH	NH <sub>4</sub> OH	HNO <sub>3</sub>	H <sub>2</sub> SO <sub>4</sub>	H <sub>3</sub> PO <sub>4</sub>	CH <sub>3</sub> COOH	HCl	HClO <sub>4</sub>	
SSi <sub>3</sub> N <sub>4</sub>	$f=0.04$ (a)	0.03	0.05, 0.05	0.03, 0.04	0.02	0.04	0.15	0.04, 0.02	0.02, 0.03	0.01	0.79
	$k_w=1.2$ (b)	0.39	0.41, 0.27	1.9, 1.9	0.36	0.30	0.13	0.09, 0.08	0.55, 0.11	0.09	0.61
HIP-RBSi <sub>3</sub> N <sub>4</sub>	0.02, 0.02 (a)	0.04, 0.04	0.03, 0.03	0.31, 0.02	0.02	0.02	0.03, 0.02	0.02	0.03	0.02	0.90
	1.6, 0.48 (b)	0.05, 0.08	0.07, 0.09	1.3, 0.89	0.39	0.43	0.07, 0.11	0.11	0.63	0.10	0.82
SSiC	0.03, 0.02 (a)	0.04, 0.03	0.03	0.01	0.02	0.03	0.02	0.02	0.02	0.02	0.66
	0.52, 0.45 (b)	0.52, 0.48	0.41	0.32	0.48	0.59	0.50	0.41	0.48	0.45	1.3
SiSiC	0.18 (a)	0.18	0.21, 0.19	0.21	0.19	0.14, 0.20	0.20	0.22	0.15	0.19	0.62
	4.1 (b)	2.3	2.5, 1.4	4.8	4.8	4.1, 4.8	4.5	4.5	3.2	4.5	1.6
MgO-ZrO <sub>2</sub>	0.37 (a)	0.42	0.43, 0.35	0.44	0.41	0.70	0.42	0.28, 0.18	0.30	0.34, 0.27	0.89
	0.21 (b)	0.15	1.2, 0.04	0.11	0.55	0.17	0.08	0.30, 0.17	0.34	0.06, 0.05	50.0
Al <sub>2</sub> O <sub>3</sub>	0.22, 0.26 (a)	0.14	0.14	0.14	0.15	0.15	0.18	0.14	0.15	0.14	0.49
	0.006, 0.003 (b)	0.34	0.23	0.16	0.13	0.13	0.21	0.13	0.14	0.06	0.003

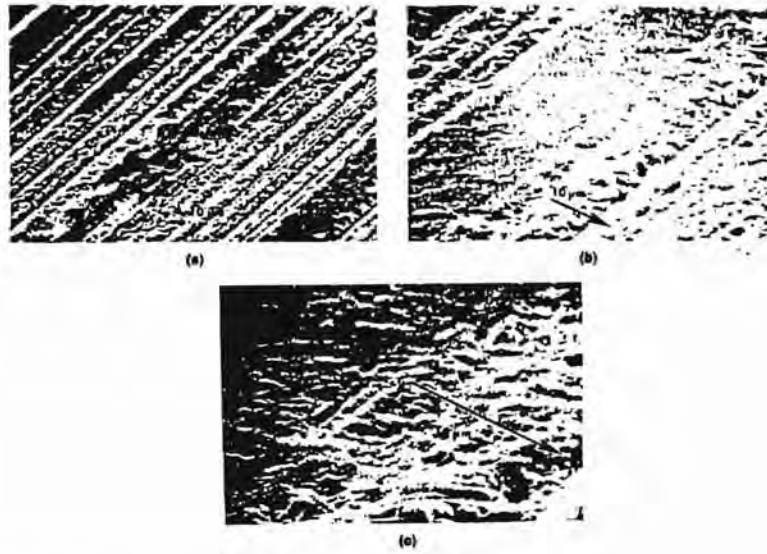


Figure 2.1.1.9 Wear behavior of silicon nitride rubbed in hexadecane and 0.5 % stearic acid [Jahanmir and Fisher, 1988]

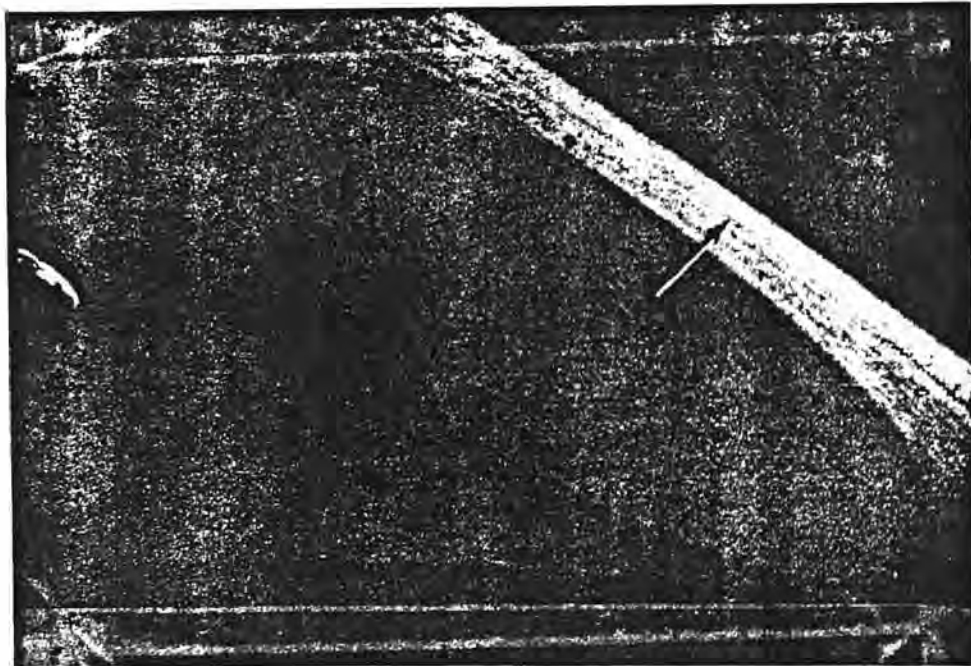


Figure 2.1.1.10 SEM of the wear scar of silicon nitride rubbed in water [Fisher, 1988]

Figure 2.1.1.10 shows a SEM micrograph of the wear scar of silicon nitride rubbed in water [Fisher, 1988]. Figures 2.1.1.11 show (a) and (b) a SEM micrographs of silicon carbide surfaces before and after rubbing in water. These ceramics can form low shear strength hydroxide films on the surface.

Couples of silicon carbide exhibited higher friction coefficients, which may have been caused by roughening the sliding surfaces through rapid dissolution of the silicon phase. The friction coefficients of alumina couples had similar values but the friction mechanism was quite different. Aluminum hydroxide films may form on the sliding surfaces and their dissolution in aqueous solutions may influence the tribological behavior. Figure 2.1.1.12 shows a SEM micrograph of a worn surface of alumina sample after rubbing in water [Gates et al, 1989]. It indicates the presence of a film on the contact region. The film had the appearance of a coherent compact material with the ability to flow. The shear strength of these films may be higher than that of the silicon hydroxide films on silicon nitride and silicon carbide. Alumina had higher wear coefficients in aqueous solutions than in air. Intercrystalline stress corrosion cracking probably enhanced wear. Its subcritical crack propagation velocity increased in the presence of water [Chen and Knapp, 1977].

Figure 2.1.1.13 shows a SEM micrograph of the wear scar of zirconia rubbed in water [Fischer, 1988]. The wear coefficient of magnesia stabilized zirconia was decreased in the presence of water. The high friction coefficients of the couples of magnesia stabilized zirconia may be favoured by the low heat conductivity of the ceramic, so that the partial disorption of water molecules can occur due to local frictional heating. However, Lancaster et al. [1992] reported increased wear rates of zirconia in the presence of water. One reason for this difference in wear behavior of zirconia is that it is extremely sensitive to its composition. The cubic form of zirconia, stabilized with magnesia and with a relatively low fracture toughness, shows a reduction in wear rates because of lower friction, reduced tensile stress, and consequent lower susceptibility to crack propagation. With the tougher, tetragonal form, however, water increases the wear rate by accelerating the rate of crack growth.

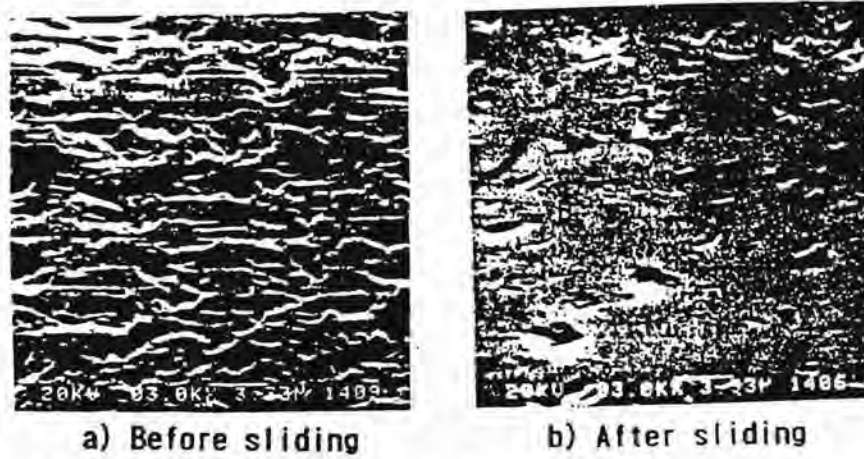


Figure 2.1.1.11 SEM of silicon carbide surfaces before and after rubbing in water [Mizutani et al., 1990]



Figure 2.1.1.12 SEM of a worn surface of alumina sample after rubbing in water [Gates et al., 1989]

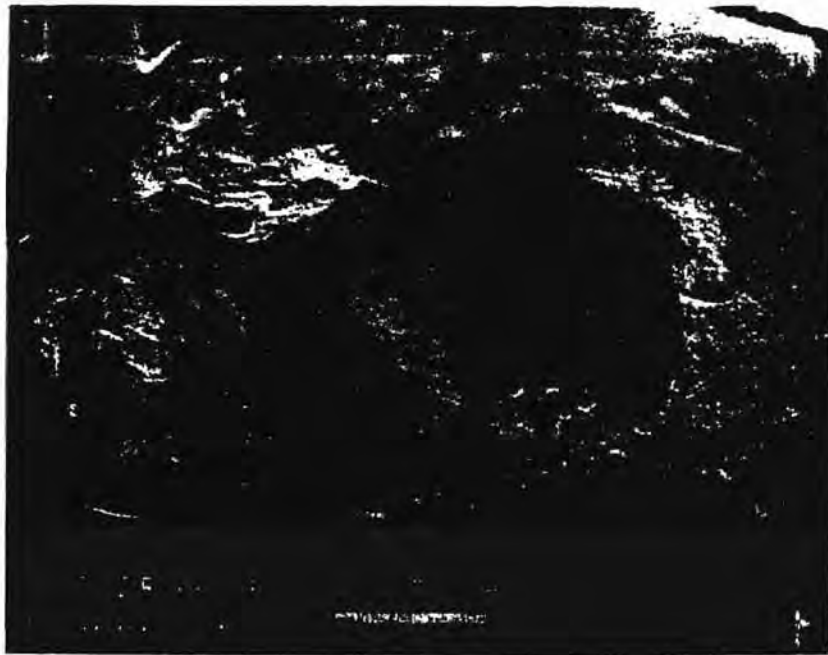


Figure 2.1.1.13 SEM of the wear scar of zirconia rubbed in water [Fisher,1988]

## 2.2. ANALYSIS OF REACTION PRODUCTS

The chemical reaction rates are often governed by the reaction products that accumulate on the surface and through which the reagent species must diffuse. There are several mechanisms by which such reactions are accelerated by friction, including the following: 1) wear removes the protective later reaction product and exposes fresh surfaces, 2) frictional stresses cause deformation or microfracture in the layer (or the solid) and produce diffusion paths (or high energy sites) of increased activity, 3) frictional heat increases the local temperature, and 4) the forming and breaking of bonds that accompany friction create highly reactive intermediate states. Since tribochemical reactions occur only where friction takes place, they can modify the surface geometry and lead to surface polishing. This modifies the local contact stress and decreases mechanical wear. On the other hand, this interaction can accelerate the chemical attack in which case it is called corrosion wear.

The reaction products generated during tribochemical studies have been investigated by various researchers using different techniques and is reviewed in this section.

### OXIDE CERAMICS

Oxide ceramics, such as alumina and zirconia are stable oxides and are incapable of undergoing further oxidation reactions. For some non-oxide based ceramics the formation of oxide layers are responsible for the reduction in wear. Alumina has been an important ceramic material for different applications ranging from abrasives to hip joint replacements [Gates et al., 1989]. Tribochemical reactions of this material have been of much interest for generating smooth surfaces. Tribochemical wear behavior reported in the literature is somewhat ambiguous in the sense that a reduction as well as increase, in wear rates were reported [Lancaster et al, 1992]. However, the formation of some form of aluminum hydroxide during rubbing in water is accepted. Figure 2.2.1 is an ion microprobe spectrum of an alumina surface during rubbing in water [Sugita et al, 1979]. The spectrum indicates the presence of  $AlH^+$  and  $AlOH^+$  species, suggesting that hydroxides are developed on the surface. In this technique, while the argon gas ions impinge on the surface at an extremely low current density and sputter off the surface atoms and molecules, the ionized fractions are analyzed with a mass spectrometer. The rate of removal by ion bombardment is about 0.2 Å/sec.



Figure 2.2.2 shows X-ray diffraction spectrum of alumina wear debris obtained from polishing with silica [Yasunaga et al, 1979]. Wear debris was heat treated at 970 and 1270<sup>0</sup> C for 2 hours. The spectrum indicates the presence of mullite as a reaction product.

Reflection electron diffraction patterns of alumina single crystal polished with diamond, silicon carbide, silica, and cerium oxide abrasives are shown in Figures 2.2.3 (a) to (e) [Namba and Tsuwa, 1977]. Figures 2.2.3 (a) and (b) show Debye rings, a characteristic of a rough polycrystalline structure in the case of diamond and silicon carbide. According to Namba and Tsuwa, the mechanism of lapping of sapphire with these abrasives involves a combination of the surface flow of the asperities by plastic deformation and microfracture. The specimen which was chemically polished [Figure 2.2.3 (c)] in a 1:1 H<sub>2</sub>SO<sub>4</sub> and H<sub>2</sub>PO<sub>4</sub> mixture showed excellent crystallographic quality. The patterns of the sapphire surface polished with silica and cerium oxide abrasives [Figures 2.2.3 (d) and (e)] had appearance similar to that of the chemically polished surface. Many Kikuchi lines are visible on the surface patterns, indicating a high degree of crystal perfection. It can be seen that the ring pattern, a typical characteristic of polycrystalline layer, is absent. The lapping damage on the sapphire specimen is completely recovered without the introduction of further damage, so that the mechanism of this ultrafine polishing must be microfracture with no dislocation or with a minimal surface damage.

Wear particles of alumina rubbed in water were analyzed using a thermogravimetric analyzer (TGA). Figure 2.2.4 shows the TGA scans of  $\gamma$ -alumina and  $\gamma$ -alumina-water reaction products [Gates et al,1989]. The low temperature product was thermally decomposed at 272<sup>0</sup> C and was identified by XRD as Bayerite, Al(OH)<sub>3</sub>. The higher temperature reaction product that was decomposed at 510<sup>0</sup> C was identified to be Bohemite Al(OH).

## NON-OXIDE CERAMICS

Non-oxide based ceramics are capable of undergoing oxidation reactions at higher temperatures. Tribochemical reactions in non-oxide ceramics can generate oxidation products on the surface. Figure 2.2.5 shows an X-ray microanalysis of a wear particle obtained during dry rolling of silicon nitride [Kato, 1990]. The particle shows the presence of oxygen, silicon, and nitrogen.

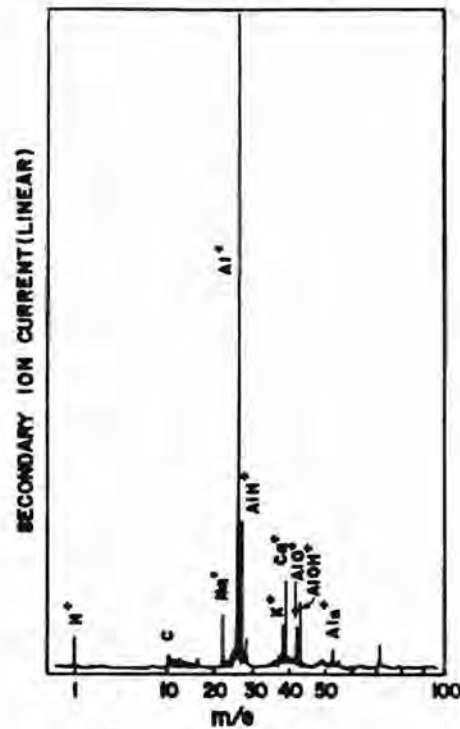


Figure 2.2.1 Ion microprobe spectrum of an alumina surface during ribbing in water [Sugita et al., 1979]

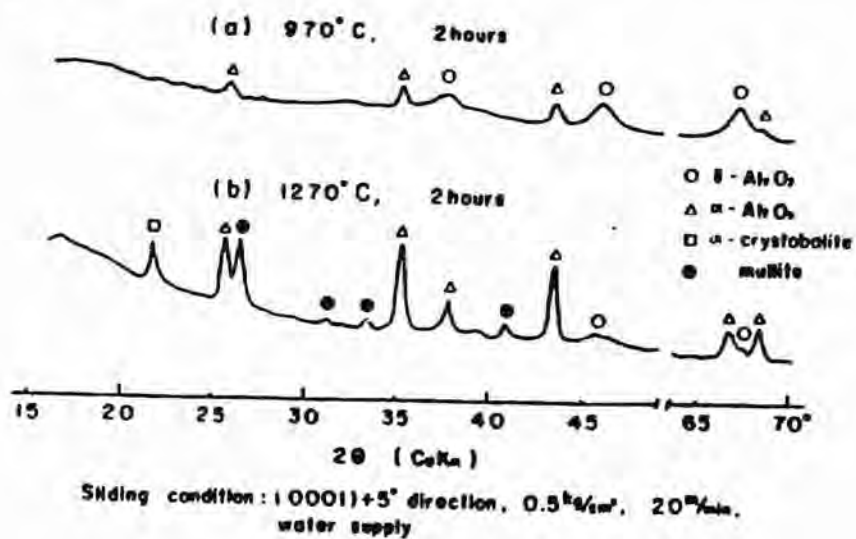


Figure 2.2.2 X-ray diffraction spectrum of alumina wear debris obtained from polishing with silica [Yasunaga et al., 1979]

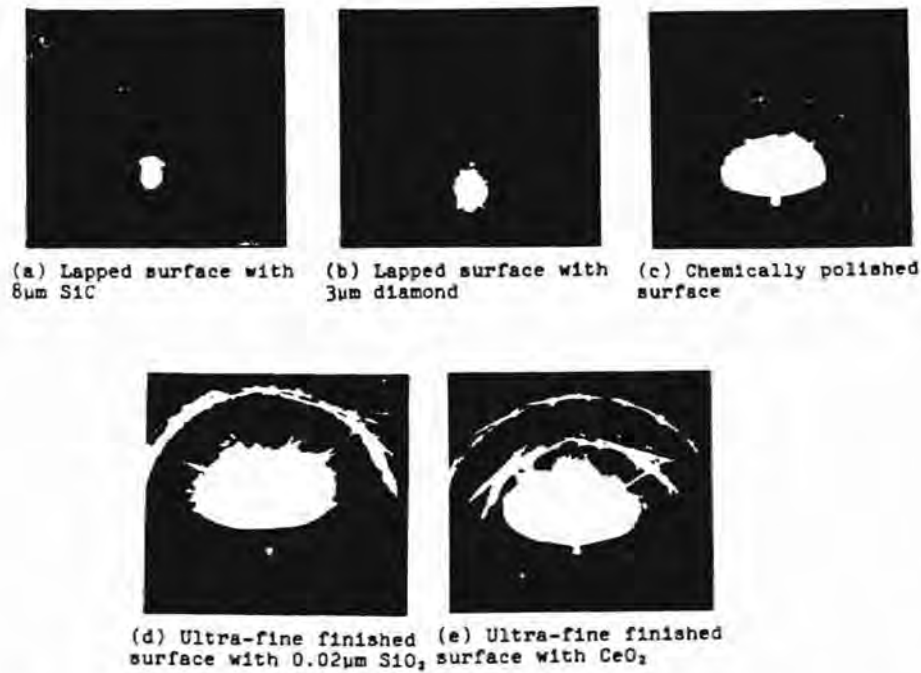


Figure 2.2.3 Alumina single crystal polished with various abrasives [Namba and Tsuwa, 1977]

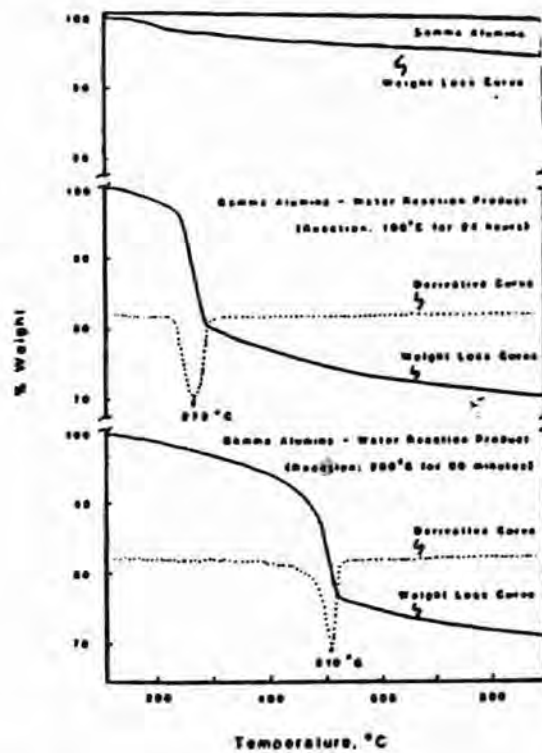


Figure 2.2.4 TGA scans of gamma-alumina and gamma-alumina-water reaction products [Gates et al., 1989]

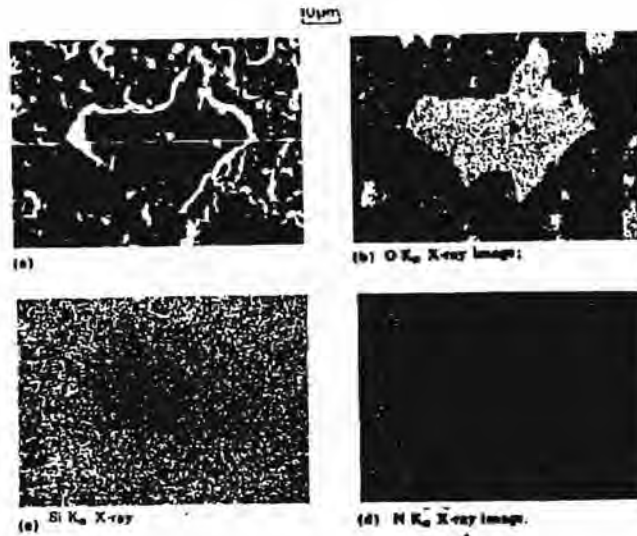


Figure 2.2.5 X-ray microanalysis of a wear particle obtained during dry rolling of silicon nitride [Kato, 1990]

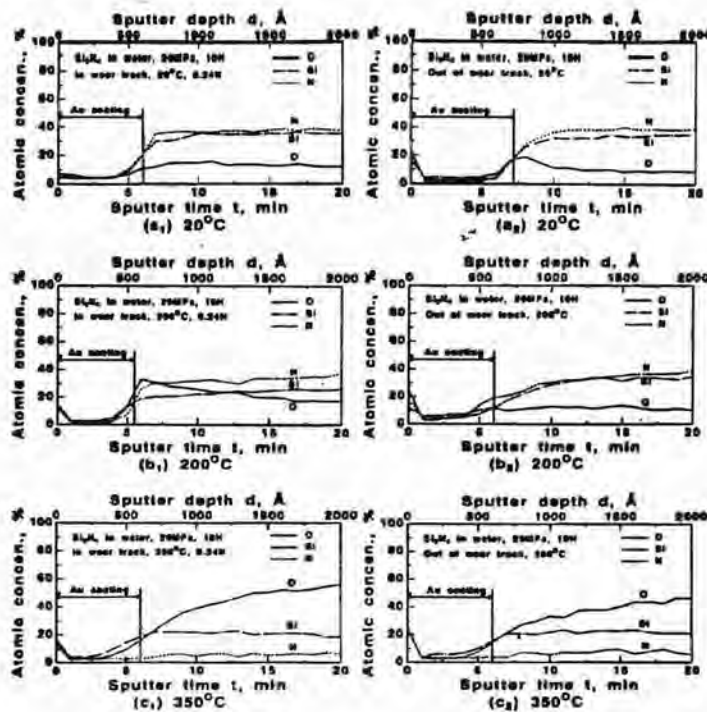


Figure 2.2.6 Auger-electron spectroscopy analysis conducted on the inside and outside of the wear tracks of silicon nitride after rubbing in water [Xu et al., 1993]

Figure 2.2.6 shows the Auger Electron Spectroscopy (AES) analysis conducted on the inside and outside of the wear tracks of silicon nitride after rubbing in water [Xu et al, 1994]. At low temperatures of sliding, the oxygen intensity is the same inside and outside the wear tracks. At intermediate temperatures, oxygen intensity inside the wear track was found to be higher. Consequently, the oxide film grows because of frictional activation. In the high temperature range, the oxide intensity has reduced inside the wear tracks due to removal of the material inside the wear tracks by microfracture and exposing the less oxidized surface. Figure 2.2.7 shows an infrared (IR) spectra obtained from a similar test [Akazawa et al, 1986]. The structure of the particles coincided with that of quartz. Therefore, the debris may have silica structure suggesting that oxidation of the silicon nitride surface is in progress.

Figure 2.2.8 shows the light element energy dispersive x-ray spectroscopy of the wear tracks obtained from a similar test [Gee and Butterfield, 1993]. The spectra, at 0.53 m/sec, 0 % RH indicates the presence of both nitrogen and oxygen suggesting that the oxidation of silicon nitride is in progress. As the humidity increases, it clearly shows the presence of oxygen in greater amounts suggesting that oxidation progresses rapidly in the presence of humidity to form a lubricious layer in the wear tracks. Another similar observation was made using electron energy loss spectroscopy (EELS) of the wear particles obtained from scratching silicon nitride in hexadecane [Jahanmir and Fischer, 1988]. Figure 2.2.9 shows the TEM micrographs obtained from amorphous and crystalline wear particles and their electron energy loss spectra. The amorphous particles showed the presence of oxygen and the crystalline particles showed the presence of oxygen and nitrogen suggesting that the oxidation product is amorphous silica and the crystalline product is silicon nitride which is in the process of oxidation.

Figure 2.2.10 shows X-ray photoelectron spectroscopy data obtained from the worn surfaces of silicon nitride with varying intensities [Cranmer, 1989]. In general, the oxygen peak in the etched film occurs at 532.2 eV and is associated with oxy-nitride structure. As more oxygen is included in the structure, the peak shifts towards 532.8 eV, which is typical of Si - O bond formation in silica. The Si peak associated with the Si - N bond in etched silicon nitride occurs at 101.4 eV and increases to 103.8 eV as the film oxidizes to form silica. The N peak associated with the Si - N bond in silicon nitride occurs at 397.4 - 397.9 eV and shifts towards 398.4 eV as the nitride incorporates oxygen in the

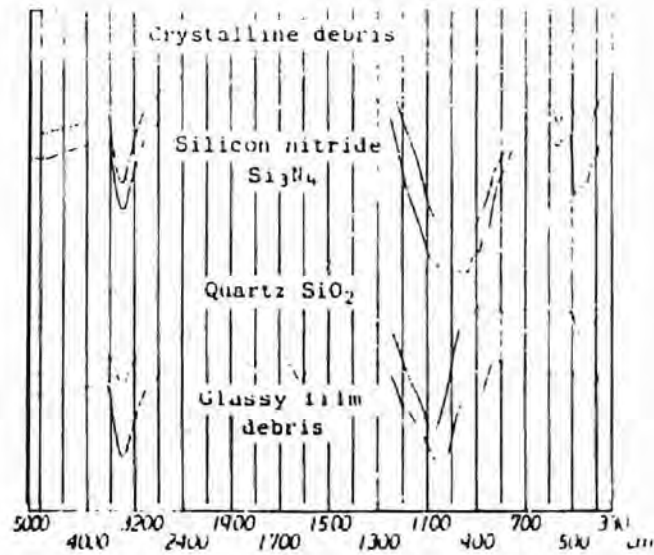


Figure 2.2.7 Infrared spectra obtained during a dry rollig test [Akazawa et al., 1986]

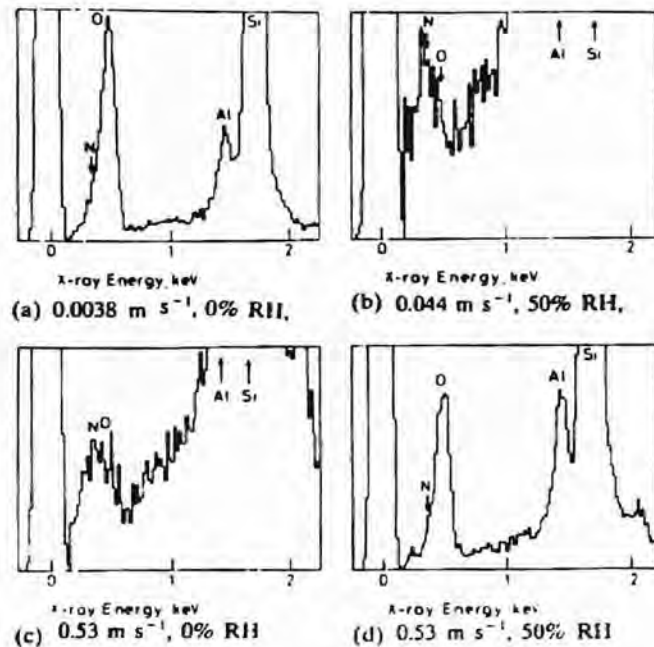


Figure 2.2.8 Light element energy dispersive x-ray spectroscopy of the wear tracks of silicon nitride during a dry rolling test[Gee and Butterfield, 1993]

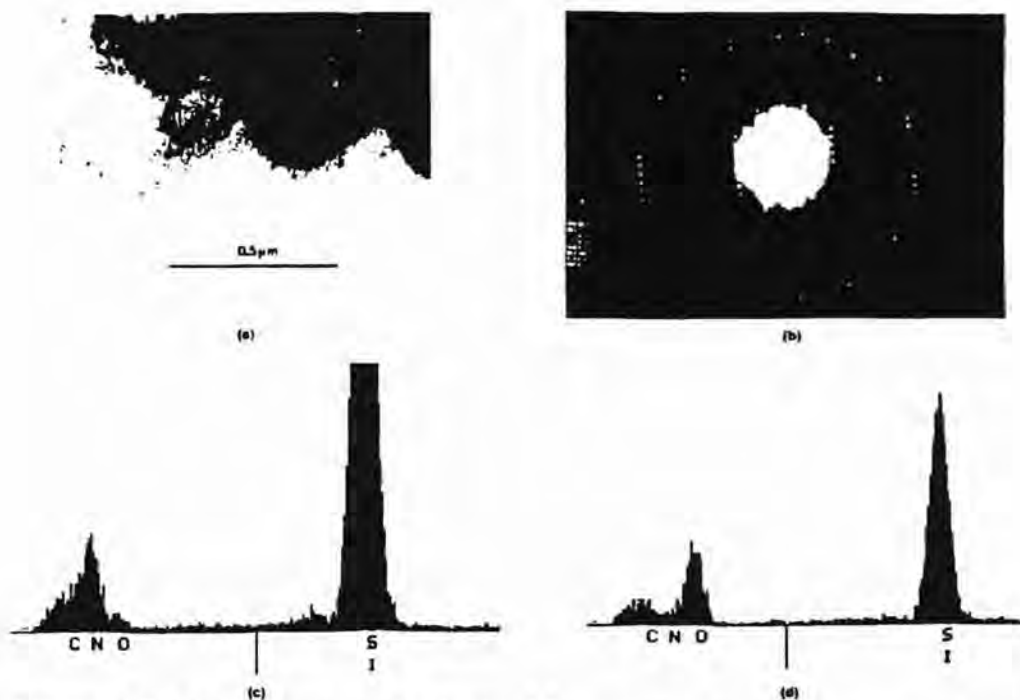


Figure 2.2.9 TEM micrographs obtained from amorphous and crystalline wear particles and their electron energy loss spectra [Jahanmir and Fischer, 1986]

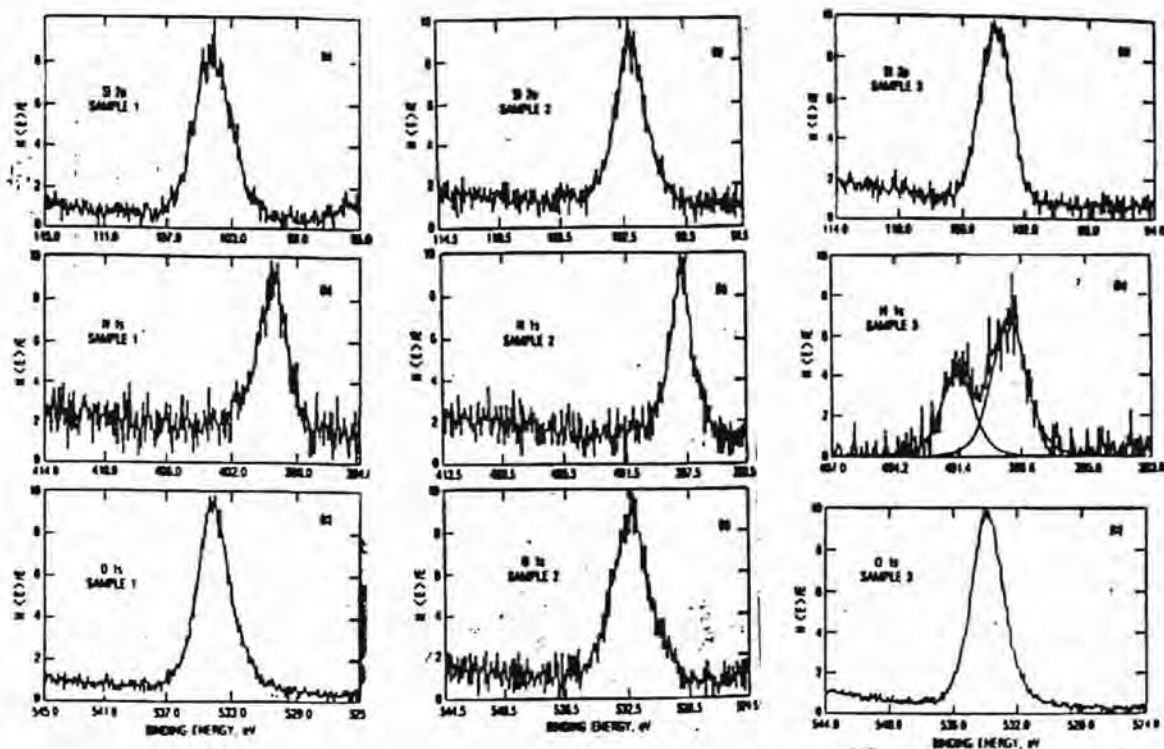


Figure 2.2.10 X-ray photoelectron spectroscopy data obtained from the worn surfaces of silicon nitride [Cranmer, 1989]

structure as oxy-nitride. These results suggest that the worn surfaces have oxidized to form silicon oxy-nitride.

Figures 2.2.11 (Figures (a) and (b) show the spectra obtained from an ion microprobe mass spectrometer as a function of the number of scans of the polished surface, fractured surface and baked surface, respectively [Sugita et al, 1984]. The polished surface had been generated under a normal load of 10 N at a rubbing velocity of 0.25 m/sec in water. The surfaces after fracturing with and without baking treatments, were observed. The baking treatment was done at 1170 °K for 1 hour. The sputtering depth, according to the scan, was about 30 Å. It was found that the SiH<sup>+</sup> was plentiful on the polished surface after rubbing; it has decreased to the same level as in the fractured surface after the baking treatment. Also, there is a large amount of SiO<sup>+</sup> present on the polished surface, for which the intensity level in the spectrum is not changed even after the baking treatment. From these results, it appears that by rubbing silicon nitride on silicon nitride in water, silica is produced initially on the work piece and subsequently silicon hydrate formed.

The wear debris in water after rubbing were examined using XRD. Figures 2.2.12 (a) and (b) show the XRD data of the wear debris as obtained and after the baking treatment at 1270<sup>0</sup> K for 1 hour. The as-received debris showed no peaks in the spectrum suggesting that they were probably amorphous products or very fine grained particles. But, after the heat treatment, the data showed the presence of  $\alpha$ -cristobalite, a form of silica. Therefore, it was assumed that  $\alpha$ -cristobalite existed in amorphous form and/or an amorphous silicon hydrate existed in the as-received remnants. The color of the remnants changed from light pink to white upon heating. This also suggests that the structure and the material must have been converted to another form.

Thus, tribochemical reactions occur in ceramic materials depending on the material and its structure as well as the environment. These studies suggest possible chemo-mechanical polishing mechanisms which may be applicable to fine polishing. The various mechanisms of chemo-mechanical polishing are discussed in the following.



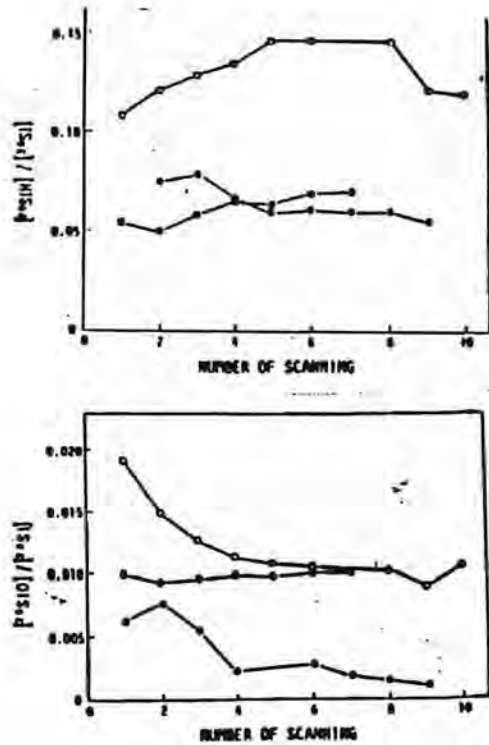


Figure 2.2.11 Spectra obtained from an ion microprobe mass spectrometer as a function of the number of scans of the polished surface, fractured surface and baked surface [Sugita et al., 1984]

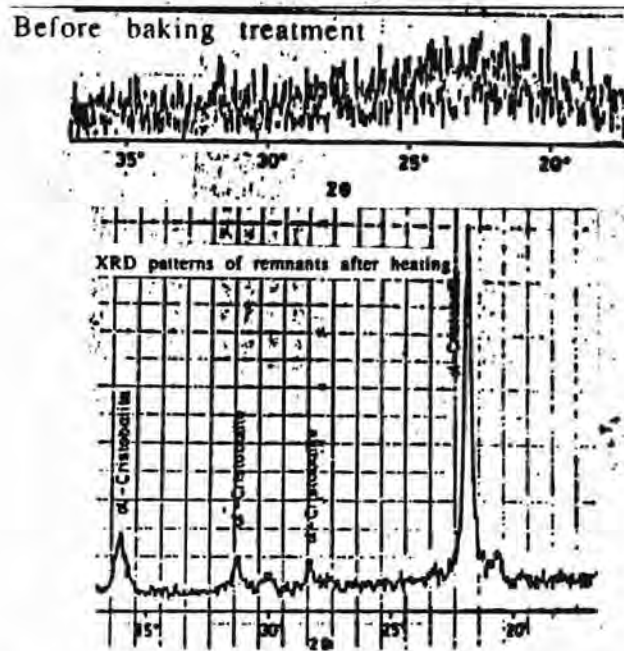


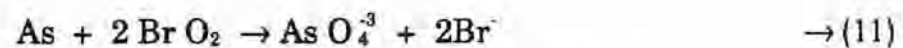
Figure 2.2.12 XRD data of the wear debris before and after the baking treatment [Karaki-Doy et al., 1989]

### 2.3. CHEMO-MECHANICAL POLISHING MECHANISMS

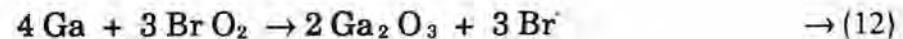
From a review of literature, it is reasonable to infer that chemo-mechanical action at the interface between two materials in frictional contact can occur, if the materials exhibit high chemical affinity. The material removal is, generally, much lower than mechanical removal (abrasion) because the reaction takes place only at the real areas of contact. The reaction products, as well as the material removal mechanisms, depend based on the reactions progressing between two materials in relative contact. In the following, the mechanisms of material removal on various ceramic workmaterials with different abrasives are discussed.

In the chemo-mechanical polishing of semiconductor materials, sodium bromite (Trade name Brodesizer) is used [Karaki-Doy, 1989]. A typical composition used is given by  $\text{NaBrO}_2$  (69.0%),  $\text{NaBrO}_3$  (1.8%),  $\text{NaOH}$  (0.6%) and water (27.3%). Amongst them,  $\text{NaOH}$  has a remarkable effect on polishing. It was found that the polishing rate increases with the pH of the reagent and reaches a maximum at 12.5. However, the surface roughness was also found to increase.

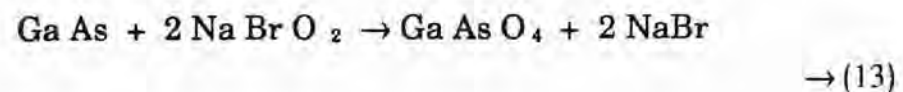
Comparing the standard oxidation-reduction potentials of Ga and As, As has a higher corrosion rate and is considered to diffuse in the solution as soon as it contacts the  $\text{NaBrO}_2$  solution.



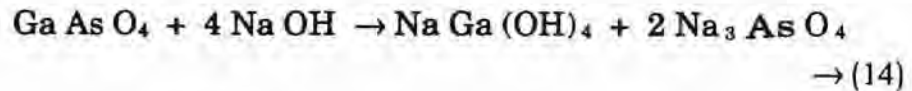
Ga when reacted with  $\text{NaBrO}_2$  solution would oxidize to Gallium oxide and most of it would stick to the surface as follows.



Since Ga dissolves more slowly than As, the GaAs substrate is visualized as a microscopically porous structure. Rearranging the above process, it actually produces the following two-step reaction:

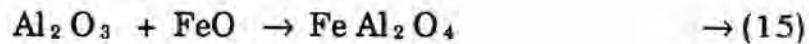


The resultant GaAsO<sub>4</sub> is an insoluble film that reacts with NaOH as follows:

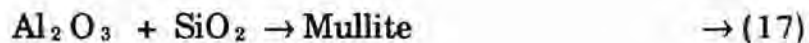
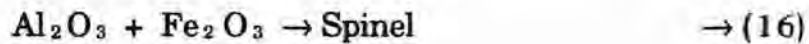


The above product is a thin soluble soft layer which is subsequently removed by the mechanical action of the abrasives.

In an investigation on the wear of sapphire on steel, the formation of chemical reaction products at the interface was confirmed [Yasunaga et al., 1977]. It may be the chemical reaction between Wustite, which is expected to be form due to oxidation of steel caused by friction, and alumina which finally forms the reaction product called Hercynite (FeAl<sub>2</sub>O<sub>4</sub>).

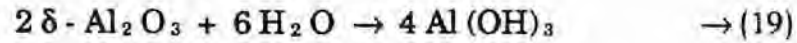
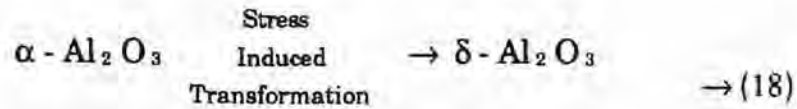


Alumina was also polished chemo-mechanically using softer abrasives, such as SiO<sub>2</sub> and Fe<sub>2</sub>O<sub>3</sub> [Yasunaga et al, 1977]. The mechanisms of polishing are given by:



Spinel and mullite form a thin layer on alumina which is subsequently removed by the mechanical action of the abrasives.

Alumina, when tested under water for tribological studies, has resulted in the formation of aluminium hydroxide. TGA results, reported earlier showed reactivity of  $\gamma$ -alumina with water. But, no reaction has been observed between  $\alpha$ -alumina and water. Therefore, it is anticipated that  $\alpha$ -alumina undergoes a stress induced transformation, as seen in the case of partially stabilized zirconia. In fact, it was observed when  $\alpha$ -alumina is subjected to abrasion in unlubricated wear tests, particles of  $\delta$ -alumina were observed in the transition phases which is quite similar to  $\gamma$ -alumina [Hines et al., 1979]. Therefore, the complete reactions are given by,



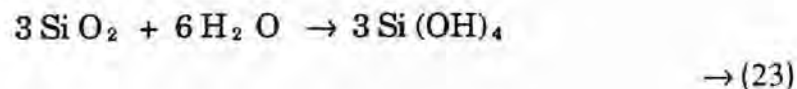
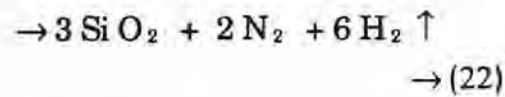
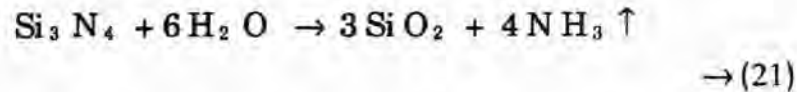
Aluminium hydroxide, a layered structure that forms, is subsequently removed by the mechanical action of the abrasives.

Silicon carbide, when polished with chromium oxide, resulted in very good surface finish [Kikuchi et al, 1992]. Kikuchi et al. suggested the following mechanism of material removal. In the oxidation reaction,



According to Kikuchi et al., oxygen is supplied from the surrounding atmosphere but not from chromium oxide. Therefore, chromium oxide acts merely as a catalyst and hastens the oxidation process to form amorphous silica which, in turn, is removed by the mechanical action.

Silicon nitride is known for its oxidation resistance at high temperatures [Tighe, 1982]. The amorphous silica which is formed as a result of the oxidation process grows with a parabolic growth law which indicates that the reaction is rate controlled by the diffusion of ions through the oxide layer. Oxidation of silicon nitride is accelerated in the presence of humidity [Singhal, 1976 (b); Contet et al., 1987; Sato et al., 1991]. Silica surfaces adsorb water to form  $\text{Si}(\text{OH})_4$ . The reactions are given as follows :



Generation of  $\text{NH}_3$  gas was confirmed experimentally during wet grinding of silicon nitride powder [Kanno et al, 1983]. Silicon nitride, when investigated for its tribological behavior, resulted in the formation of  $\text{NH}_3$  in appreciable amounts. Thus, the formation of chemical reaction products can be beneficial during polishing of advanced ceramics for obtaining desired finish and accuracy. However, control of the reaction rates is necessary for optimum material removal rates and good finish.

Fischer et al., (1989) used the following method to determine the nature of the material removal mechanism in stating, namely, whether it is assisted by the formation of chemical reaction products or not. The material removal is determined as a function of rubbing speed in two different ways. The first one is calculated from the rubbing time (time dependent material removal rate) and the second one calculated from the rubbing distance (the distance related material removal rate). He found that the distance dependent removal rate decreases with increased rubbing speed, but the time dependent material removal rate is independent of the rubbing speed. If the removal mechanism is by abrasion, the removal volume should be proportional to the distance. Thus, the distance dependent removal rate should remain constant for all rubbing speeds, but the time dependent material removal rate should increase with rubbing speed, since for a given time, a greater distance will be covered at greater speeds. If the removal mechanism is based on a chemical reaction, the removal volume will depend on the volume of chemicals produced at the interface, which is proportional to the total contact time. Thus, for wear due to chemical reactions, the time dependent removal rate remains constant at all rubbing speeds. Since the removal volume depends only on the contact time, the distance dependent removal rate decreases with increasing rubbing speed with decreasing contact time.

Based on the literature review, during polishing of silicon nitride with chromium oxide, it appears the oxidation of silicon nitride takes place with the oxygen available from surrounding atmosphere and not from the chromium oxide abrasive. Thus, the role of chromium oxide is considered as a mere catalyst and does not take part in the chemo-mechanical action. While chromium oxide is a well known catalyst, it will be shown in this investigation that chromium oxide does in fact take part in the chemo-mechanical polishing of  $\text{Si}_3\text{N}_4$ .

## CHAPTER 3

### PROBLEM STATEMENT

In order to minimize scratches and other defects on the finished surfaces of advanced ceramics, a novel polishing technique, namely, chemo-mechanical polishing was developed by some researchers using abrasives softer than the workpiece. Chemo-mechanical polishing combines chemical and mechanical actions between soft abrasive grains and a harder workmaterial, to provide a smooth surface. This investigation focuses on the chemo-mechanical polishing of silicon nitride workmaterial with chromium oxide abrasive (under both dry and wet conditions).

Based on the review of literature, although many researchers have identified the possibility of chemo-mechanical polishing  $\text{Si}_3\text{N}_4$  with  $\text{Cr}_2\text{O}_3$ , the role of chromium oxide was identified only as a catalyst for enhancing the oxidation of silicon nitride. No evidence of any compound formation of silicon nitride workmaterial with chromium oxide abrasive, in a given environment (water or dry), was given. It was decided to investigate further into the chemo-mechanical action of chromium oxide abrasives on the polishing of silicon nitride and to determine whether there is any compound formation or the action is entirely catalytic. This necessitated systematic investigation wherein silicon nitride is polished with not only chromium oxide but also other abrasives, such as boron carbide and silicon carbide. Both boron carbide and silicon carbide are harder than silicon nitride. Hence, mechanical abrasion would be the predominant material removal mechanism. Because of similar surface chemistry, polishing of  $\text{Si}_3\text{N}_4$  appeared to be more mechanical and negligible chemo-mechanical. Chromium oxide on the other hand is about the same or lower hardness than silicon nitride. Hence, mechanical abrasion would not be the predominant mode. The smooth finish generated on the silicon nitride workmaterial must be associated with a chemical mechanism of material removal.

To identify possible compound formation during chemo-mechanical polishing of silicon nitride with chromium oxide abrasive, it is necessary to investigate the polished workmaterial as well as the wear debris by various characterization techniques. This

includes the use of scanning electron microscope, with an energy dispersive X-ray microanalyzer, as well as X-ray diffraction studies. The former provides surface features as well as elemental information, while the latter can provide information on compound formation.

The activation of chemical reaction between a soft abrasive and a hard workmaterial, at several contacting points, depends on the high temperatures and pressures generated in the micro-reaction zones. After the reaction, the reaction product is removed by the soft abrasive due to mechanical forces. Therefore, this mechanism can be controlled by the mechano-chemical reaction rates, i.e., by selecting a proper combination of soft abrasive grain material and a hard workmaterial, and sliding conditions such as polishing pressure, contact temperature, and sliding speed. So, it is necessary to determine the temperatures generated at the asperities of contact during polishing. Also, it is necessary to identify various compounds that can be formed during chemo-mechanical polishing, using thermodynamic analysis. To accomplish these, the following studies are undertaken:

Experimental study of the wear debris generated in polishing of silicon nitride with different abrasives; examination of the wear debris, as well as the finished balls and rollers, in a scanning electron microscope with an energy dispersive X-ray microanalyzer and X-ray diffraction studies; analytical determination of the flash temperatures generated at the actual points of contact during polishing; identification of possible compound formation using Gibb's free energy of formation coupled with a phase diagram study; and, finally, development of a plausible model for the chemo-mechanical polishing of silicon nitride with chromium oxide abrasive.

## CHAPTER 4

### EXPERIMENTAL APPARATUS AND CHARACTERIZATION OF THE WORKMATERIAL AND THE ABRASIVES

To study the chemo-mechanical polishing of silicon nitride workmaterial with chromium oxide abrasive, two magnetic field assisted polishing techniques, currently under active investigation at OSU, were used. The magnetic field assisted polishing experiments were conducted by the author's colleagues (Mr.M. Raghunandan and Mr. Michel. Fox). Samples of the finished  $\text{Si}_3\text{N}_4$  balls and rollers, as well as the wear debris with each of the abrasive, were provided to the author for chemo-mechanical investigation. In this chapter, the two magnetic field assisted polishing techniques used at OSU are described briefly along with typical polishing conditions. This is followed by the characterization of the  $\text{Si}_3\text{N}_4$  workmaterial as well as that of the other abrasives used. Water-based magnetic fluid was used in magnetic float polishing, for polishing silicon nitride balls since water has been found to be effective in the oxidation of silicon nitride. Magnetic abrasive finishing was conducted in air, for polishing silicon nitride rollers.

#### 4.1 MAGNETIC FIELD ASSISTED POLISHING OF $\text{Si}_3\text{N}_4$ BALLS AND ROLLERS

The requirements of high finish and accuracy, and absence of any surface defects, by the conventional methods of grinding and polishing cost effectively, necessitated the investigation of alternate manufacturing technologies as part of ARPA's Ceramic Bearing Technology Program. The recent support provided by the National Science Foundation towards an understanding of chemo-mechanical polishing of silicon nitride using  $\text{Cr}_2\text{O}_3$  abrasive is the basis for this investigation. Two methods of finishing  $\text{Si}_3\text{N}_4$  balls and rollers based on magnetic field assisted polishing are the techniques used in this investigation. They are: i. Magnetic float polishing of ceramic balls, and ii. Magnetic abrasive finishing of ceramic rollers.



The salient features of magnetic field assisted polishing techniques are the following:

1. Very high finish and accuracy can be obtained,
2. Very little (or no) surface damage, such as microcracks to the ceramic parts during the finishing operation, due to extremely low forces (on the order of 1 N/ball or less),
3. The finishing operation can be significantly faster than by conventional techniques. This is due to higher spindle speeds possible by this technique,
4. Small polishing batch. Very few ceramic balls are needed in a batch for polishing, unlike in conventional polishing where a large number are required for alignment and accuracy requirements. The number of balls depend on the size of the balls as the float pad can be changed to suit the size of the balls,
5. Fewer polishing steps are needed. The balls can be processed from the rough to finished state in one operation, by varying the strength of the magnetic field intensity. It is, therefore, not necessary to change the polishing machines for roughing and finishing or clean the balls during the polishing cycle.

In the following, the two magnetic field assisted polishing techniques are briefly described.

#### 4.1.1 MAGNETIC FLOAT POLISHING OF $Si_3N_4$ BALLS

The magnetic float polishing technique was developed on the basis of the magneto-hydrodynamic behavior of a magnetic fluid that can float non-magnetic abrasives suspended in it by a magnetic fluid. The process is considered highly effective for finish polishing, because a buoyant levitational force is applied to the abrasives in a controlled manner. Hence, the forces applied by the abrasives to the part are extremely small and highly controllable. The magnetic fluid is a colloidal dispersion of extremely fine (100 to 150 Å) sub-domain ferromagnetic particles, usually magnetite ( $Fe_3O_4$ ), in various carrier fluids, such as water or kerosene. The ferrofluids are made stable against particle agglomeration by the addition of surfactants. When a magnetic fluid is placed in a magnetic field gradient, it is attracted towards the higher magnetic field side. If a non-magnetic

substance (e.g., abrasives in this case) is mixed in the magnetic fluid, they are discharged towards the lower side. When the field gradient is set in the gravitational direction, the non-magnetic material is made to float on the fluid surface by the action of the magnetic levitational forces. The polishing operation in this process occurs due to the magnetic buoyant levitational force.

Figure 4.1.1.1 is a diagram of the magnetic float polishing apparatus, showing permanent magnets located at the base of the apparatus. These magnets are located alternate N and S on top of the float vessel. A guide ring is mounted on top of the float vessel to contain the magnetic fluid. Magnetic fluid containing fine abrasive particles, fills into the chamber. Silicon nitride blanks for balls are located between the drive shaft and the float. The end of the drive shaft can be chamfered and a flat float can be used underneath, or alternately, the shaft end can be flat and the top surface of the float can have a V- groove to fit the balls. Three point contact is preferred. When a magnetic field is applied, the ceramic balls, abrasive grains, and the float of non-magnetic material all float and are pushed upwards by the magnetic fluid. The ceramic balls are pressed against the drive shaft and are finished by the rotation of the drive shaft. The time required to finish the balls to the same accuracy or better by this technique is reported to be at least one to two orders of magnitude faster than by conventional polishing techniques. Consequently, this technique can be extremely cost effective and a viable method for the manufacture of ceramic balls.

Typical polishing conditions are:

Polishing capacity	:	12 balls/batch (up to 0.5 in. in diameter)
Spindle speed	:	2,000 ~ 6,000 rpm
Levitational force, $F_M$	:	0 ~ 33 lb
Polishing load, $P_l$	:	1 N/ball
<b><u>Magnets</u></b>		
Maximum energy product	:	32 MGO
Residual induction, $B_r$	:	13 KGauss

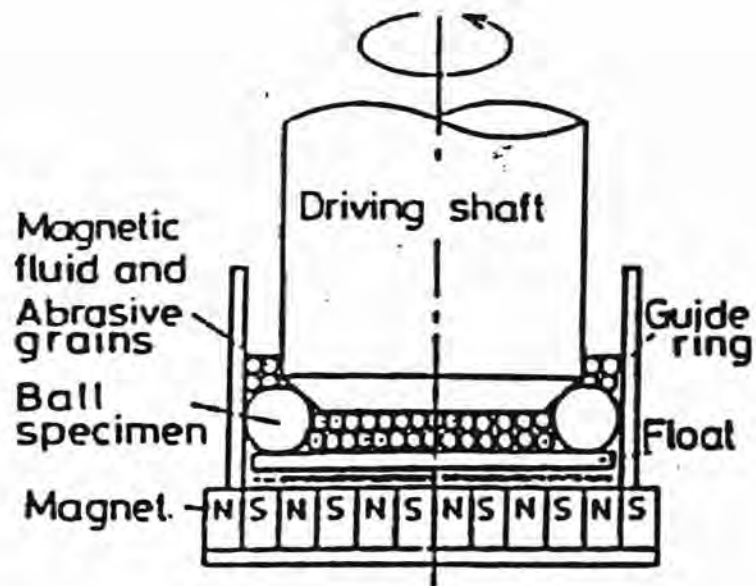


Figure 4.1.1.1 Diagram of the magnetic float polishing apparatus

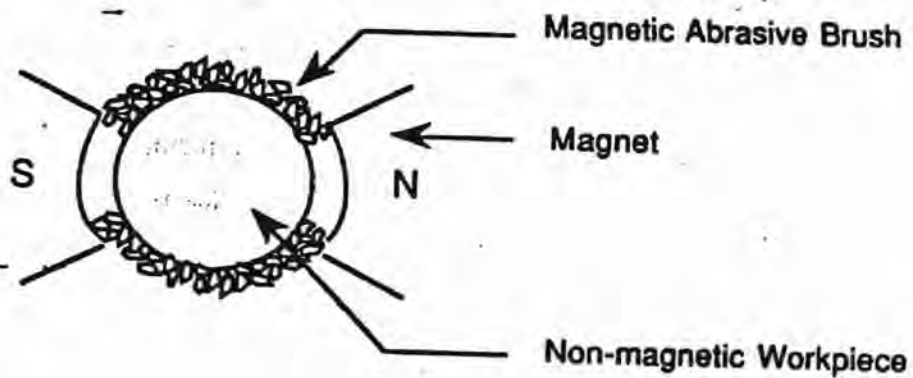


Figure 4.1.2.1 Schematic of the magnetic abrasive finishing process

#### 4.1.2 MAGNETIC FIELD ASSISTED POLISHING OF $\text{Si}_3\text{N}_4$ ROLLERS

In the magnetic abrasive finishing process, a magnetic-abrasive agglomerate is used. The finishing pressure is exerted by the magnetic field. Figure 4.1.2.1 is a schematic of the magnetic abrasive finishing process. The magnetic abrasives are linked to each other magnetically between the magnetic poles N and S along the lines of magnetic force, forming flexible magnetic abrasive brushes. A cylindrical workpiece, such as a  $\text{Si}_3\text{N}_4$  roller, is clamped to the chuck of the spindle providing a rotary motion. Axial vibratory motion is introduced in the magnetic field by the oscillating motion of the magnetic poles. The rollers can be magnetic or non-magnetic. Hence, this technique is equally applicable to both steel and ceramic rollers. The process is highly efficient and the removal rate and finish depend on the workpiece circumferential speed, magnetic flux density, working clearance, workpiece material, size of the magnetic abrasive conglomerate, including the type of abrasive used, its grain size and volume fraction in the conglomerate. The size of the magnetic abrasive conglomerates is about 50 to 300 mm and the abrasives are in the 1 to 25 mm range.

Typical conditions used for finishing of  $\text{Si}_3\text{N}_4$  rollers follow:

Machine Tool	: 1.5 hp Hardinge Precision Lathe,
Workpiece size	: 5-15 mm diameter x 120 mm long cylindrical roller
Polishing capacity	: 45 mm long
Lathe speed	: 500, 1,000, and 2,000 rpm (corresponding to 20, 40, and 80 m/sec.)
Current density	: 0.5, 1, and 2A
Magnetic field density	: 0.5-1.2 T
Vibrational frequency	: 15 Hz,
Vibrational amplitude	: 0.06 in,
Magnetic pressure	: 0-40 KPa
Magnetic core	: 0.16% carbon steel
Magnetic abrasives	: B <sub>4</sub> C, SiC, and Cr <sub>2</sub> O <sub>3</sub> abrasive (5-10 μm) in a matrix of iron particles (100-400 μm)
Lubricant	: dry, oil, zinc stearate

## 4.2 SILICON NITRIDE WORKMATERIAL

Silicon nitride has been at the forefront of developments in high-strength, high-temperature materials, because of the possibility of its use in the development of more efficient ceramic gas turbine engine that can run at temperatures far beyond the capability of conventional superalloys currently used [Katz, 1985, 1983, 1989, 1994; McColm, 1983]. In addition, silicon nitride is also being used as balls and rollers in hybrid bearing applications, where higher stiffness, higher precision, higher specific weight, higher wear resistance, higher speed capability, and higher temperature capability are some of the considerations.

Silicon nitride is predominantly a covalent (75 %) solid built up of  $\text{Si}_3\text{N}_4$ -tetrahedra joined in a three dimensional network by sharing corners [Katz, 1985, 1983, 1989, 1994; McColm, 1983].  $\beta$ - $\text{Si}_3\text{N}_4$  has a hexagonal structure. Although it was originally believed that an  $\alpha$ -form exists that form was found to be a defective silicon nitride containing one oxygen for every 30 nitrogen atoms, and is therefore regarded as an oxynitride. Silicon nitride can be processed by sintering, reaction bonding, hot-pressing, and HIP'ing. Ytria or magnesia are the common sintering aids. During the high-temperature hot-pressing of silicon nitride with, small amounts of MgO addition, a complex glassy phase is found to form at the grain boundaries. It is primarily a magnesium silicate modified by Ca, Fe, Al, and other impurities initially present in  $\text{Si}_3\text{N}_4$ . At temperatures around 1100 °C, grain boundary sliding occurs under load. Additions of yttria to  $\text{Si}_3\text{N}_4$ , generally leads to a crystallization in the glassy phase at the grain boundaries instead of pure glassy phase with MgO. However, the oxidation resistance of this material was found to be inferior to those with MgO additions [Katz and Gazza, 1983]. For this reason, MgO added  $\text{Si}_3\text{N}_4$  is increasingly used in high temperature applications.

Hot-pressed  $\text{Si}_3\text{N}_4$  is produced either by conventional uniaxial hot-pressing or HIP'ing. One starts with an  $\alpha$ - $\text{Si}_3\text{N}_4$  powder that has a densification aid, such as MgO,  $\text{Y}_2\text{O}_3$  or  $\text{SiBeN}_2$ . Under pressures of 14 MPa and temperatures in the range of 1650 °C to 1750 °C, some of the  $\alpha$ - $\text{Si}_3\text{N}_4$  reacts with the additive and a thin layer of  $\text{SiO}_2$  is formed that coats each particle of  $\text{Si}_3\text{N}_4$ , producing a liquid silicate in which the remaining  $\alpha$ - $\text{Si}_3\text{N}_4$  dissolves and re-precipitates as elongated  $\beta$ - $\text{Si}_3\text{N}_4$  grains. On completion of the  $\alpha$  to  $\beta$  transformation, the elongated  $\beta$ -grains are surrounded with a residual silicate oxynitride grain boundary phase. The elongated nature of these grains, that are typically 0.5 to 4  $\mu\text{m}$ , gives hot-pressed  $\text{Si}_3\text{N}_4$  its high strength.

The apparent limitations of the hot-pressed  $\text{Si}_3\text{N}_4$  are due to the nature of the grain boundary phase and not intrinsic to the  $\text{Si}_3\text{N}_4$  [McColm, 1983]. So, attention was focussed on controlled modification of the grain boundary, such as grain boundary crystallization in hot-pressed  $\text{Si}_3\text{N}_4$  with  $\text{Y}_2\text{O}_3$  additions. While such a modification was found to provide higher strength at both room and elevated temperature (1400 °C) as well as better creep and oxidation resistance, this material was found to suffer from an intermediate temperature oxidation (1000 °C) problem. This material is also found to be difficult to finish by grinding and polishing. Consequently, complex parts made of this material are rather expensive, once again shifting the emphasis to  $\text{Si}_3\text{N}_4$  with MgO additions.

Relatively pure  $\text{Si}_3\text{N}_4$  material was found to be elastic to fracture exhibiting practically no plasticity. This is understandable in view of the predominantly non-ionic nature of bonding in this material. Impurities in the material seem to enter into the grain boundary glassy phase and lower its viscosity. Thus, the high-temperature mechanical properties of hot pressed  $\text{Si}_3\text{N}_4$  appear to be controlled by impurities and, more likely, the hot-pressing aid. Grain boundary sliding is the suggested mechanism for subcritical crack growth, plasticity, and creep.

In this investigation, HIP'ed silicon nitride balls (NBD 200) acquired from Norton Ceramics were used. Table 4.2.1 gives a summary of some of the properties of this material. Figure 4.2.1 is a scanning electron micrograph of a polished and etched (with HF) silicon nitride showing interlinked columnar  $\beta$ -silicon nitride grains.

#### 4.3 ABRASIVES USED:

The boron carbide, silicon carbide, and chromium oxide used in this investigation, were obtained from Norton Co. Figures 4.3.1 to 4.3.3 show scanning electron micrographs of silicon carbide, boron carbide and chromium oxide abrasives, respectively. The lower magnification shows an aggregate sample and higher magnification shows details of the abrasive. It can be seen that both boron carbide and silicon carbide have sharp fracture facets while the chromium oxide abrasive appears as an agglomerate of fine particles. Later in the results, the wear debris of all the three abrasives are compared to determine the severity of abrasion. Table 4.3.1 shows the hardness of various abrasives. It can be noticed that the hardnesses of silicon nitride and chromium oxide are in the same range, while boron carbide is the hardest abrasive used in the present investigation.

Table 4.2.1 Properties of HIP'ed silicon nitride used in the present investigation

Tensile Strength, MPa	400
Flexural Strength, MPa	800
Compressive Strength, MPa	
Fracture Toughness, MPa-m <sup>1/2</sup>	4.1
Density, gm/cc	3.3
Elastic Modulus, GPa	320
Poisson's Ratio	0.26
Hardness Vickers (10 Kg), GPa	16.6
Thermal Expansion Coefficient, 10 <sup>-6</sup> /°C	2.9
Thermal Conductivity, W/m-K	29.3
Maximum Use Temperature, °C	1000

Table 4.3.1 Hardness values of the abrasives used [Schnieder, 1991]

Material	Density g/cc	Hardness, MPa	Melting Point °C
Diamond (C)	3.5	>5000	4500°
Boron Carbide (B <sub>4</sub> C)	2.5	2800 - 3500	2450
Silicon Carbide (SiC)	3.2	2300 - 2700	2400
Silicon Nitride (Si <sub>3</sub> N <sub>4</sub> )	3.2	1600 - 2200	1900
Chromium Oxide (Cr <sub>2</sub> O <sub>3</sub> )	5.2	1600 - 2000	2265
Aluminium Oxide (Al <sub>2</sub> O <sub>3</sub> )	4.0	1600 - 2000	2040

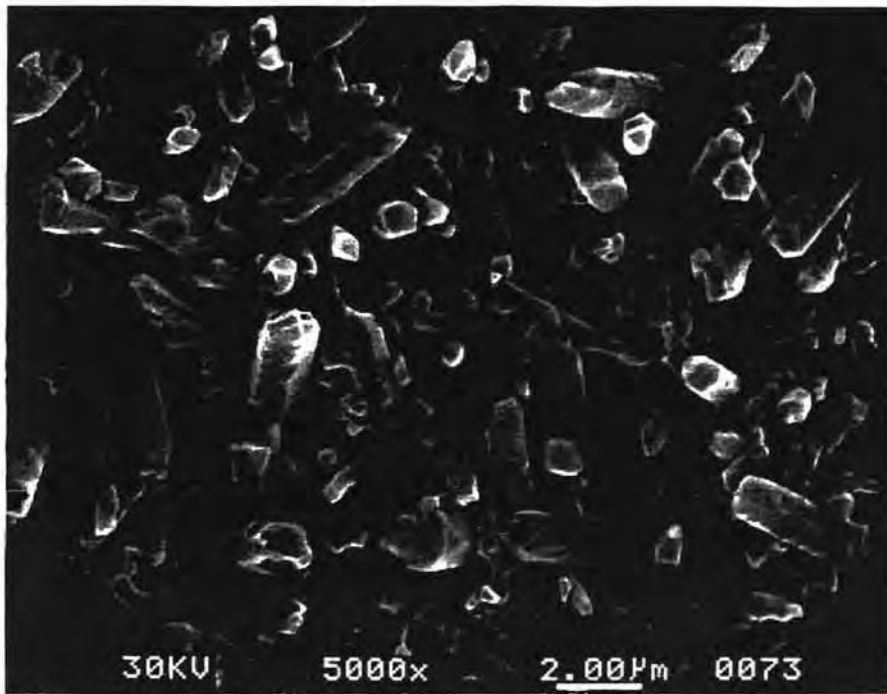


Figure 4.2.1 SEM micrograph of a polished and etched silicon nitride showing internal linked columnar beta-silicon nitride grains



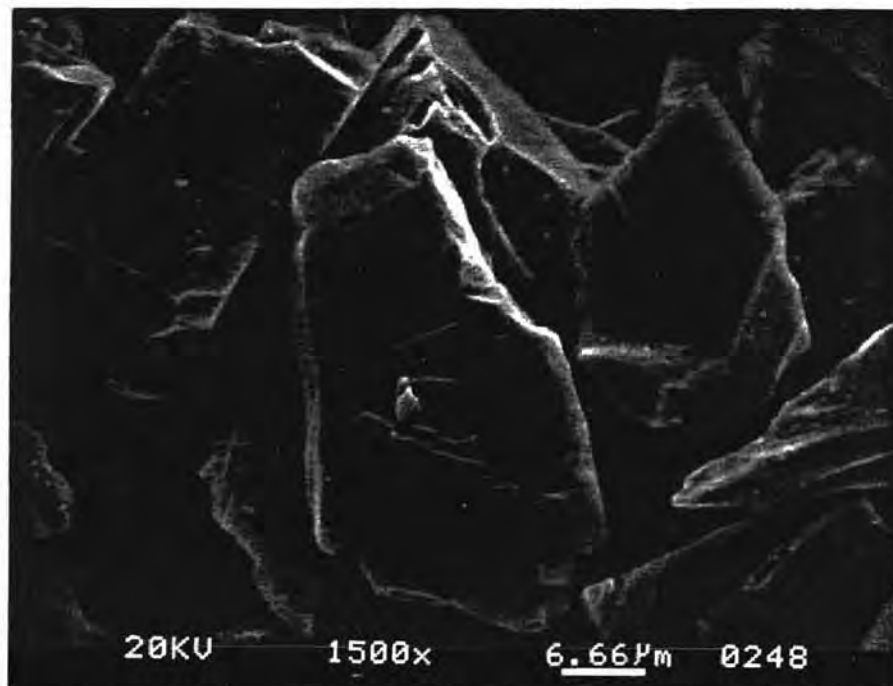
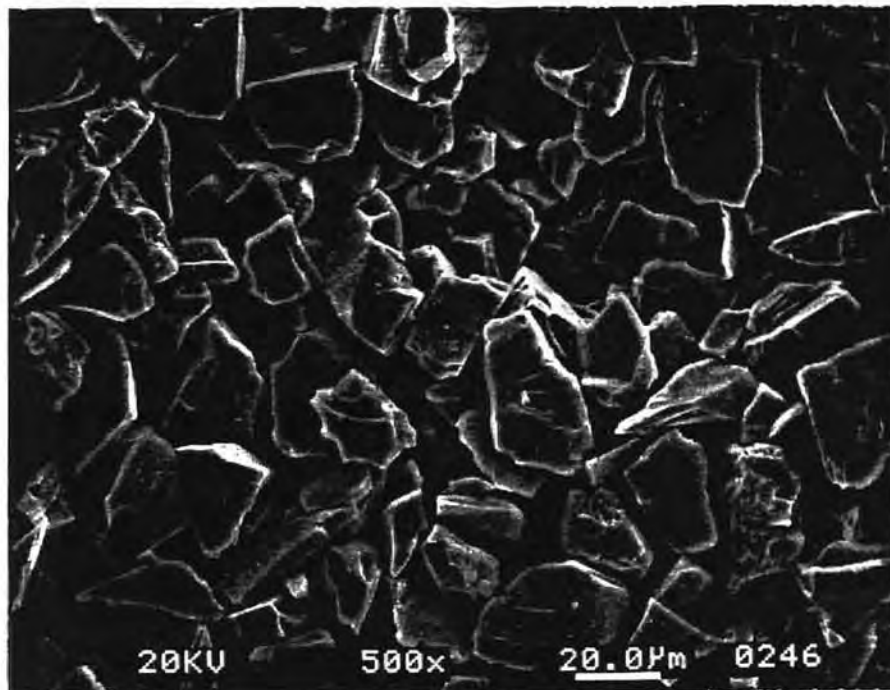


Figure 4.3.1 SEM micrograph of as received silicon carbide abrasives

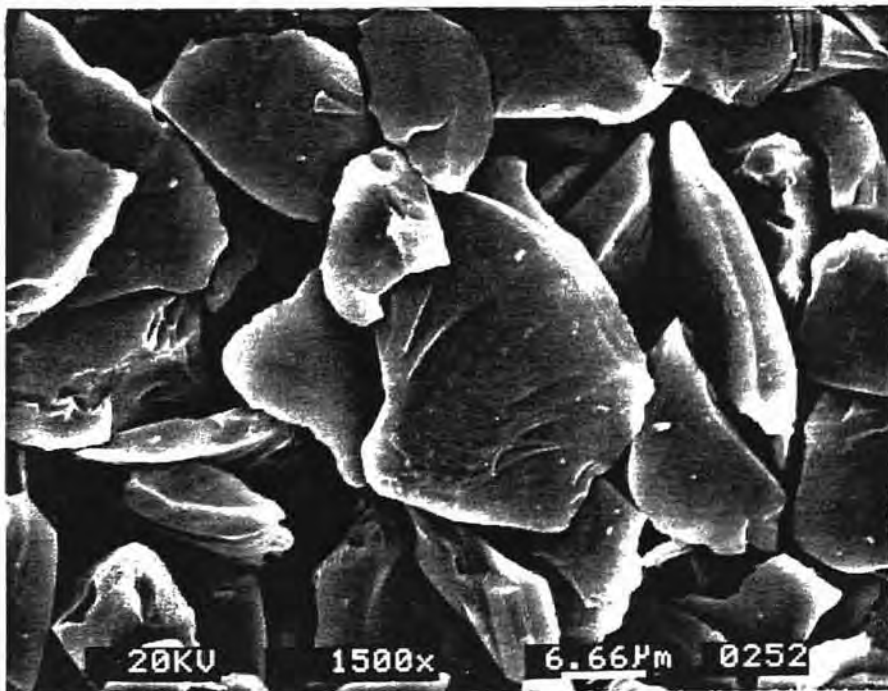
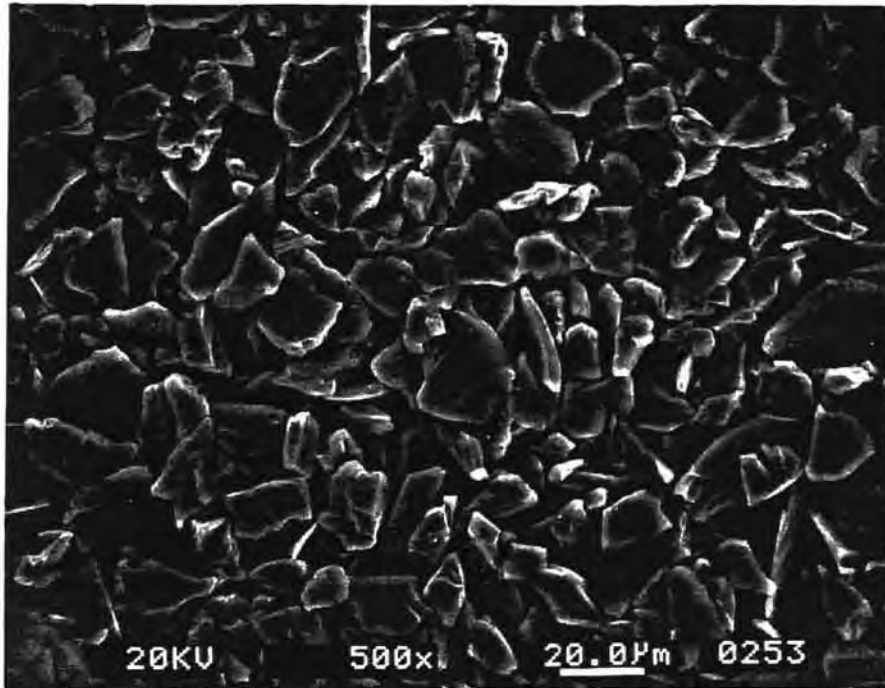


Figure 4.3.2 SEM micrograph of as received boron carbide abrasives

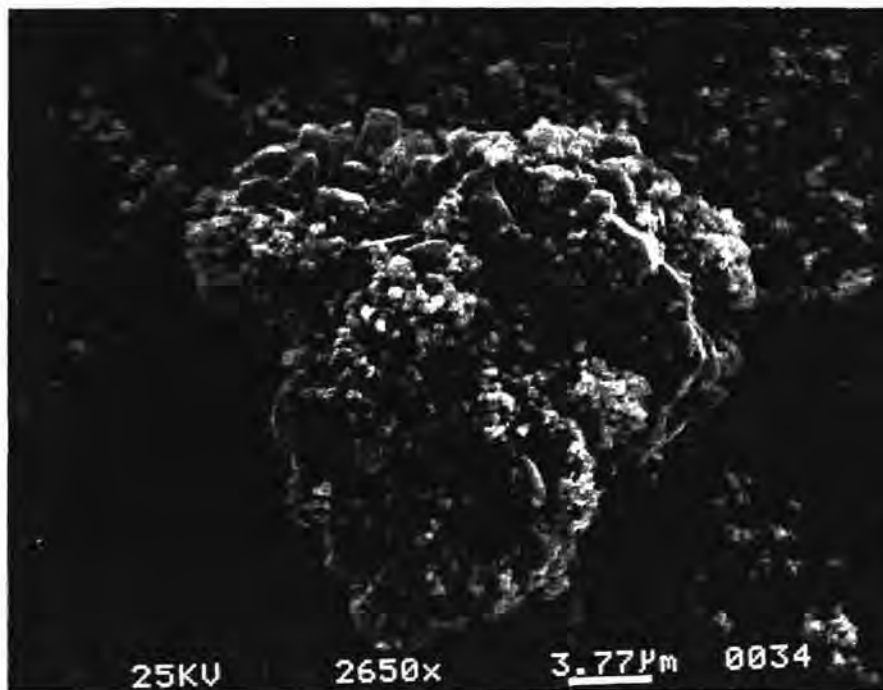
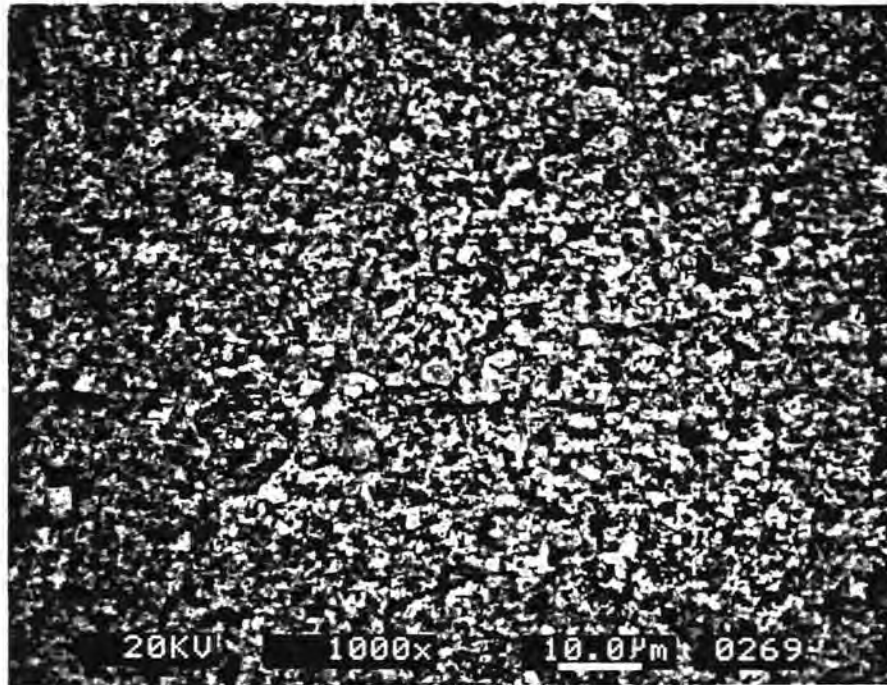


Figure 4.3.3 SEM micrograph of as received chromium oxide abrasives

Carbide abrasives are capable of undergoing oxidation, resulting in the formation of thin films of oxide on the abrasives. As a result, surfaces of silicon carbide are covered with silica, which is the same oxidation product as that of silicon nitride. Boron carbide abrasive on the other hand, contains thin layer of oxide, which may participate in the chemical reaction during polishing.

## CHAPTER 5

### THERMODYNAMIC AND HEAT TRANSFER ANALYSES

In this chapter, a thermodynamic analysis, namely, is conducted at the flash temperatures generated in polishing of silicon nitride with different abrasives, to determine the various compounds that can be formed. This is followed by the modeling of the flash temperatures generated at the real areas of contact. Using the model recently developed, for a moving disk heat source, by Hou and Komanduri [1994] and Jaeger's solutions for this problem, flash temperatures generated in magnetic abrasive finishing are estimated. The effect of various process conditions, such as pressure exerted by the abrasive on the workmaterial and rotational speed of the workmaterial on the flash temperature generated, are considered here. Finally, a phase equilibrium study is made to consider the various phases that may form between the silicon nitride workmaterial and the abrasives. This study should facilitate the identification of different compounds that may form at a given temperature.

#### 5.1 THERMODYNAMIC ANALYSIS

The tribological and tribochemical behavior of silicon nitride, examined in the literature, suggest that oxidation is the main reaction mechanism. However, in the case of silicon nitride, the action of the abrasive in the reaction process is not as well understood as the case of alumina. Ammonia formation was detected during the wet grinding of silicon nitride suggesting that oxidation was in progress. No evidence was shown of the abrasive actually taking part in the reaction.

Oxidation kinetics studies reported in the literature shows that silicon nitride gets oxidized in air [Munro and Dapkunas, 1993; Cubicciotti and Lau, 1978 and 1979; Singhal, 1976 (a); Kiehle et al., 1975; Echeberria and Castro, 1990; Lange, 1979; Clarke and Lange, 1980; and Falk and Engstrom, 1991], and humidity helps in enhancing the process. Experimental results indicate that the activation energy required was 375 KJ/mole as compared to 488KJ/mole in the case of air [Singhal, 1976 (b); Contet et al., 1987; Sato et

et al., 1991 and Xu et al., 1994]. As the relative humidity increases, the oxidation also increases. The activation energy required in the presence of water was found to be 108 KJ/mole [Xu et.al, 1994].

A Gibb's free energy analysis was performed, keeping the above factors in mind, to determine the most effective environment for chemo-mechanical polishing. The results indicate that water not only enhances oxidation but also dominates the process until 700 °K, beyond which oxidation is favoured in the presence of air. The various steps involved in the calculations of Gibbs free energy are :

1) Determine the enthalpy of the reaction at 298 °K

$$\Delta H^{\circ}_{298} = \Sigma \Delta H^{\circ}_{298 \text{ of the products}} - \Sigma \Delta H^{\circ}_{298 \text{ of the reactants}}$$

2) Determine the entropy of the reaction at 298 °K

$$\Delta S^{\circ}_{298} = \Sigma \Delta S^{\circ}_{298 \text{ of the products}} - \Sigma \Delta S^{\circ}_{298 \text{ of the reactants}}$$

3) Determine the heat capacity of the reactants

$$\Sigma C_p = \Sigma C_p \text{ of the products} - \Sigma C_p \text{ of the reactants}$$

4) Determine  $\Delta S^{\circ}_T$  according to the equation

$$\Delta S^{\circ}_T = \Delta S^{\circ}_{298} + \int_{298}^T \frac{\Delta C_p dT}{T}$$

5) Determine  $\Delta H^{\circ}_T$  according to the equation

$$\Delta H^{\circ}_T = \Delta H^{\circ}_{298} + \int_{298}^T \frac{C_p dT}{T}$$

6) Finally, evaluate  $\Delta G^\circ_T$  according to the equation

$$\Delta G^\circ_T = \Delta H^\circ_T - T\Delta S^\circ_T$$

Table 5.1.1 gives the values of enthalpies, entropies, and specific heats obtained from the literature [Kubashevski and Block, 1979]. Table 5.1.2 gives the Gibb's free energy values obtained for the case of air and water, upto 900 °K. From Table 5.1.2, it can be seen that water is effective until 700 °K and air is effective above that. Therefore, chemomechanical polishing can be done in water at much lower temperatures. This result is used in the experimental work in which water is used as the medium of polishing.

Table 5.1.1 : Thermodynamic Values of Compounds in the Oxidation of  $\text{Si}_3\text{N}_4$

Substance	$\Delta H_{298}^0$ (Kcal)	$\Delta S_{298}^0$ (Kcal/mole.) °K	$C_p = a + b.T + c.T^2$ cal/mol.°K		
			a	b (x 10 <sup>+3</sup> )	c (x 10 <sup>-5</sup> )
$\text{Si}_3\text{N}_4$	-178	27.0	16.86	23.6	0
$\text{H}_2\text{O}$	-57.795	45.1	7.17	2.56	0.08
$\text{SiO}_2$	-217.6	9.91	4.28	21.06	0
$\text{NH}_3$	-10.98	46.05	7.11	6.00	-0.37
$\text{O}_2$	0	49.0	7.16	1.0	-0.40
$\text{N}_2$	0	45.77	6.83	0.9	-0.12

Table 5.1.2 Values of Gibb's Free Energy of Formation  
(from calculations)

<p>SILICON NITRIDE OXIDATION IN AIR</p> <p><math>2 \text{Si}_3\text{N}_4 + 6\text{O}_2 \rightarrow 6 \text{SiO}_2 + 4\text{N}_2 \uparrow</math></p> <p><math>\Delta G_T^0 = 208267 - 18.32 T \cdot \ln.T - 365 T - 0.16 \cdot 10^{-3} \cdot T^2 + 1.74 \cdot 10^{-5} \cdot T^{-1}</math></p>
--

Table 5.1.2 Continued.....

Gibb's Free Energy at different Temperatures	$\Delta G_{300^\circ\text{K}}^0$	$\Delta G_{400^\circ\text{K}}^0$	$\Delta G_{500^\circ\text{K}}^0$	$\Delta G_{600^\circ\text{K}}^0$	$\Delta G_{700^\circ\text{K}}^0$	$\Delta G_{800^\circ\text{K}}^0$	$\Delta G_{900^\circ\text{K}}^0$
Values obtained KCal/mol.	67.9	18.7	- 30.7	-80.8	- 131	- 181	- 232
<b>HYDROTHERMAL OXIDATION OF SILICON NITRIDE</b>  $\text{Si}_3\text{N}_4 + 6\text{H}_2\text{O} \rightarrow 3\text{SiO}_2 + 4\text{NH}_3\uparrow$  $\Delta G_T^0 = -169073 + 18.6 T \cdot \ln T + 156.47 T - 22.61 \cdot 10^{-3} \cdot T^2 + 0.98 \cdot 10^{+5} \cdot T^{-1}$							
Gibb's Free Energy at different Temperatures	$\Delta G_{300^\circ\text{K}}^0$	$\Delta G_{400^\circ\text{K}}^0$	$\Delta G_{500^\circ\text{K}}^0$	$\Delta G_{600^\circ\text{K}}^0$	$\Delta G_{700^\circ\text{K}}^0$	$\Delta G_{800^\circ\text{K}}^0$	$\Delta G_{900^\circ\text{K}}^0$
Values obtained KCal/mol.	- 147	- 138	- 129	- 121	- 113	- 105	- 97

## 5.2 HEAT TRANSFER ANALYSIS

The temperatures generated at the contact points are crucial in the chemo-mechanical polishing. They affect the rates of reactions occurring at the contacting interface and bring additional routes of reaction into play. There are two components to the interface temperature. The first one is the bulk temperature, which is the average temperature of the surface layers of the specimen. The second one is the flash temperature, which is the temperature reached by the individual contact points between the abrasive and the workmaterial [Gee and Butterfield, 1993].

Measurement of the temperatures in the vicinity of the contact points during polishing is difficult and not practicable in most situations. Analytical work performed by previous authors, however, concentrates on metals in which plastic deformation and junction growth at the contact asperities are considered [Archard, 1959; and Ashby et al.,



1991]. The same analysis cannot be used for ceramics owing to their brittle nature and lack of junction growth. Therefore, a mathematical analysis was performed in which the flash temperatures developed at the contact surfaces are determined.

#### 5.2.1. FLASH TEMPERATURE DETERMINATION

A moving disc heat source model was used in the present investigation for the calculation of flash temperatures at the real areas of contact between the abrasive and the workmaterial. In this model, the abrasive particles sliding over the workmaterial generates heat which in turn is dissipated into the surrounding material. Hou and Komanduri [1994] have developed a mathematical analysis for the calculation of flash temperatures generated in a moving disk heat source. In this investigation, their analysis was used for the calculation of the flash temperatures generated in magnetic abrasive finishing of silicon nitride rollers.

Temperature distributions in the polishing of silicon nitride rods were studied using the abrasive contact approach. Abrasives contact the surface with a certain velocity during polishing which raises the workpiece temperature due to frictional energy generated. This energy is used to calculate the flash temperatures at the contact points. The amount of heat generated can be calculated by the frictional energy. The contact area between the abrasive and the work material forms the heat source.

The present problem is the estimation of heat generated during polishing of  $\text{Si}_3\text{N}_4$  rod. The rod is rotated in the spindle of a lathe and the magnetic abrasives are held by the magnetic poles. The poles alongwith the abrasives are made to oscillate along the length of the rod during polishing. Abrasives traverse along the length of the rod with sliding velocity, which can be determined by the combination of rotational speed of the rod and the oscillating speed of the abrasives. A magnetic abrasive agglomerate is used in the polishing operation. Often, additional iron powder is mixed with the magnetic abrasive to aid in polishing. The polishing pressure is determined by the strength of the magnet as well as the magnetic abrasive.

Flash temperatures obtained for magnetic abrasive finishing of silicon nitride rollers are in the range of  $1200^\circ\text{C}$  -  $2000^\circ\text{C}$ , for a polishing pressure of 7.5 p.s.i. and rotational speed in the range of 2000- 4000 rpm. The oscillating speed of the pneumatic head was 25 Hz. Flash times were on the order of 1.5- 22  $\mu\text{sec}$ , which are much lower than the time

taken for the adjacent abrasive to travel. From the results obtained it is confirmed that the flash temperatures are not cumulative and the reaction occurs at a nanometer level.

The results also show that the temperatures (flash temperature) developed at the contact point of the abrasive increase as the pressure is increased (see Figure A.1. in Appendix A for details). As the rotational speed of the  $\text{Si}_3\text{N}_4$  rod is increased, the temperatures developed in the work piece also increases (see Figure A.2. in Appendix A for details). However, the length of the heat source did not have any effect on the temperature rise. This is true, because, the rise in temperature was mainly a function of sliding velocity and polishing pressure and is independent of the length of travel of the abrasives. Variations in the amplitude and frequency for the same reason did not have any effect on the flash temperatures. The volume fraction of the iron powder had an effect owing to the differences in the heat dissipation.

To determine the reaction products in chemo-mechanical polishing of silicon nitride, using different abrasives, the characteristics of the surfaces of these materials have been studied. Predictions are made using the phase diagram study, coupled with the flash temperature analysis regarding the reactions that would proceed during polishing.

### 5.3 PHASE DIAGRAM STUDY

The surface characteristics of silicon nitride workmaterial and the abrasives have been studied in detail. The surface of hot pressed silicon nitride with magnesia as the sintering aid, essentially consists of silica and forsterite (a form of magnesium silicate,  $\text{Mg}_2\text{SiO}_4$ ) at high temperatures. This further reacts with the oxide surfaces of the abrasives. The surfaces of carbide abrasives are also covered with oxide layers of finite thickness. Therefore, the reaction products can be studied from the phase diagrams of the oxide systems formed in each case. The lowest temperatures at which liquids form in the above systems are tabulated. Table 5.3.1 shows the reaction data with oxide abrasives and silicon nitride and Table 5.3.2 shows the reaction data with carbide abrasives and silicon nitride.

Table 5.3.1 Reaction Data Of Oxide Abrasives With Silicon Nitride

Type of Abrasive	Reactants	Melting Temp (°C)	Composition	Ref. Ernest, 1956
MgO	MgO - SiO <sub>2</sub>	1545	35% MgO - 65 % SiO <sub>2</sub>	Fig. 83
Cr <sub>2</sub> O <sub>3</sub>	MgO - Cr <sub>2</sub> O <sub>3</sub>	2100	90% Cr <sub>2</sub> O <sub>3</sub> - 10% MgO	Fig. 81
	Cr <sub>2</sub> O <sub>3</sub> - SiO <sub>2</sub>	1723	96% SiO <sub>2</sub> - 4% Cr <sub>2</sub> O <sub>3</sub>	Fig. 122
	MgO - Cr <sub>2</sub> O <sub>3</sub> - SiO <sub>2</sub>	1546	34.5% MgO - 1% Cr <sub>2</sub> O <sub>3</sub> - 64.5% SiO <sub>2</sub>	Fig. 387
	MgO - Cr <sub>2</sub> O <sub>3</sub> - SiO <sub>2</sub>	1550	39% MgO - 2% Cr <sub>2</sub> O <sub>3</sub> - 59% SiO <sub>2</sub>	Fig. 387
FeO	FeO - MgO	1800	90% FeO - 10% MgO	Fig. 71
	FeO - MgO - SiO <sub>2</sub>	1250		Fig. 363
CaO	CaO - MgO	2300	62% CaO - 38% MgO	Fig. 40
	CaO - Fe <sub>2</sub> O <sub>3</sub>	1200	18% CaO - 82% Fe <sub>2</sub> O <sub>3</sub>	Fig. 46
	CaO - Fe <sub>2</sub> O <sub>3</sub> - SiO <sub>2</sub>	1185	45% of 2CaO. Fe <sub>2</sub> O <sub>3</sub> - 55% of CaO.SiO <sub>2</sub>	Fig. 344
	CaO - SiO <sub>2</sub>	1436	65% SiO <sub>2</sub> - 35% CaO	Fig. 48
	MgO - CaO - SiO <sub>2</sub>	1388-1450		Fig. 278

Table 5.3.1. Continued.....

	MgO - CaO - SiO <sub>2</sub>	1388-1450		Fig. 278
CeO <sub>2</sub>	MgO - CeO <sub>2</sub>	2280		Fig. 82
	CeO <sub>2</sub> - Fe <sub>3</sub> O <sub>4</sub>	1500		Fig. 126
	CeO <sub>2</sub> - Fe <sub>3</sub> O <sub>4</sub>	1500		Fig. 126

Table 5.3.2. Reaction Data Of Carbide Abrasives With Silicon Nitride

Type of Abrasive	Reactants	Melting Temp. (°C)	Composition	Reference
B <sub>4</sub> C	MgO - B <sub>2</sub> O <sub>3</sub>	988	99.2% B <sub>2</sub> O <sub>3</sub> - 0.8 MgO	Davis, 1945
	MgO - B <sub>2</sub> O <sub>3</sub>	1381	53.6% MgO - 46.4% B <sub>2</sub> O <sub>3</sub>	Davis, 1945
	MgO - B <sub>2</sub> O <sub>3</sub>	1366	63.5% MgO - 36.5% B <sub>2</sub> O <sub>3</sub>	Davis, 1945
	MgO - B <sub>2</sub> O <sub>3</sub>	1358	72% MgO - 28% B <sub>2</sub> O <sub>3</sub>	Davis, 1945
	BaO - B <sub>2</sub> O <sub>3</sub> - SiO <sub>2</sub>	≈ 800	53.5% B <sub>2</sub> O <sub>3</sub> - 46.5% SiO <sub>2</sub>	Ernst, 1956 and Babushkin, 1985.
SiC	Same reactions as in the case of MgO abrasive would occur because of the presence of SiO <sub>2</sub> layer on the surface [ Ernst, 1956].			

Formation of liquids or viscous fluids (near liquid regions) can be favorable in the polishing of silicon nitride in achieving a high quality surface with minimal damage. The data collected in this section will be used as a basis for the results obtained from SEM and XRD to determine the reaction mechanisms in each case.

## CHAPTER 6

### RESULTS

The results obtained from the chemo-mechanical polishing of silicon nitride are presented in this section. Silicon nitride rods were polished in air and silicon nitride balls were polished in a water base magnetic fluid to which different abrasives were added. Abrasives mixed with iron powder were used in the Magnetic Abrasive Finishing of rollers. The iron content was kept constant at 60 wt% with all three abrasives.

In the case of Magnetic Float Assisted Polishing of balls, the abrasive content was kept constant at 10% by volume. The results obtained from the magnetic float polishing of balls are discussed in the section 6.1 with all the three abrasives. The first part presents the surface characteristics obtained from the balls from SEM and Talysurf. Analyses of the wear debris from the EDXA and SEM are presented for each abrasive in the second part. The results from the XRD are discussed in the third part.

In section 6.2, the first part discusses the results obtained from the surface characterization studies, during magnetic abrasive finishing of rollers, using chromium oxide abrasives. Results from the wear debris analysis using EDXA and SEM are presented in the second part. Finally, the XRD results obtained in this case are presented in the third part of section 6.2.

#### 6.1 MAGNETIC FLOAT POLISHING OF SILICON NITRIDE BALLS

##### PART I

##### 6.1.1 SURFACE CHARACTERIZATION OF THE BALLS

Figure 6.1.1.1 shows the SEM micrographs of the silicon nitride ball polished with SiC abrasives. The low magnification picture shows the general features obtained as a

result of polishing. At higher magnification, scratches and microcracks produced during the polishing can be noticed. These suggest the severity of the abrasive action.

Figure 6.1.1.2 shows the SEM micrographs of the silicon nitride ball polished using  $B_4C$  abrasives. At low magnification, cracks developed during the polishing can be observed. High compressive stresses developed during the polishing may have resulted in the cracks and causing surface damage to the ball. At higher magnification the scratches produced on the surface can be seen.

Figure 6.1.1.3 shows the SEM micrographs of the ball obtained after it was polished using chromium oxide abrasive. At lower magnifications, reduction in the extent of surface damage can be observed. At higher magnification, it can be seen that the gentle action of the abrasive coupled with chemical action resulted in yielding a surface with minimal surface damage. Surface cracks present in the other cases were almost absent with chromium oxide polished ball. Oxidation of silicon nitride in higher amounts and the subsequent hydrolization of the oxide phase resulted in a smooth surface finish.

Figure 6.1.1.4 shows the surface roughness plots obtained using Talysurf surface measurement technique. The peak to valley surface roughness ( $R_a$ ) value obtained in the case of ball polished with boron carbide was maximum with a value of  $0.20 \mu m$ , while that of obtained with SiC was in the comparable range with  $0.18 \mu m$ , the least being the value obtained was about  $0.04 \mu m$  obtained in the case of ball polished with chromium oxide.

These suggest the severity of action in the case of carbide abrasives. Material removal is by multi grain pullout and cleavage resulting in a rougher surface with extensive surface damage. In the case of chromium oxide, the surface roughness was the least among the three cases suggesting that the material removal is superficial and the surface integrity is maintained causing minimal damage to the silicon nitride ball.

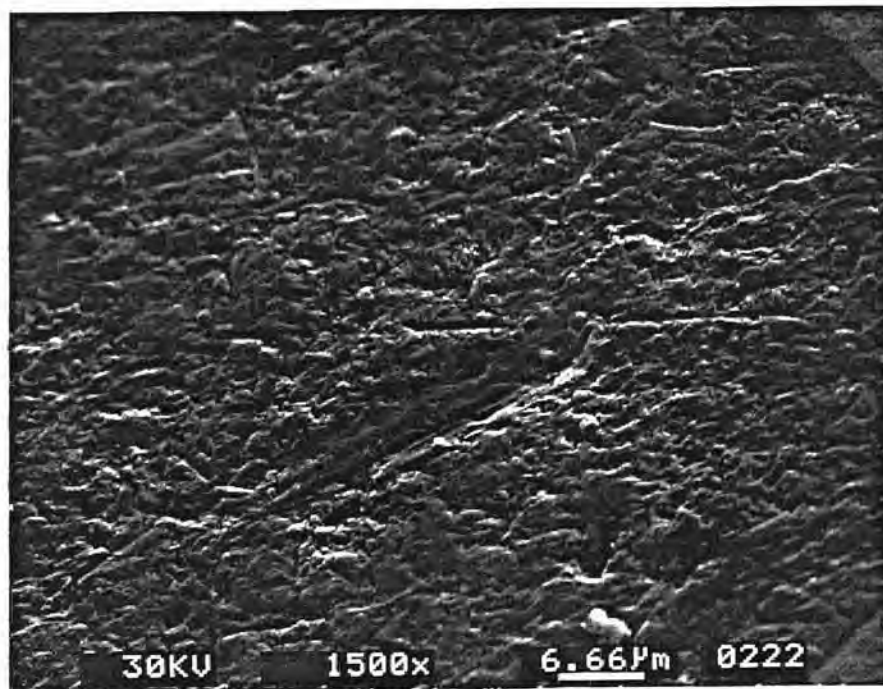
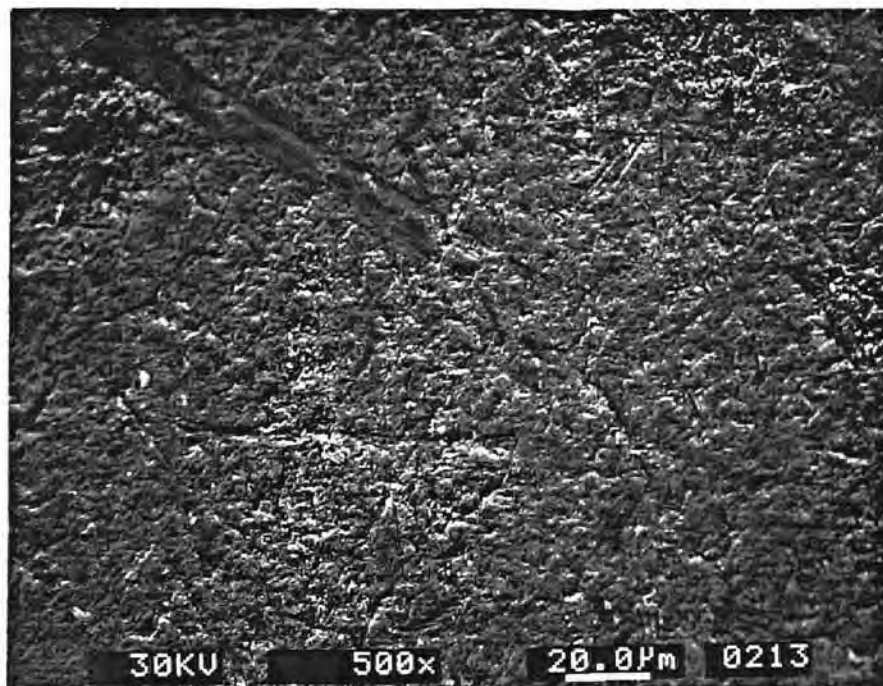


Figure 6.1.1.1 SEM micrographs of the silicon nitride ball polished with silicon carbide abrasives

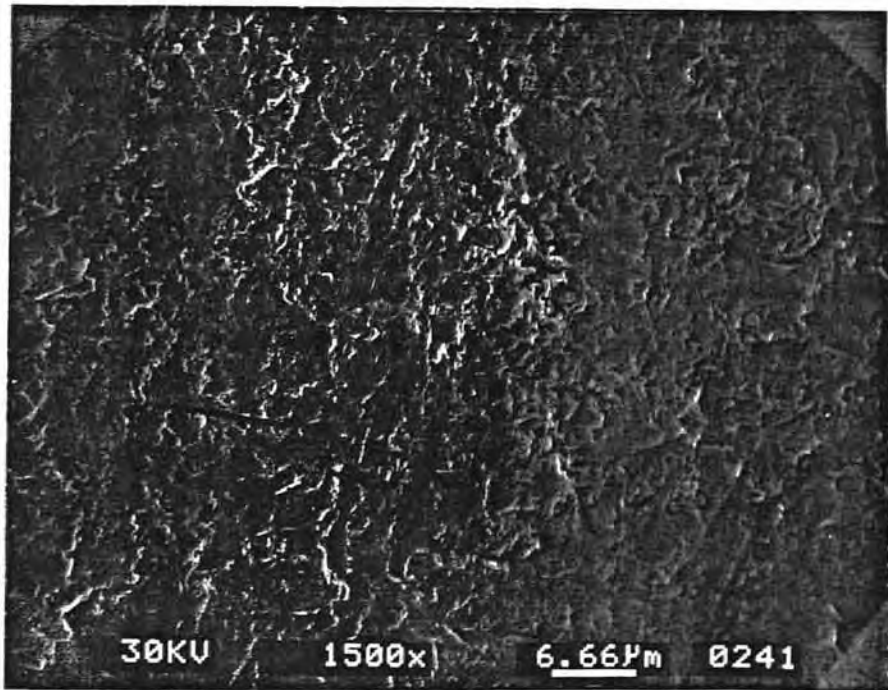
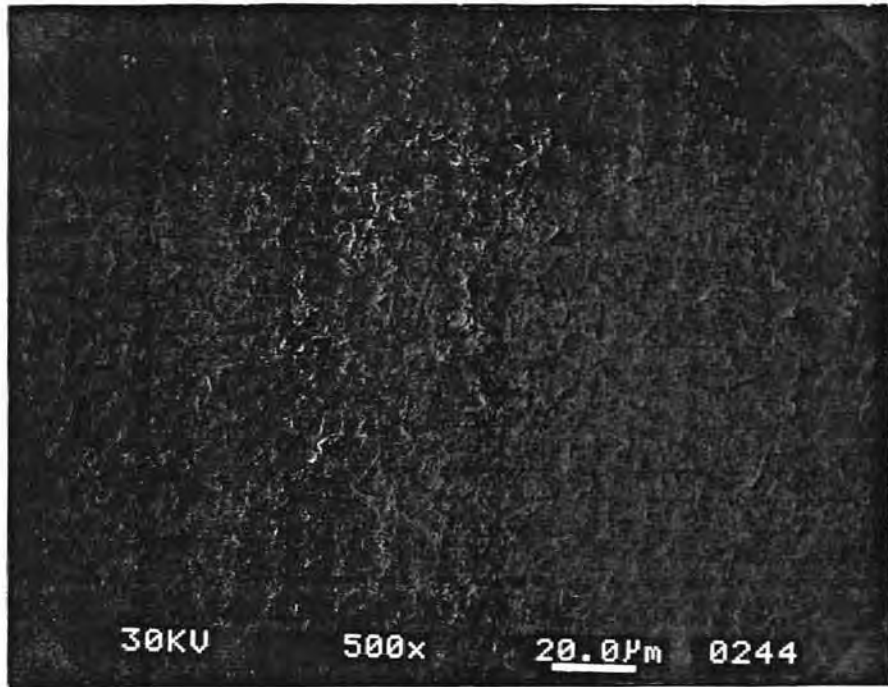


Figure 6.1.1.2 SEM micrographs of the silicon nitride ball polished with boron carbide abrasives



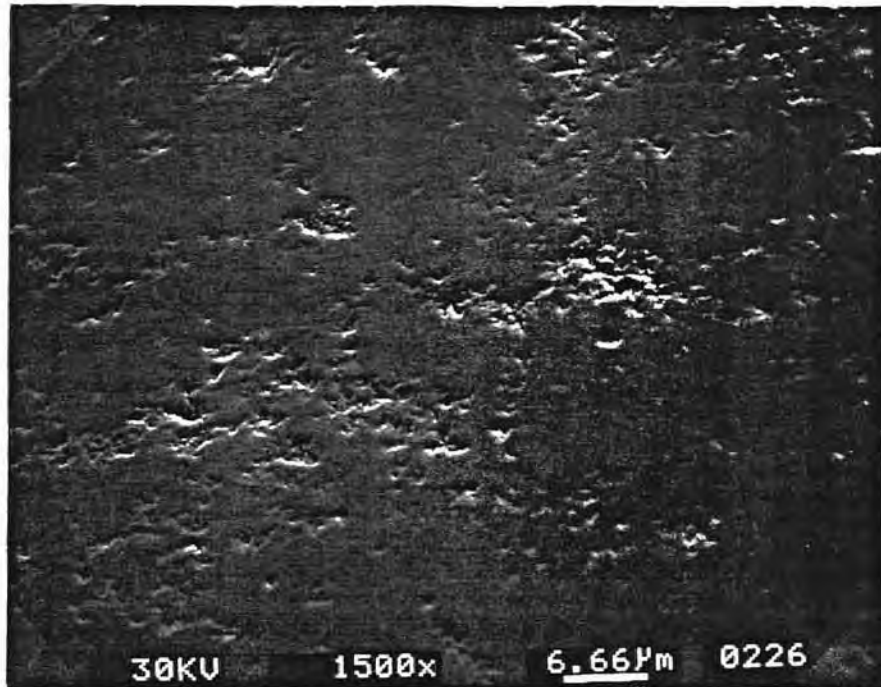


Figure 6.1.1.3 SEM micrographs of the silicon nitride ball polished with chromium oxide abrasives

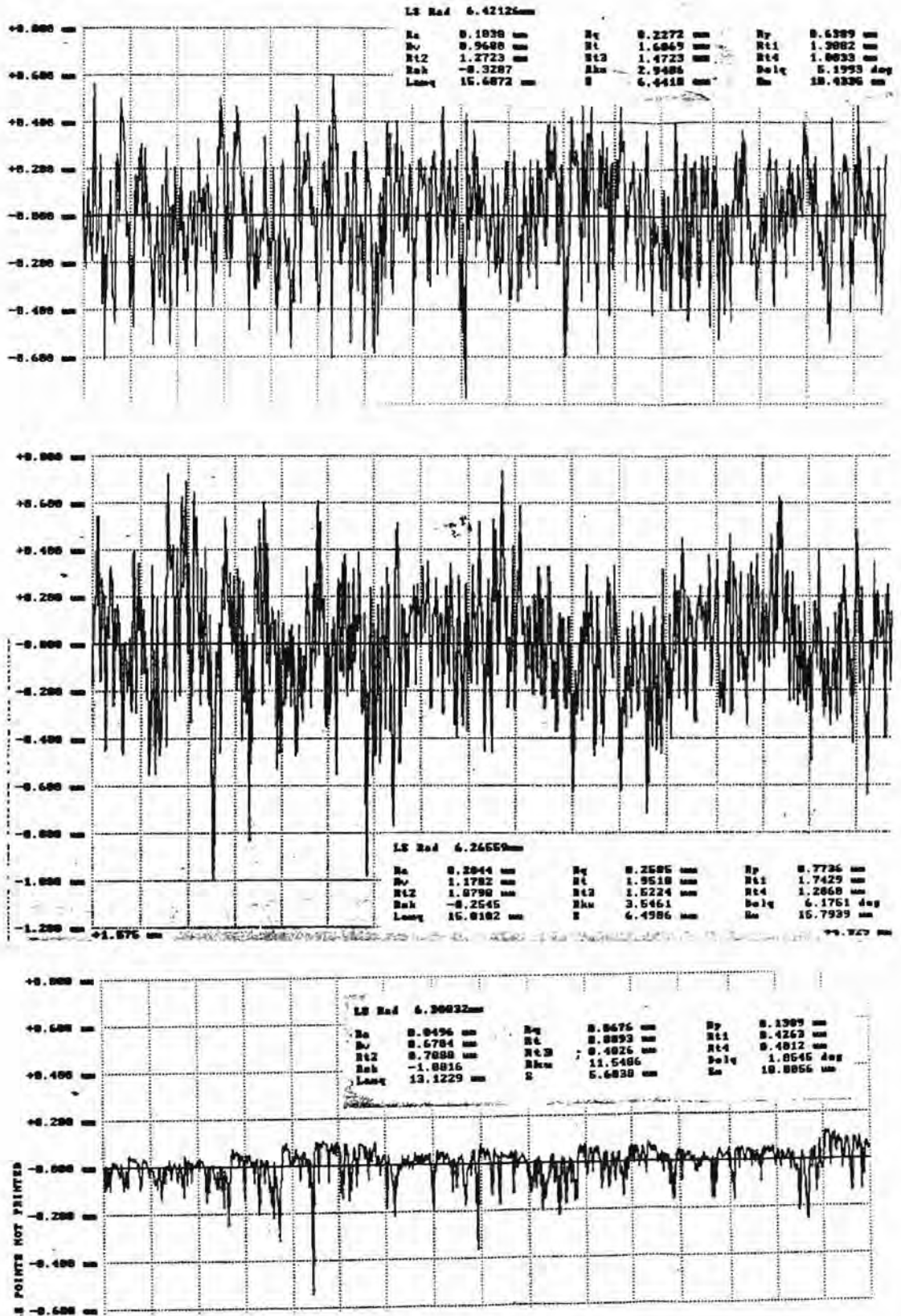


Figure 6.1.1.4 Talysurf surface roughness plots of the silicon nitride ball polished with silicon carbide, boron carbide and chromium oxide

## PART II

### 6.1.2 ANALYSIS OF THE WEAR DEBRIS

Wear debris obtained from polishing was washed in methanol to remove the surfactants adhering to the particles. It was made into a colloidal solution in a ultrasonic cleaner, to remove most of the iron particles. Later they were physically separated by centrifuge to collect the wear particles. The wear debris obtained was dried prior to the examination to reduce the agglomerate content. In the case of Magnetic Abrasive Finishing, the particles were physically separated from relatively coarser iron particles by physical separation.

#### SILICON CARBIDE

Figure 6.1.2.1 shows the SEM micrograph of the wear particle and the EDXA microanalysis obtained during polishing with SiC. The particle size is about 10.0  $\mu\text{m}$  and it had suffered severe mechanical damage. A part of the surface was cleaved during polishing. The EDXA analysis of the wear particle shows the presence of silicon in major amounts and iron in minor amounts. This suggests that the particle may be silicon carbide. Fig 6.1.2.2 shows an SEM micrograph of the wear debris. Particles appear to be a result of particle cleavage. The EDXA analysis shows the presence of silicon. Comparing with the SEM micrographs of unused SiC abrasives, their fracture mode was found to be identical. Thus, they were determined to be SiC particles. This suggests that the abrasives are being subjected to high stresses causing the disintegration of the abrasives. Fig 6.1.2.3 shows another group of wear particles. The EDXA analysis shows the presence of silicon and magnesium. The presence of magnesium suggests the particles are silicon nitride. The presence of Magnesium in appreciable amount suggests that it could be a result of either oxidation or a result of severity of mechanical abrasion. Debris dimensions suggest that severity of action of the abrasives could be a more probable reason. Fig 6.1.2.4 shows the SEM micrograph of a long wear particle. Surface shows that the lateral crack has propagated from the left and removed a chunk of material from the ball. The right end of the particle shows a part of the material still hanging from the main body. The severity of the mechanical abrasion is more clear in this figure. EDXA analysis of the wear particle indicates the presence of silicon and magnesium in appreciable amounts suggesting that cracks propagated deep into the ball causing material removal by ploughing.

SiC wear debris showing  
53N4 particles 7000x 30KV

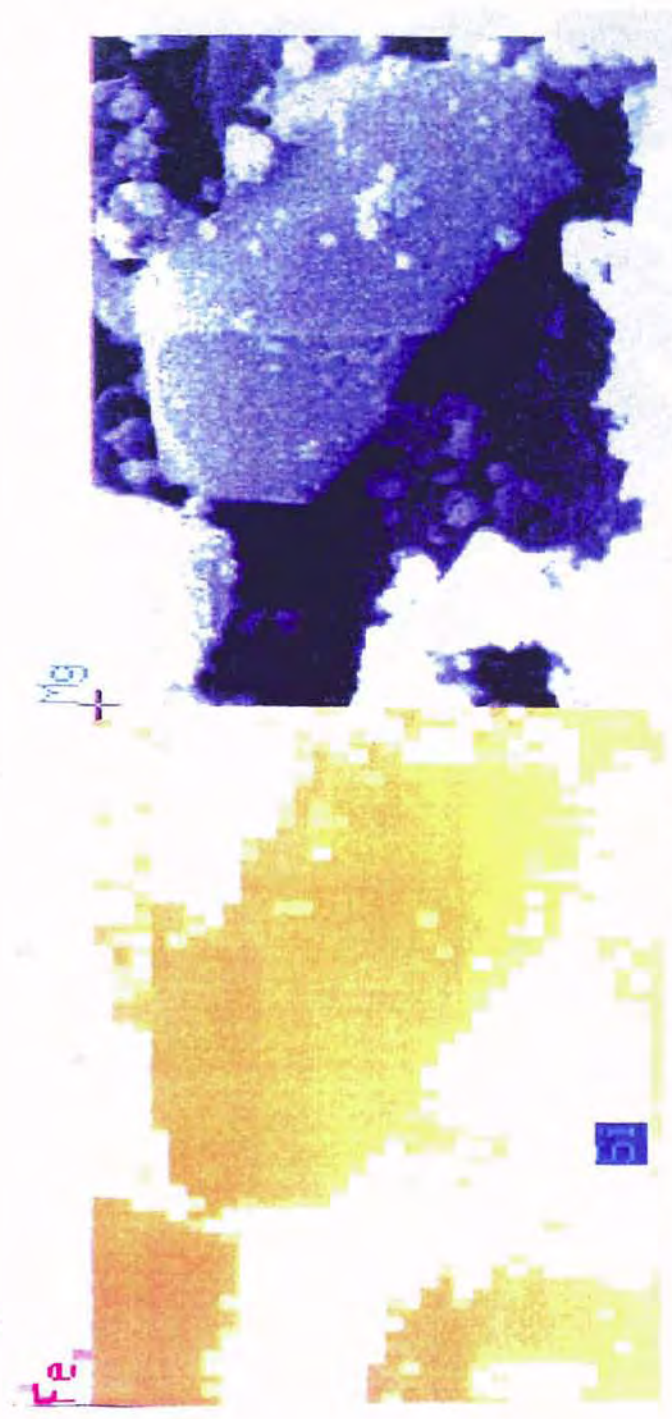


Figure 6.1.2.1 SEM micrographs and EDX analysis of the silicon carbide wear debris showing silicon carbide wear particle

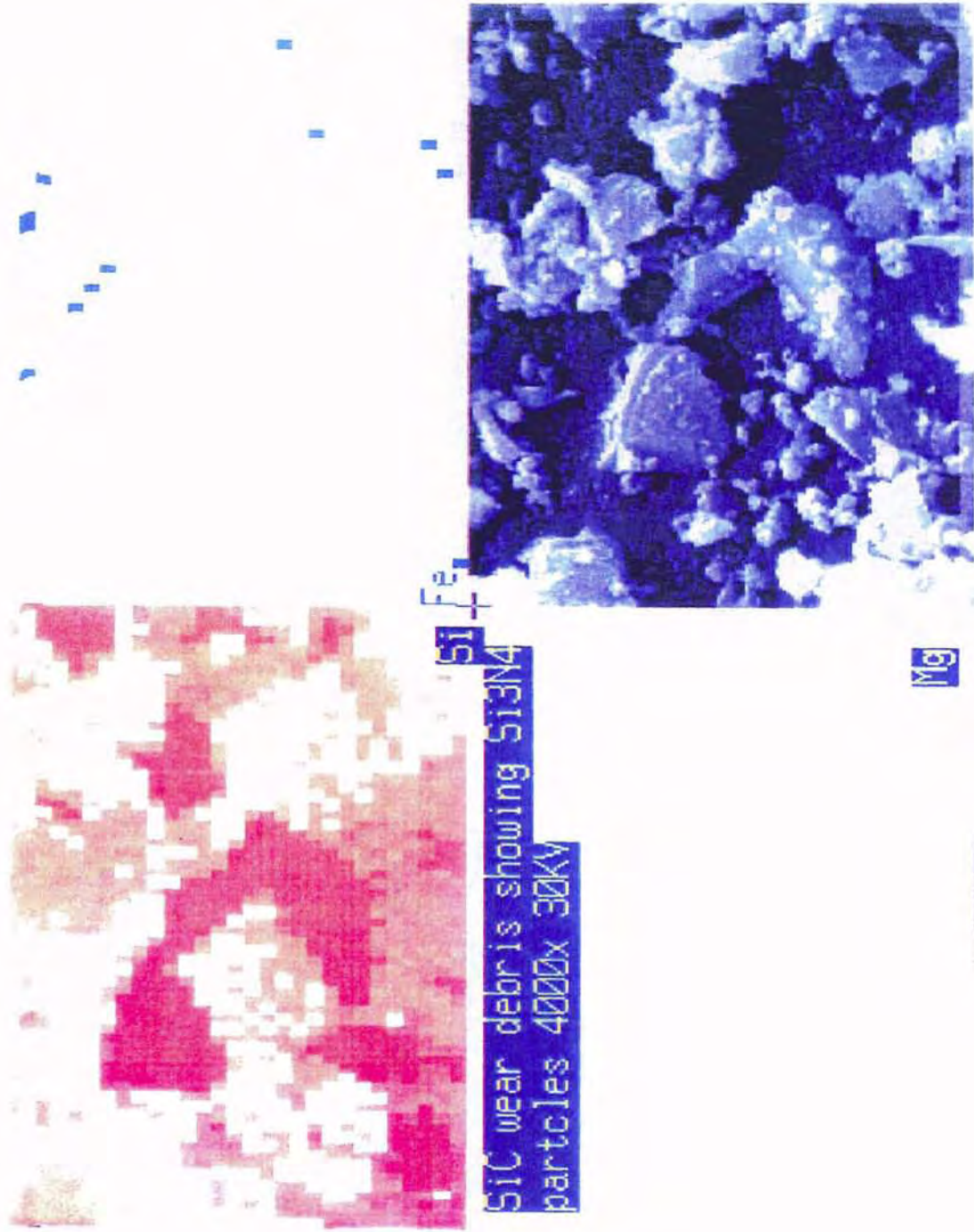


Figure 6.1.2.2 SEM micrographs and EDX analysis of the silicon carbide wear debris showing silicon carbide wear particles

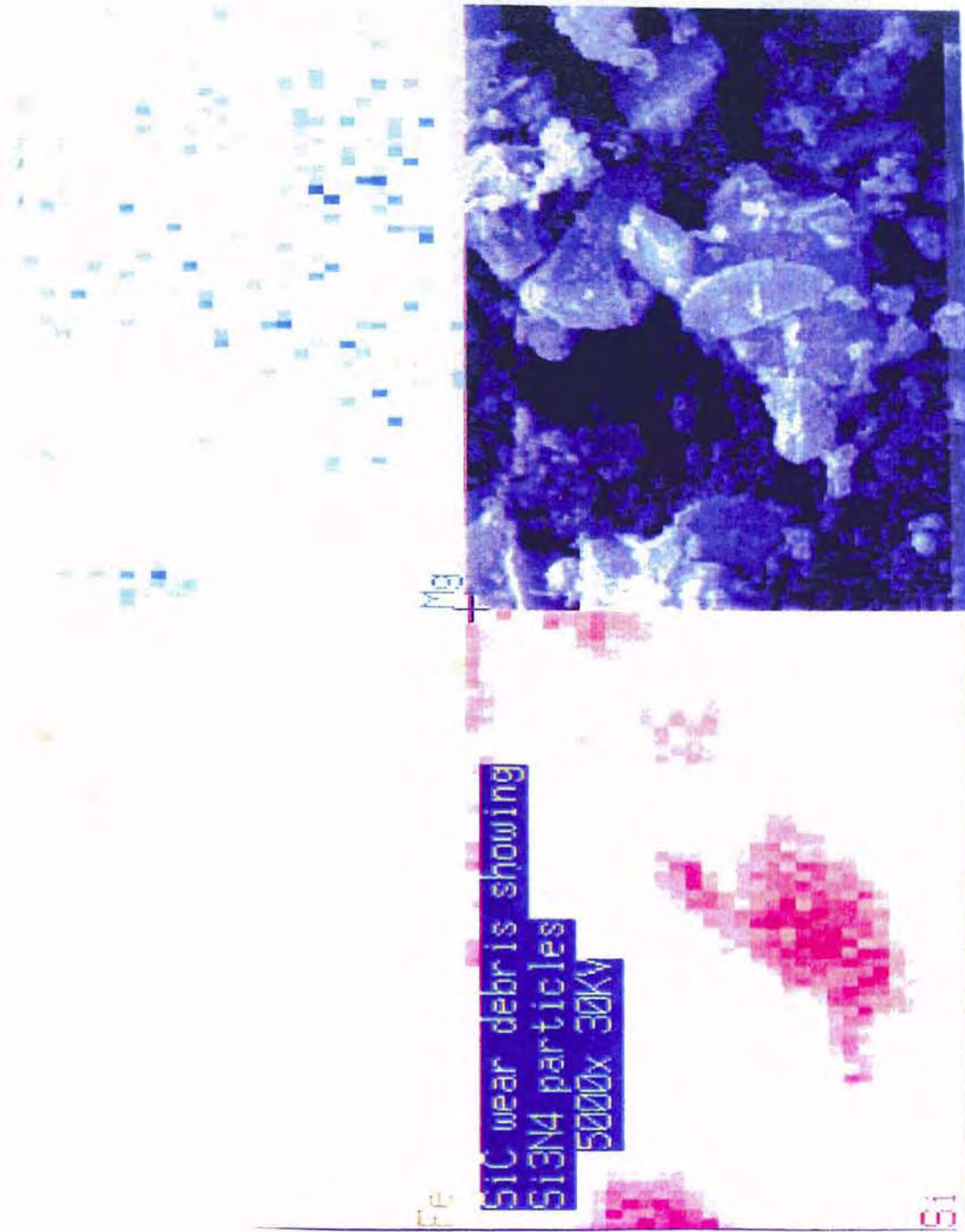


Figure 6.1.2.3 SEM micrographs and EDX analysis of the silicon carbide wear debris showing silicon nitride wear particles

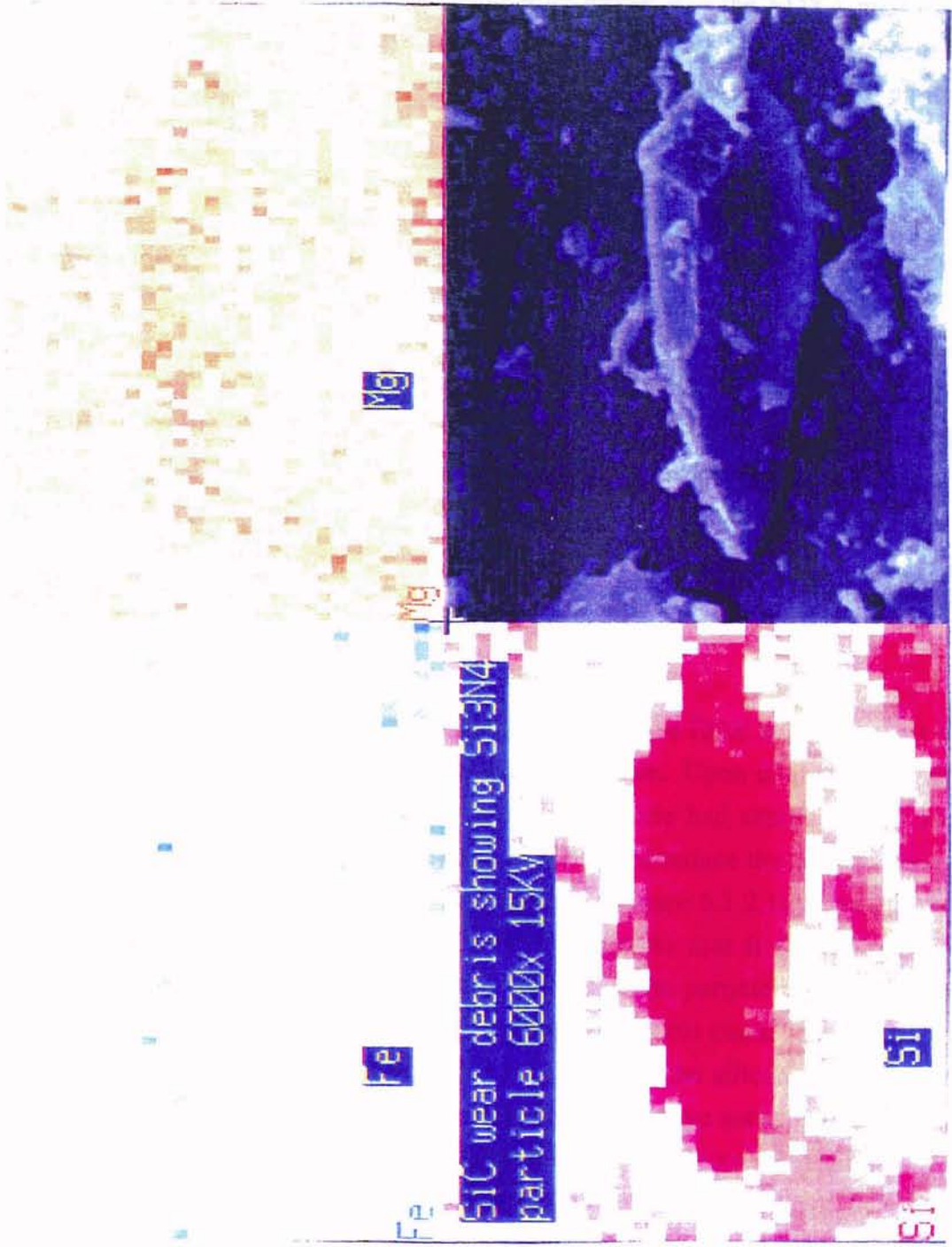


Figure 6.1.2.4 SEM micrographs and EDX analysis of the silicon carbide wear debris showing silicon nitride wear particle

## BORON CARBIDE

Figure 6.1.2.5 shows the SEM micrograph and the EDXA analysis of the wear particle obtained during silicon nitride ball polishing using Boron carbide abrasives. The EDXA analysis indicates the presence of silicon suggesting that the particle is Silicon nitride. Initial scratching marks could be observed on the particle. The particle size was about 15 to 20  $\mu\text{m}$ ., higher than that obtained from SiC wear debris. Figure 6.1.2.6 shows the SEM micrograph and the EDXA analysis of another wear particle obtained during polishing with Boron Carbide. Fracture mirror originating from the subsurface can be observed (Particle is overturned). Cleavage leading to the dislodgement of material in the form of chunk can be observed in this case. Figure 6.1.2.7 shows another particle similar to previous figure showing the propagation of surface cracks developed during the removal of the particle. Figure 6.1.2.8 shows the SEM micrograph of the Boron Carbide abrasives disintegrated during the polishing. EDXA analysis does not indicate the presence of Silicon. This could be a result of the particles (of about 3  $\mu\text{m}$  in size), containing mostly Boron which could not be detected from EDXA.

## CHROMIUM OXIDE

Figure 6.1.2.9 shows the wear particle and the EDX analysis. This suggests that the effect of abrasion would be minimal in this case. Upon comparison with the unused abrasive, It can be noticed that the abrasive particle had sharper edges which became rounded during the polishing operation. This would reduce the stresses developed on the surface of the material causing lesser damage. Figure 6.1.2.10 shows the wear particle obtained during polishing. This particles suggests that it was subjected to viscous deformation. The flow patterns on the surface of the particle can be observed. EDXA analysis indicated the presence of Silicon suggesting this could be a Silica particle, which was mechanically removed. Figure 6.1.2.11 shows the silicon nitride particle scooped from the ball. The surfaces appear smooth and crack have not propagated as in the case of Boron Carbide. EDXA analysis shows the presence of Silicon in larger amounts and traces of chromium. It was understood that the oxidation of silicon nitride particle was in progress at the time of removal. Figure 6.1.2.12 shows the SEM micrograph and the EDXA analysis of the wear particle obtained. EDXA indicates the presence of both Silicon and Chromium in major quantities corresponding to the white particle. This is assumed to be a particle of Chromium Silicate, the reaction product of chemomechanical polishing.



B4C wear debris showing Si3N4  
particle 3500X 15kV

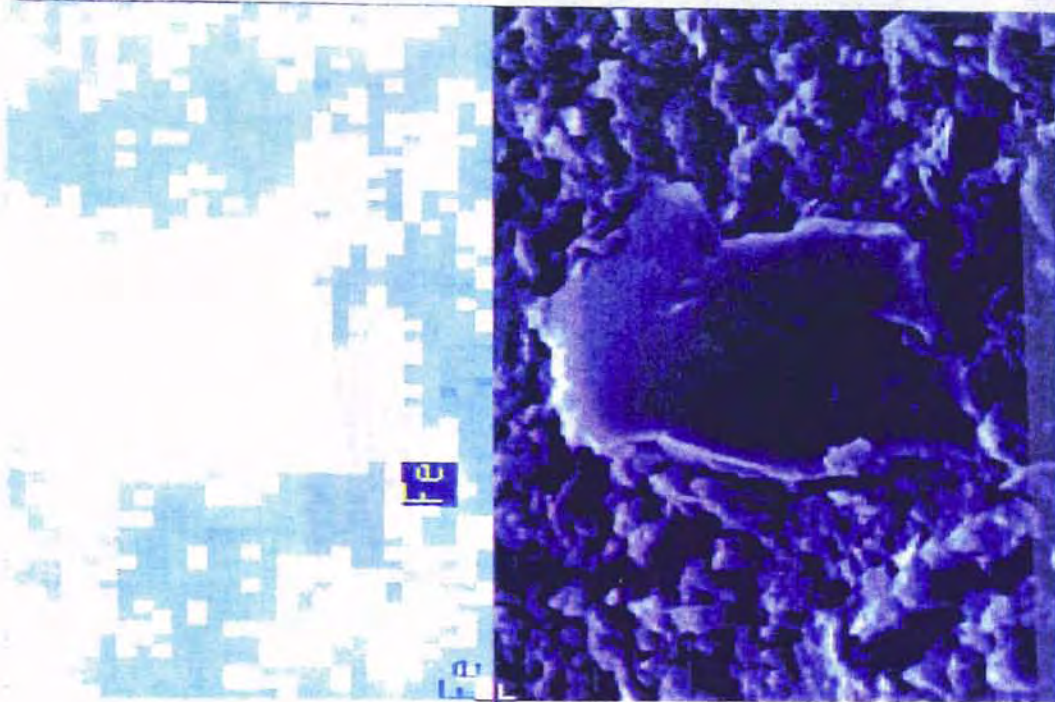


Figure 6.1.2.5 SEM micrographs and EDX analysis of the boron carbide wear debris showing silicon nitride wear particle

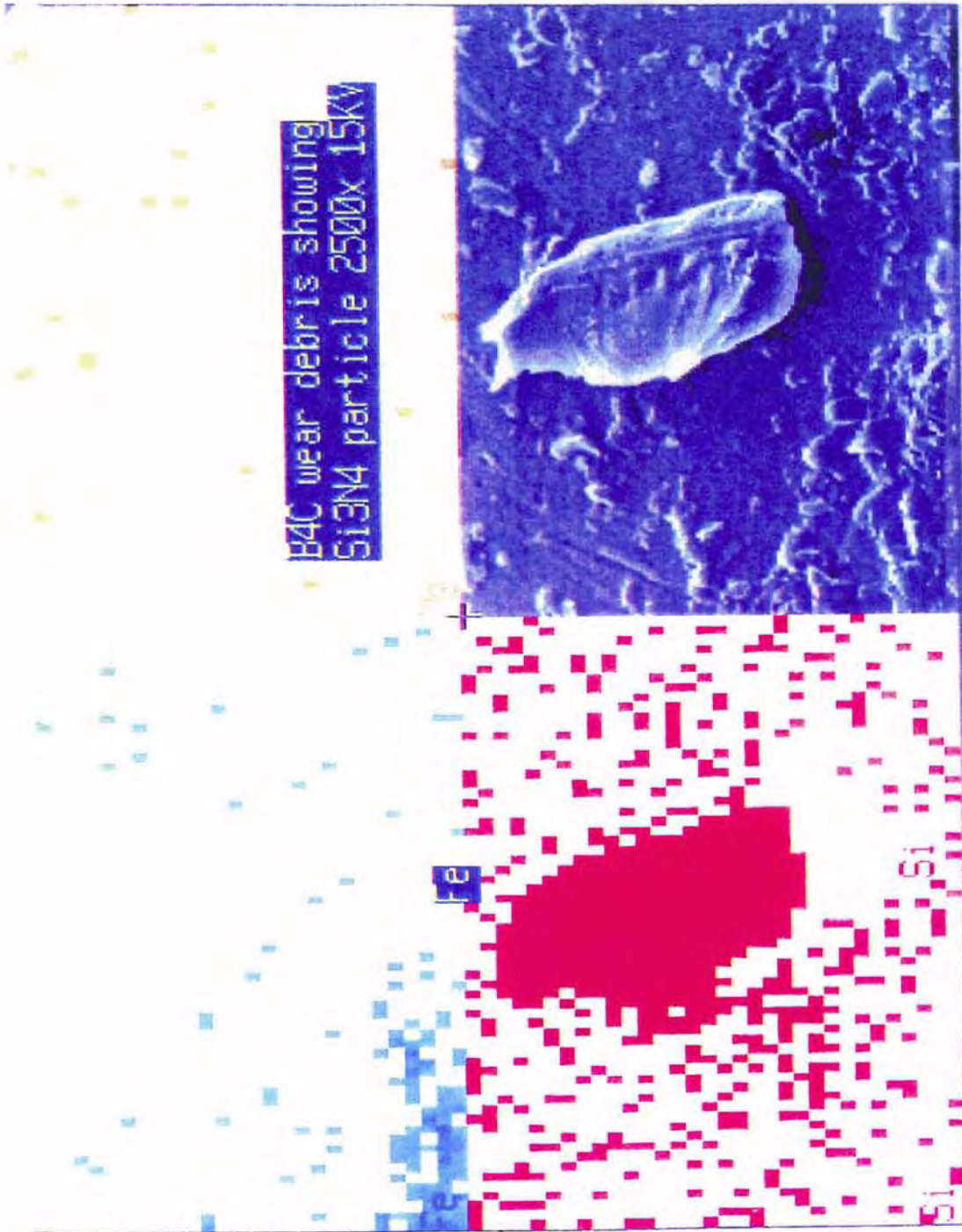


Figure 6.1.2.6 SEM micrographs and EDX analysis of the boron carbide wear debris showing cleaved silicon nitride wear particle

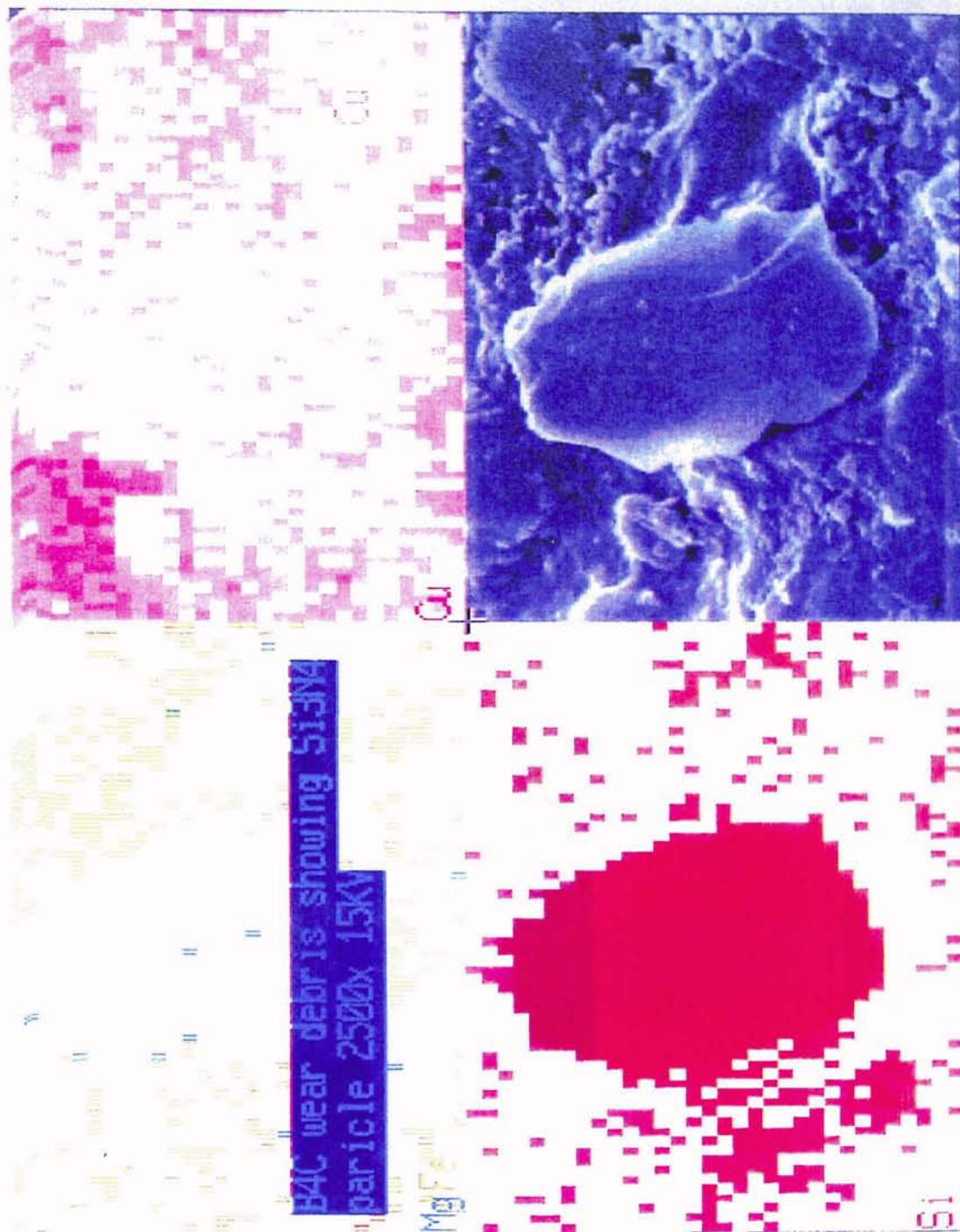


Figure 6.1.2.7 SEM micrographs and EDX analysis of the boron carbide wear debris showing silicon nitride wear particle

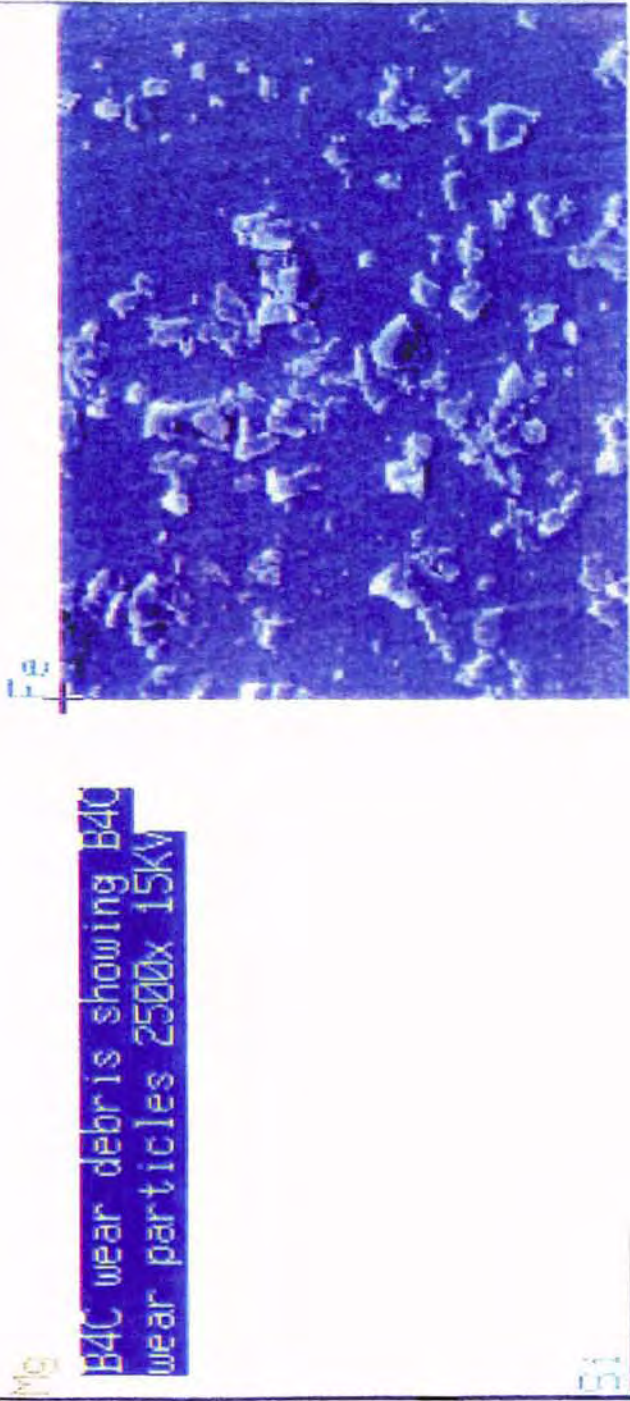


Figure 6.1.2.8 SEM micrographs and EDX analysis of the boron carbide wear debris showing boron carbide wear particle

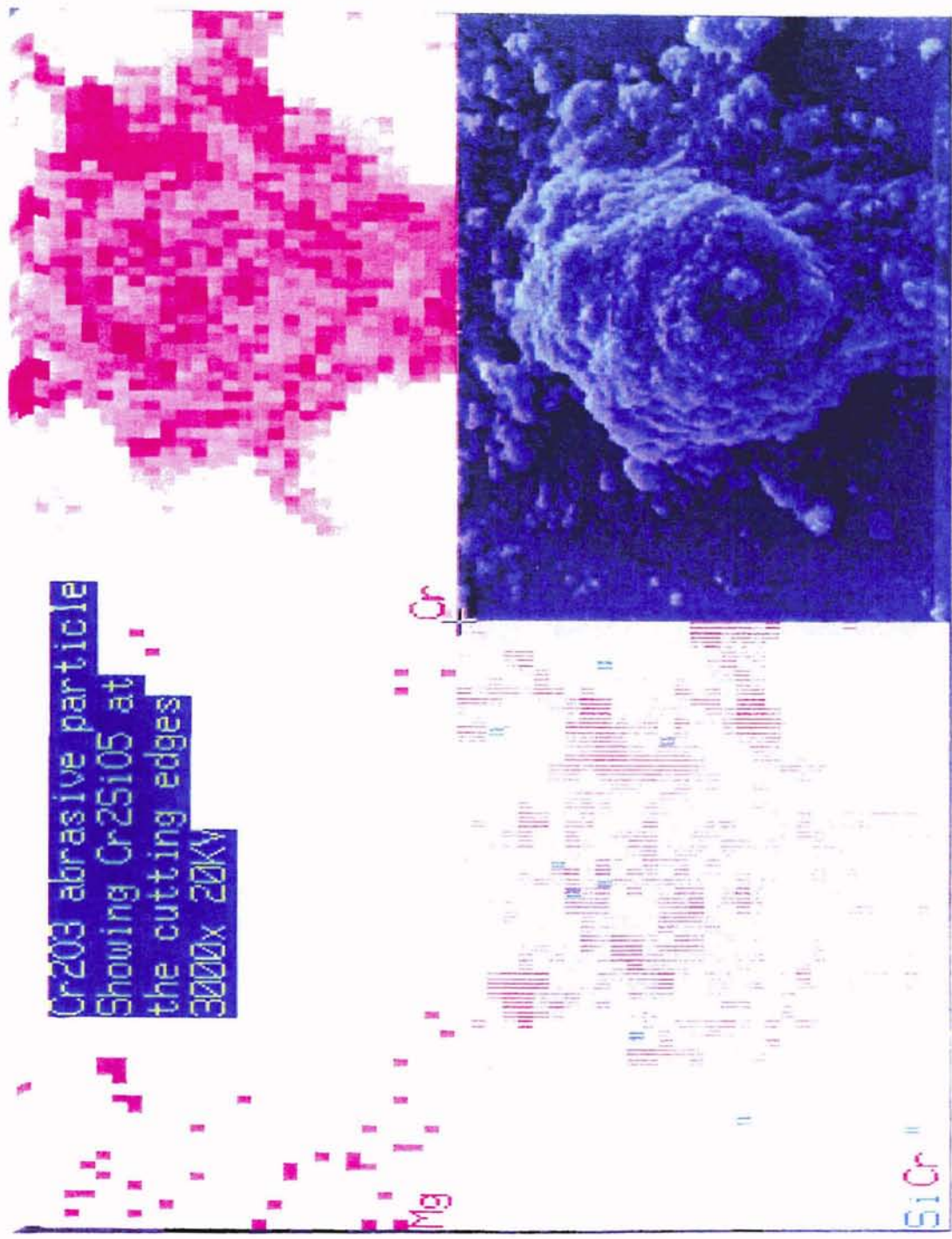


Figure 6.1.2.9 SEM micrographs and EDX analysis of the chromium oxide wear debris showing chromium oxide wear particle

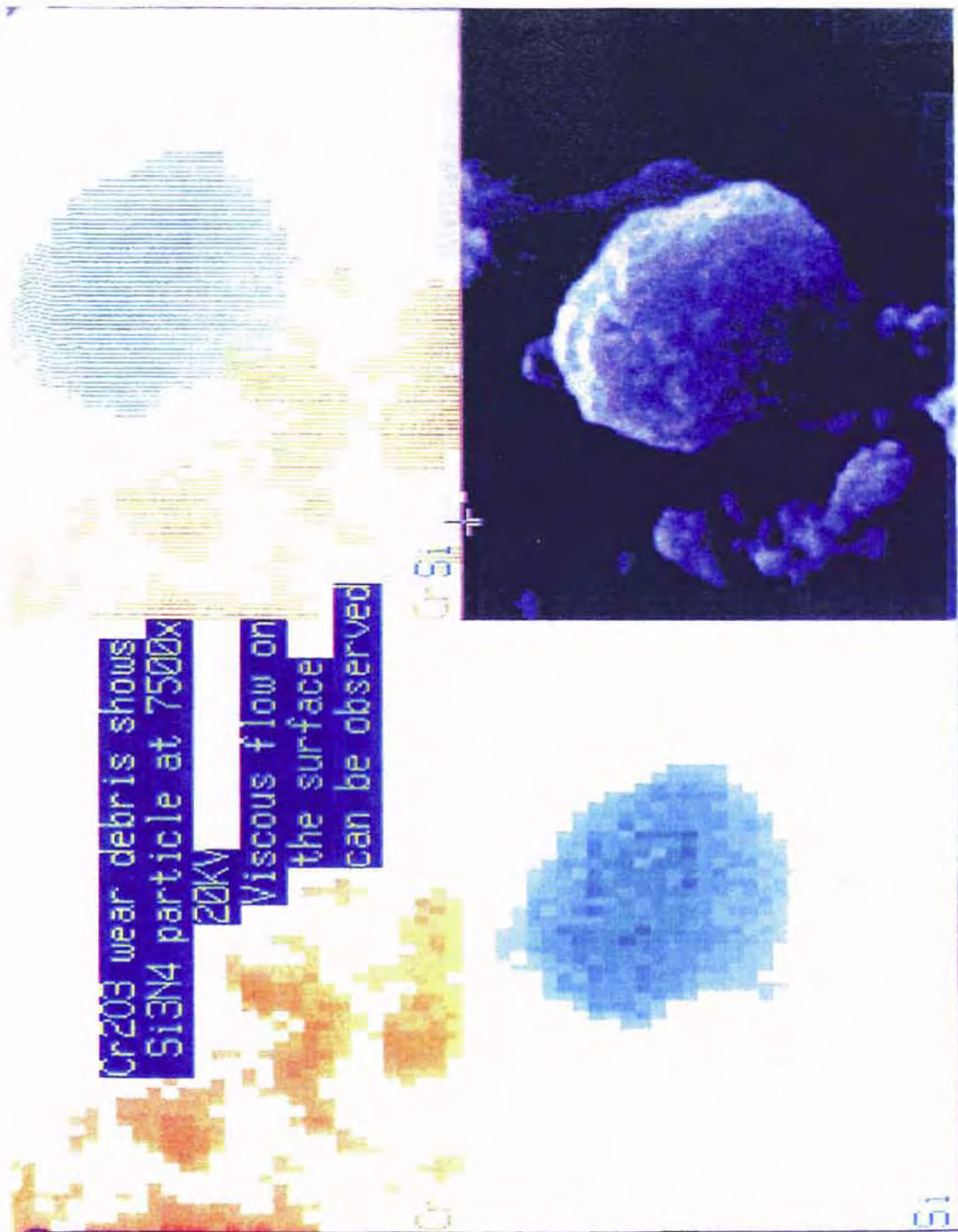


Figure 6.1.2.10 SEM micrographs and EDX analysis of the chromium oxide wear debris showing particle with viscous deformation

Cr<sub>2</sub>O<sub>3</sub> wear debris showing  
Si<sub>3</sub>N<sub>4</sub> particle scooped out  
from the work piece.  
Particle suffered least  
damage. 7000x 30Kv

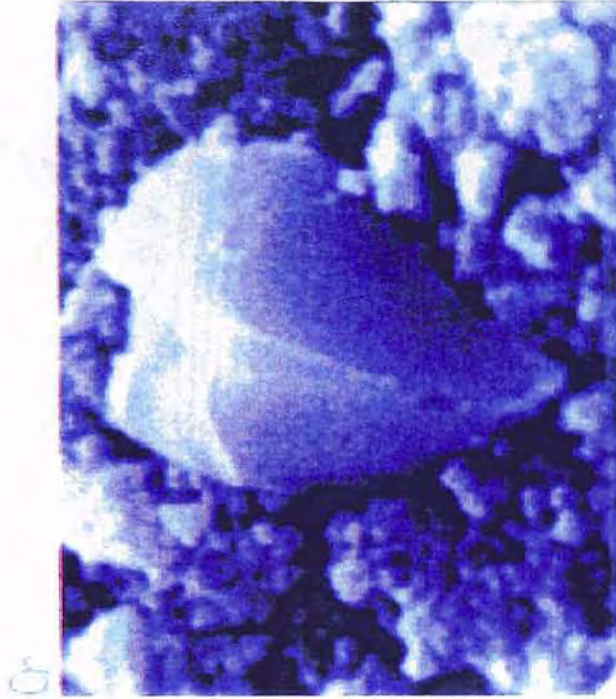


Figure 6.1.2.11 SEM micrographs and EDX analysis of the chromium oxide wear debris showing silicon nitride particle

## PART III

### XRD ANALYSIS

Figure 6.1.3.1 shows the XRD data obtained for SiC wear debris from the Magnetic Float Assisted Polishing. The data show the presence of Silica and no other reaction products. As it was understood from the literature survey, there were no other reaction products other than silica. This suggests that the material removal mechanism is mostly by abrasion. High stresses developing at the point of contact do not favour any other compound formation

Figure 6.1.3.2 shows the XRD data obtained for Boron Carbide wear debris. This shows the presence of Boron Silicate. However, it could not be detected in the wear debris.

Figure 6.1.3.3 shows the XRD data obtained in the case of Chromium oxide. The data indicate the presence of Chromium silicate and the formation of chromium nitride during the reaction with surface of silicon nitride. This will be explained in the next chapter. Chromium silicate phase, being the brittle intermetallic phase, is removed during the subsequent mechanical abrasion.

Therefore, it can be determined from the results that the interaction between the silicon carbide abrasives and the silicon nitride ball was essentially mechanical. Grain removal appears to be the main mechanism by which material removal takes place. Chemical action was minimal as the surface chemistry is the same. That silicon dioxide existed in different compositions is probably a result of flash temperature variations near the vicinity of contact during polishing.



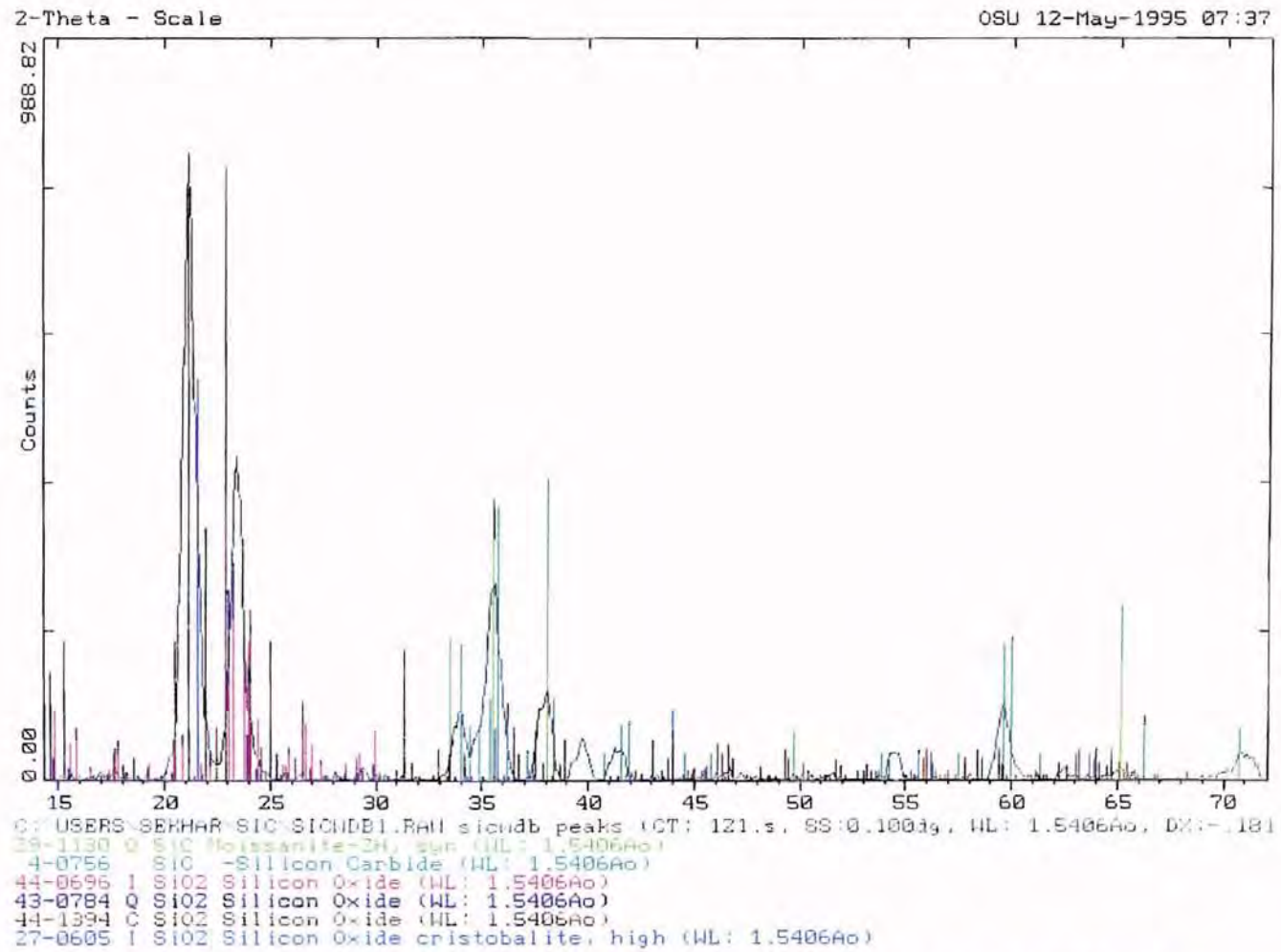


Figure 6.1.3.1 XRD pattern obtained from silicon carbide wear debris showing various forms of silica

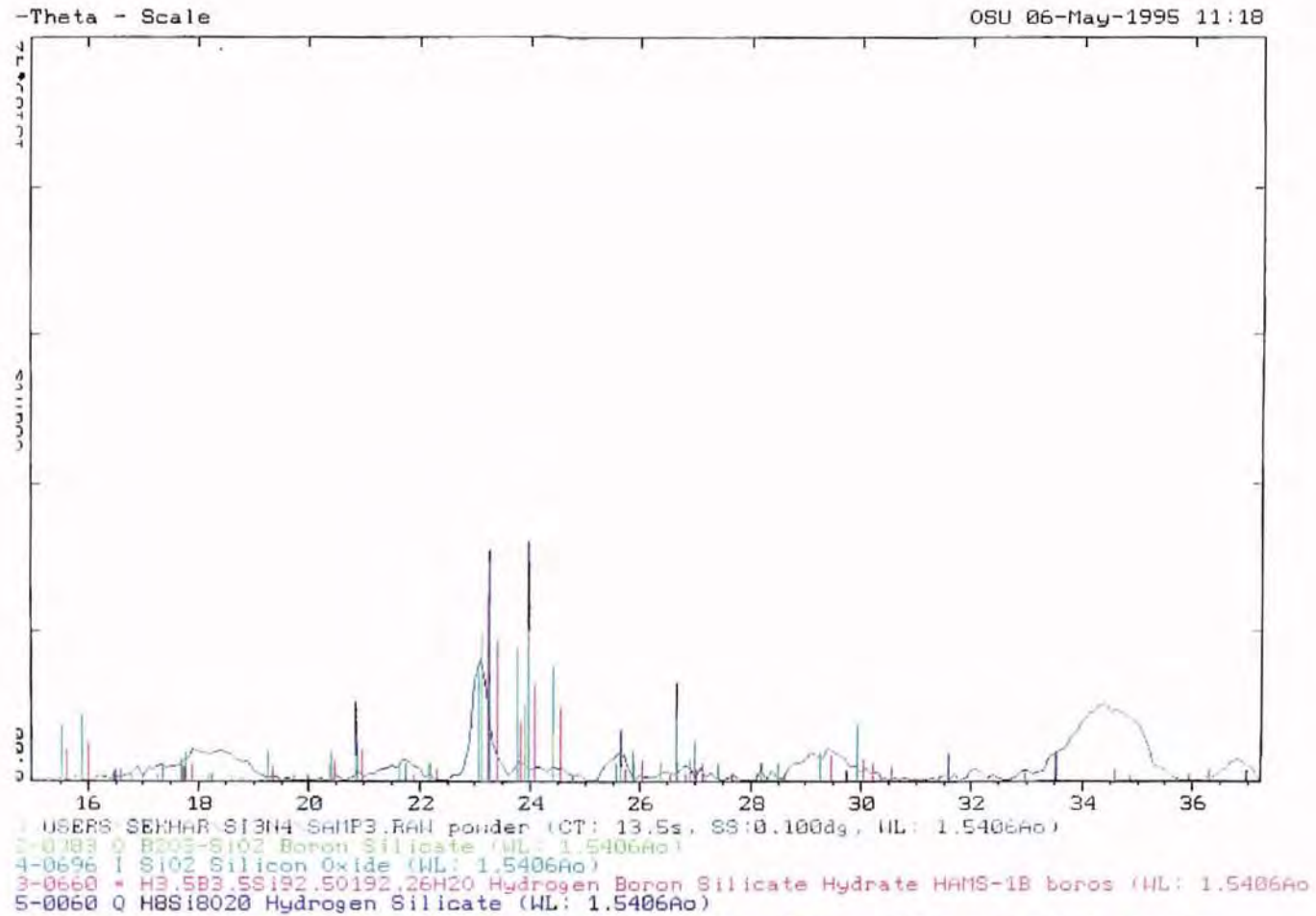


Figure 6.1.3.2 XRD pattern obtained from boron carbide wear debris showing presence of borosilicate

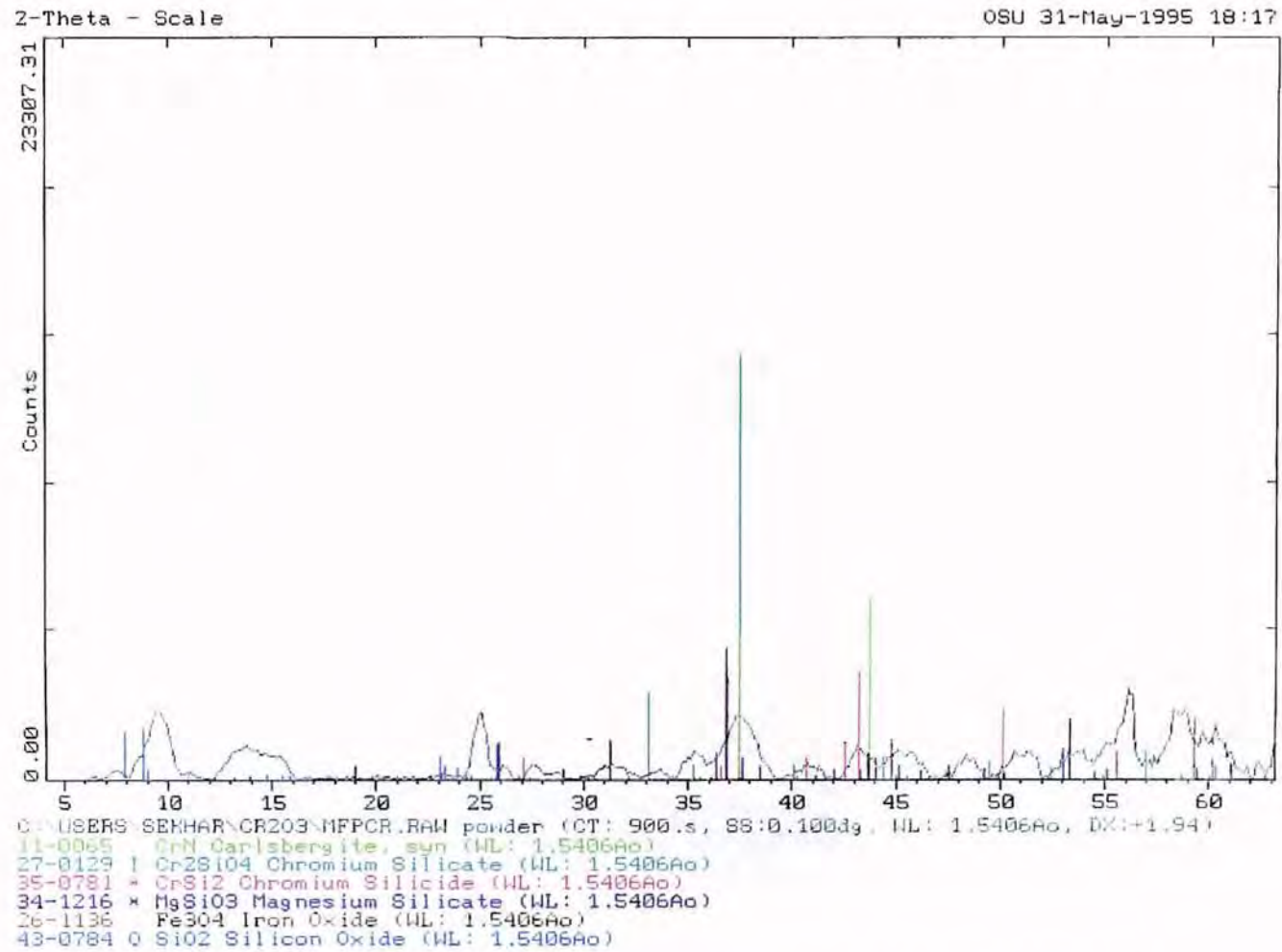


Figure 6.1.3.3 XRD pattern obtained from chromium oxide wear debris showing chromium nitride as a result of oxidation and chromium silicate as a result of chemo-mechanical action

## 6.2. MAGNETIC ABRASIVE FINISHING OF ROLLERS

### PART I

#### 6.2.1 SURFACE CHARACTERIZATION OF ROLLERS

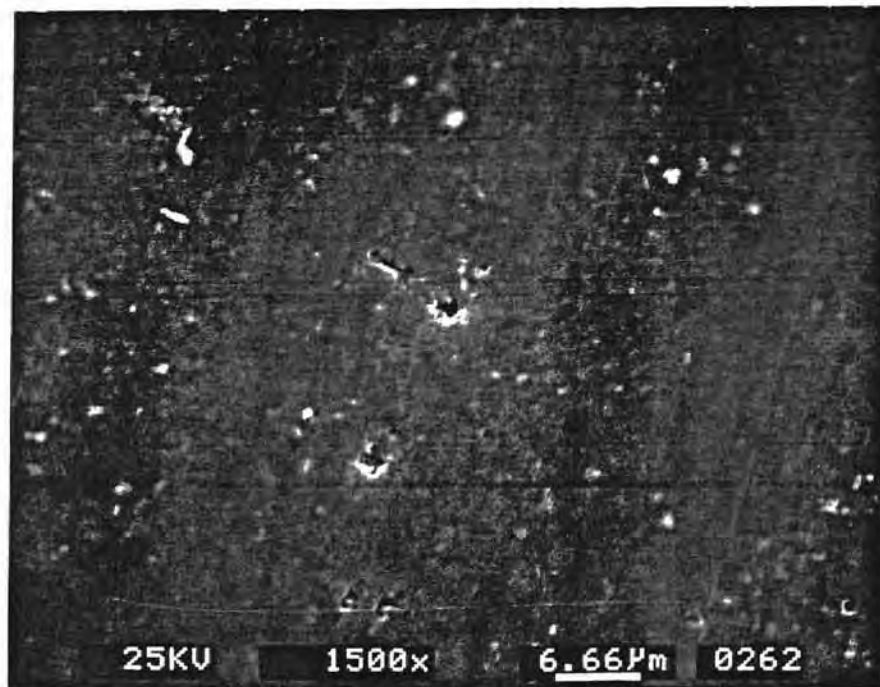


Figure 6.2.1.1 SEM micrographs showing the surface of silicon nitride rod during magnetic abrasive finishing

Silicon nitride rollers polished with chromium oxide abrasives are characterized in this section. Figure 6.2.1.1 shows the SEM micrograph of the surface obtained. The surfaces were almost free of surface defects, suggesting that the chemical reactions occurring between the abrasive and the workmaterial are predominant. There was no surface crack generation due to the polishing process itself. It could be understood that the higher temperatures (flash temperatures) produced on the surface during the polishing in air has increased the chemical reaction rates.

Figure 6.2.1.2 shows the talysurf trace obtained in this case showed the roughness value (peak to peak) of 0.0085  $\mu\text{m}$ . an order of magnitude lesser compared to that obtained while polishing in water.

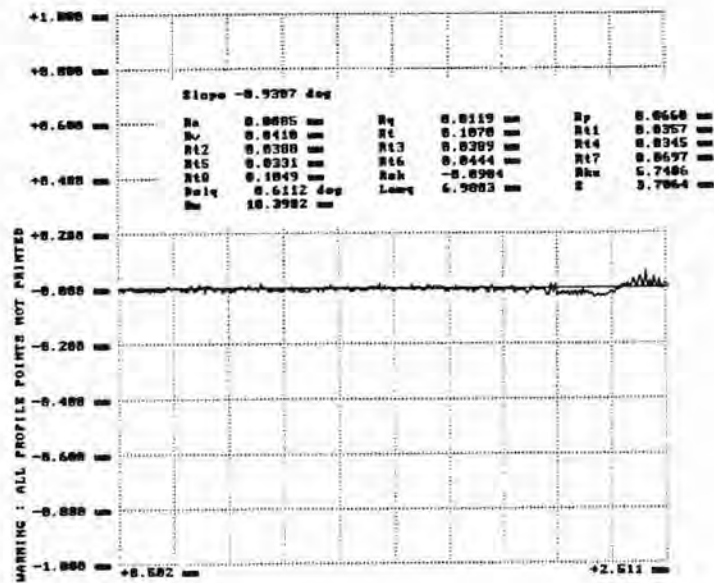


Figure 6.2.1.2 Talysurf surface roughness plot obtained during magnetic abrasive finishing of silicon nitride rod using chromium oxide abrasive

## PART II

### 6.2.2 ANALYSIS OF THE WEAR DEBRIS

Figure 6.2.2.1 shows the SEM micrograph and the EDXA analysis of the wear debris showing the rounding of edges of a chromium oxide particle, similar to that obtained when polishing in water. Figure 6.2.2.2 shows the SEM micrograph and EDXA analysis of another wear particle showing the formation of a chromium silicate phase due to the chemical reaction between the workmaterial and abrasive. Figure 6.2.2.3 shows the SEM and EDXA analysis of the wear particle showing the formation of chromium silicate. The particle appearance does not match with that of silicon nitride particle obtained from silicon carbide wear debris. It could have resulted from either the removal of silica film formed on the surface or a disintegrated particle of chromium silicate. However, chromium was not found in the EDX pattern obtained for the image. Therefore, it was understood that the particle was of silica which has undergone viscous deformation due to the stresses developed at the contact zone.

## PART III

### 6.2.3 XRD ANALYSIS

Figure 6.2.3.1 shows the XRD pattern obtained for the wear debris. Data shows the presence of Chromium nitride and Chromium silicate in greater quantities compared to that obtained when polishing in water. This could be because of the higher flash temperatures facilitating the silicate phase to increase in its crystallinity. Moreover, hydrolyzation of silica and other reaction products tend to impart amorphous nature to the wear debris which was the case shows in water. Peak intensities in both the cases show the same effect.

Cr2O3 wear debris of Si3N4 rod  
showing Cr2O3 agglomerates  
12500x 20KV

Si Fe Mg

Cr

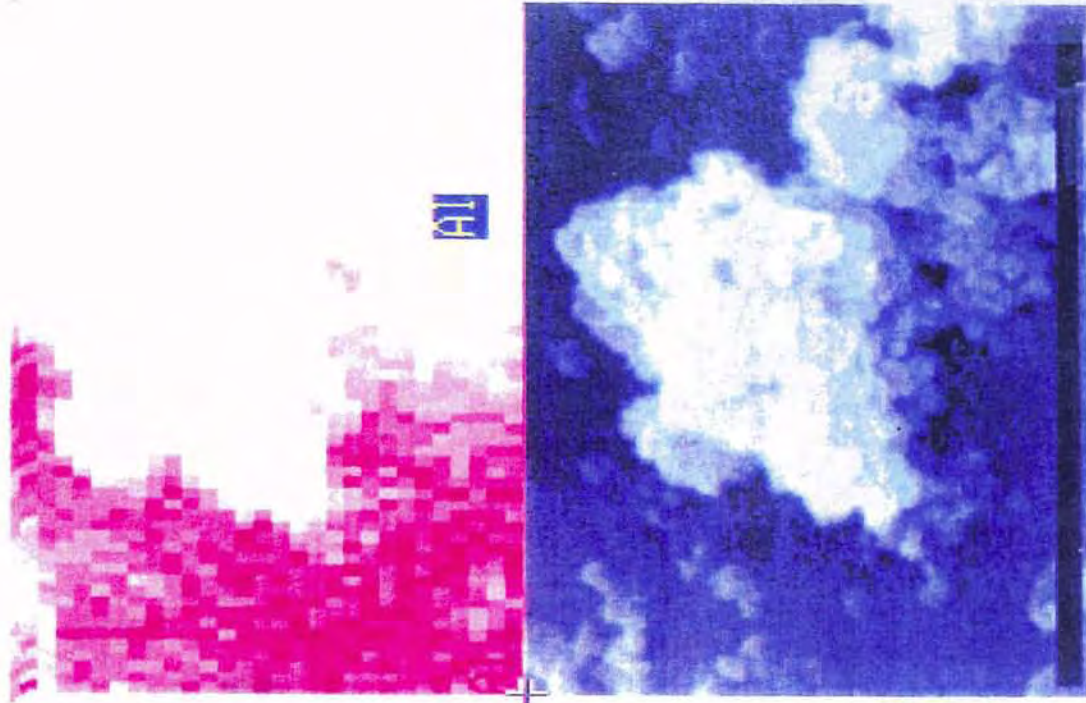


Figure 6.2.2.1 SEM micrographs and EDX analysis of the chromium oxide wear debris obtained during magnetic abrasive finishing of silicon nitride rod

Cr203 wear debris of Si3N4 rod showing Si, CR 12500x 20KV

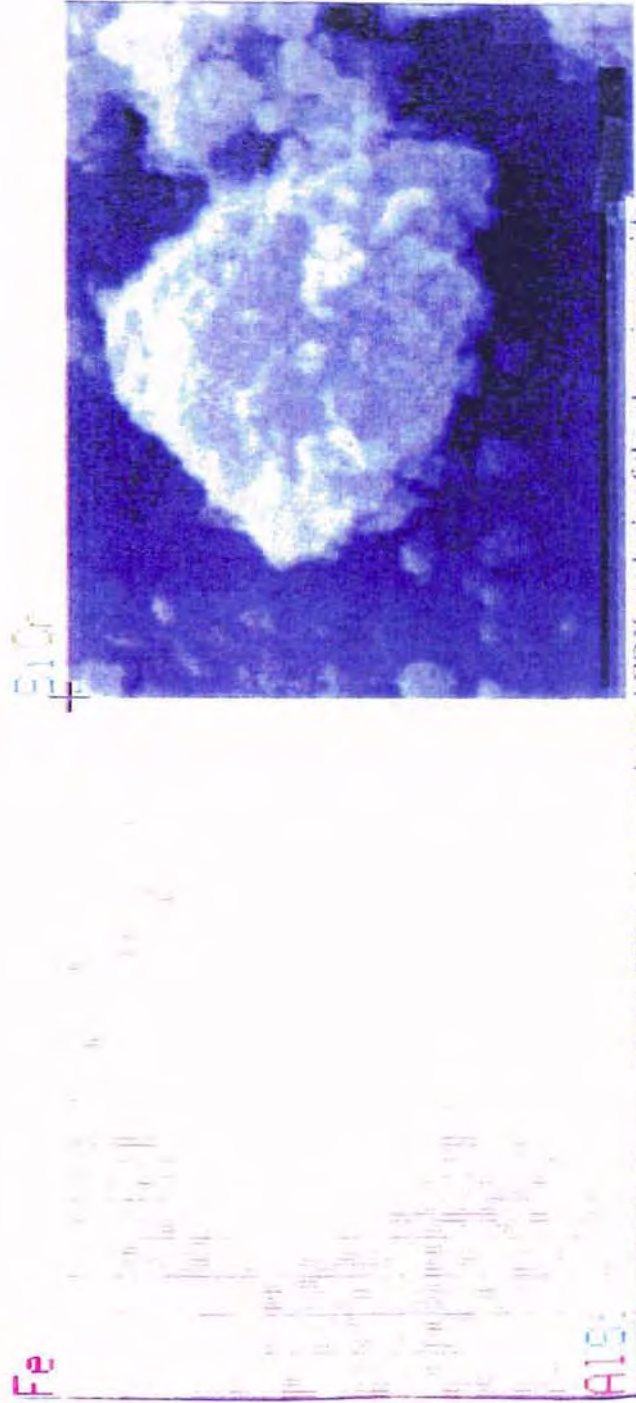


Figure 6.2.2.2 SEM micrographs and EDX analysis of the chromium oxide wear debris obtained during magnetic abrasive finishing of silicon nitride rod shows chromium silicate reaction product



Cr2O3 wear debris of Si3N4 rod showing Chromium Silicate reaction product at 20000x 20KV

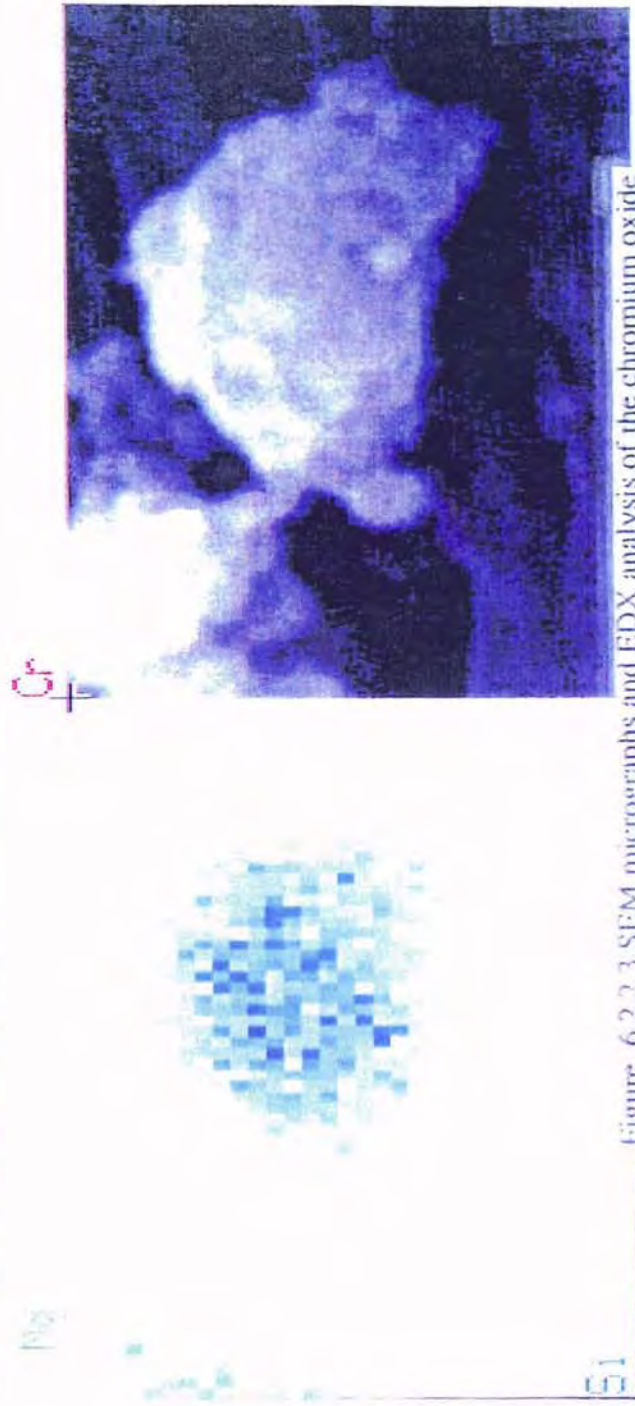


Figure 6.2.2.3 SEM micrographs and EDX analysis of the chromium oxide wear debris obtained during magnetic abrasive finishing of silicon nitride rod shows chromium silicate reaction product

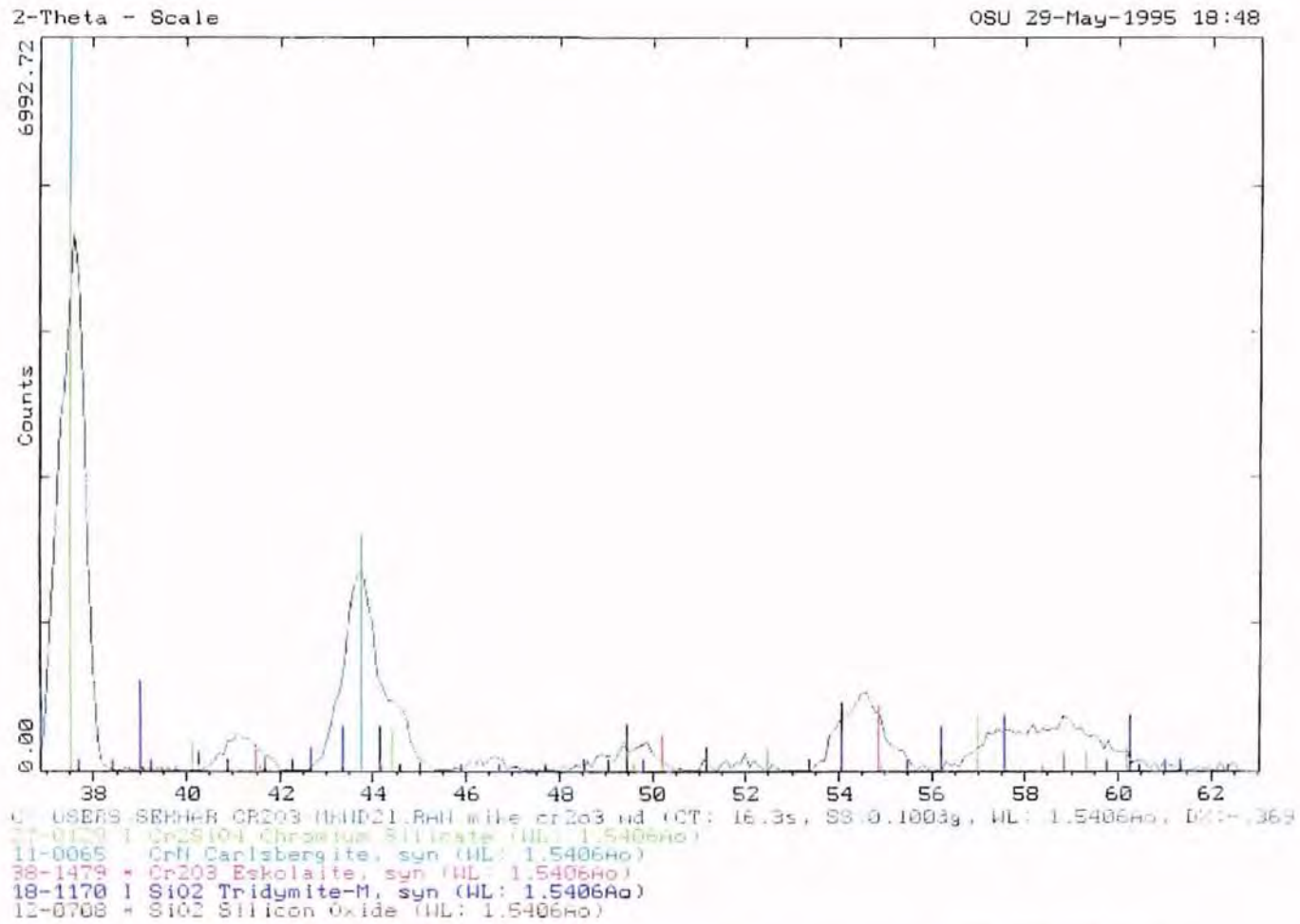


Figure 6.2.3.1 XRD pattern obtained during chemomechanical polishing of silicon nitride rod in air using chromium oxide abrasives shows the presence of Chromium nitride and chromium silicate

From these results, it is understood that chromium oxide is a material which undergoes chemical reactions with the oxidation products of silicon nitride. It also, enhances the oxidation kinetics by lowering (considerably) the activation energy required. Chromium oxide forms a silicate phase while reacting with silica, which is subsequently removed during the abrasive action. It, also, participates in the oxidation of silicon nitride by reacting with silicon nitride directly forming chromium nitride as the reaction product. Carbide abrasives do not undergo extensive chemical interactions with the workmaterial. The constituents of the silicon nitride oxidation product and the surface layer of SiC are identical. However, Boron carbide does undergo chemical reaction with silica, but may not be the sole mechanism of material removal. In fact, the reaction between oxide present on Boron carbide and silica is insignificant when compared to the mechanical abrasion in progress.

## CHAPTER 7

### DISCUSSION AND PROPOSED CHEMO-MECHANICAL MODEL

In this chapter, a new chemo-mechanical model is presented for polishing silicon nitride workmaterial with chromium oxide abrasive (both dry and in water). This model takes into account some of the ideas developed by the earlier investigators. It also takes into account results from the Gibb's free energy analysis and phase diagram study, coupled with the experimental results obtained from the present work.

#### 7.1 ANALYSIS OF THE CHEMO-MECHANICAL POLISHING MECHANISMS PROPOSED IN THE LITERATURE

Silicon nitride was mechanochemically polished by Vora et al [1982] using softer abrasives, such as  $\text{Fe}_2\text{O}_3$  and  $\text{Fe}_3\text{O}_4$  (3-5  $\mu\text{m}$  grain size). They obtained a surface finish (peak-to-valley roughness or  $R_{\text{max}}$ ) of about 20 nm. They, also, analyzed the silicon nitride samples polished with  $\text{Fe}_2\text{O}_3$  using an Auger Electron Spectroscopy (AES) and found the Auger peaks to closely resemble the oxygen rich silicon oxynitride. From this, they concluded that oxidation is a possible mechanism causing chemo-mechanical polishing of silicon nitride.

Kanno and Suzuki [1983] detected formation of ammonia during grinding of silicon nitride powder in water. Sugita et al [1984] studied the mechanism of material removal of silicon nitride rubbing in water. Ion microprobe analyses of the samples showed ions of silicon, with hydrogen and oxygen ions remaining on the polished surface. The wear debris analyses showed the material to be amorphous as they could not identify any visible peaks from the X-ray diffraction studies. However, when the sample was heat treated for one hour at 1170 °K, and examined, the X-ray diffraction data showed conversion into  $\alpha$ -cristobalite ( $\alpha$ - $\text{SiO}_2$ ). Based on this, they concluded that  $\alpha$ -cristobalite existed in an amorphous form and/or an amorphous silicon hydrate ( $\text{SiO}_2 \cdot x \text{H}_2\text{O}$ ) existed in the rubbing remnants. They postulated that oxidation of silicon nitride under the heat of friction results in the formation of an amorphous hydrate of silicon ( $\text{SiO}_2 \cdot x \text{H}_2\text{O}$ ) by the

action of water during rubbing. The amorphous hydrate of silica thus formed would subsequently be removed from the rubbing interface by the mechanical action of the abrasives.

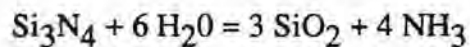
Fischer and Tomizawa [1985] conducted tribochemical studies of silicon nitride on itself in different gaseous and liquid media. In dry gases, they found wear to occur by two fracture mechanisms. Within 1 mm of the surface, they found the asperity contact to produce very large local stresses and cracking on a very fine scale. At a depth of 3-5 mm, they found the fracture to follow the weaknesses in the material, with mostly intergranular fracture and some transgranular cleavage. *They, however, found no evidence of plastic deformation.* This is an important observation as some researchers of late claim (with no real evidence) 'ductile' grinding of brittle materials. In water and in humidity saturated gases, they found the wear to be predominantly by tribochemical reaction, which produces an amorphous protective layer in humid gas and dissolution in water. They also found that humidity has a significant effect in reducing wear in silicon nitride material. They found that the oxide film formed on the surface became hydrated and supported the work material by elastohydrodynamic lubrication. However, their wear debris analysis could not result in the determination of the actual structure and composition of the reaction products. They expected it to be amorphous and contain oxygen. So, they assumed that it would be hydrated amorphous silica.

Cranmer [1987] studied the wear of silicon nitride on itself in air. He examined the wear surfaces using a scanning electron microscope with a X-ray microanalyzer and a X-ray photoelectron spectroscope (XPS). The XPS provided the distinction between Si in  $\text{Si}_3\text{N}_4$ , silicon oxynitride, and  $\text{SiO}_2$ ; N in  $\text{Si}_3\text{N}_4$ , silicon oxynitride; and O in silicon oxynitride and  $\text{SiO}_2$ . He found the oxidation of  $\text{Si}_3\text{N}_4$  to be related primarily to the distance slid. He also found that the mechanical stresses at the wearing surfaces to enhance the formation of oxide rather than oxynitride, when compared to materials exposed only to temperature.

Jahanmir and Fischer [1988] conducted tribological studies of silicon nitride lubricated by humid air, water, hexadecane, and hexadecane + 05 % stearic acid. They found a tribochemical reaction to occur between silicon nitride and water in all four environments, leading to the formation of an amorphous silicon dioxide layer on the surface. *They also found an absence of plastic deformation of the surface, similar to Fischer and Tomizawa.* Tomizawa and Fischer [1987], subsequently, found that moisture

causes the formation of amorphous silica layer as a result of tribochemical reaction. They also found that the silica layer dissolves slowly in water to form silicic acid ( $\text{H}_2\text{SiO}_3$ ). In a review of tribochemistry, at the contact points in various ceramics, Fischer [1988] pointed out that flash temperatures generated due to the frictional heat determine the tribochemical reactions occurring at the surface.

Xu et al [1993] investigated the wear behavior of silicon nitride sliding on itself at high temperature and pressure of water. They analyzed the wear tracks (both inside and outside) using Auger Electron Spectroscopy (AES), and found oxygen intensities inside the wear track to be stronger than outside the wear track in a certain range of temperatures (150-200 °C). After rubbing silicon nitride with itself in water, an analysis of that water indicated that it contained ammonium ions suggesting that dissolution of the surface film was in progress as per the following equation:



These studies unequivocally show that oxidation of silicon nitride is the crucial step in the actual tribological and tribochemical behavior of this material. All the results indicate the formation of an amorphous silica on the surface when silicon nitride was polished in air, and the formation of a hydrated silica layer when polished in water. However, the role of chromium oxide is considered to be one of a catalyst rather than directly involved in the chemical reactions. Flash temperatures generated at the contact points during polishing determine both the possibility of a given reaction(s) and its rate. Therefore, it is necessary to study the oxidation phenomenon further to clarify the conditions under which the process is favoured and determine the flash temperatures developed during polishing. Further, it is necessary to perform the Gibb's free energy analysis at these flash temperatures to determine the chemical reactions favorable in air and in water, respectively.

## 7.2 THEORETICAL CONSIDERATIONS

Silicon nitride oxidizes in air in appreciable amounts beyond 1000 °C [Singhal, 1976]. Figure 7.2.1 is a schematic showing the reaction processes occurring during oxidation of hot pressed silicon nitride [Singhal, 1976]. It was shown that the grain boundary phase plays a crucial role in the oxidation process. Apart from the diffusion of anionic species (oxygen) into the silicon nitride workmaterial, there is another step which

balances the kinetics of the process. This is the diffusion of the cationic species (i.e. sintering aids, such as Mg, Ca, Y ions) out of the grain boundaries to the surface [Cubicciotti and Lau, 1978 and 1979 ; Falk and Engstrom, 1991]. Diffusion of the cationic species was determined to be the rate controlling step in the oxidation of silicon nitride. The activation energy required was  $488 \pm 30$  KJ/mole [Cubicciotti and Lau, 1978].

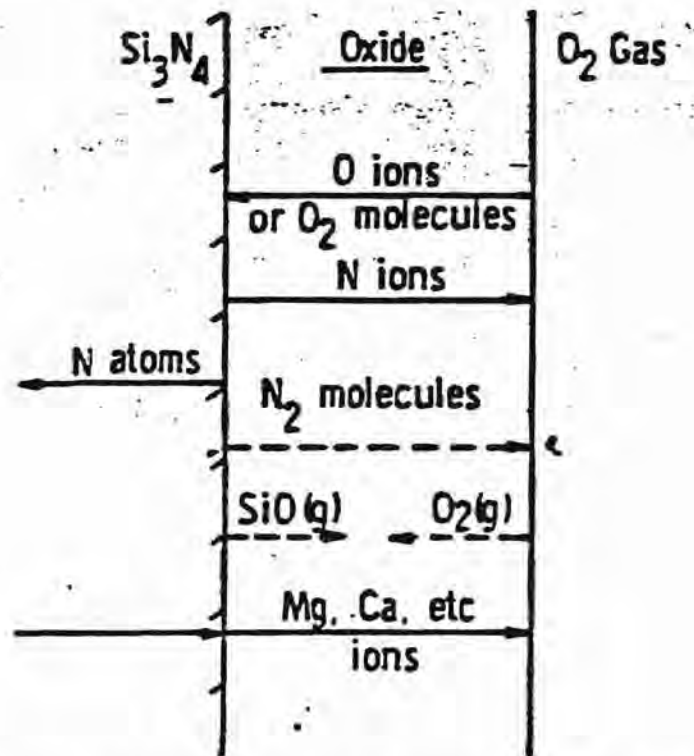
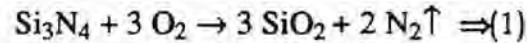


Figure 7.2.1 Schematic showing the reaction processes occurring during the oxidation of silicon nitride

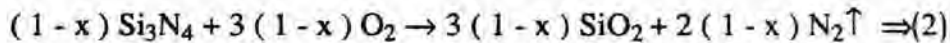
It was also found that the presence of water vapor in air greatly accelerates the oxidation of silicon nitride and catalyzes the devitrification of silica [Singhal, 1976 (a)]. The corresponding value for the activation energy in wet air is  $375 \pm 25$  KJ/mole [Singhal, 1976 (b)]. As the relative humidity increases, the oxidation increases. The activation energy required in the presence of water is 108 KJ/mole [Xu, et al , 1993].

Oxidation of silicon nitride results in the formation of a SiO<sub>2</sub> film on the surface and is given by the following equation.

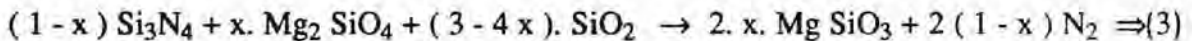


The formation of the SiO<sub>2</sub> film is associated with the formation of nitrogen gas. As the partial pressure of the gas increases in the oxidized layers, the gas is released forming pores and cracks in the film. Other reasons for the formation of cracks are the thermal expansion mismatch at the Si<sub>3</sub>N<sub>4</sub> - SiO<sub>2</sub> interface and/or the low temperature phase transformations occurring in the silica film. The nature of the SiO<sub>2</sub> film is not protective in the sense that the rate of oxidation is unaffected by the removal of the oxide scale. This suggests that oxidation is not controlled by the diffusion of oxygen into the scale alone.

Sintering additives such as MgO, CaO and Y<sub>2</sub>O<sub>3</sub> are present in HPSN and HIPped Si<sub>3</sub>N<sub>4</sub> [Kiehle et al., 1975 ; Echeberria and Castro, 1990]. In the present work, hot isostatically pressed Si<sub>3</sub>N<sub>4</sub> with MgO additions is used. The material consists of two phases Si<sub>3</sub>N<sub>4</sub> and Mg<sub>2</sub>SiO<sub>4</sub>. Oxidation of this two phase product in air can be represented as:



to yield a net reaction of

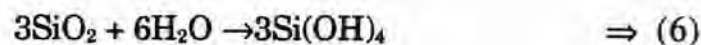
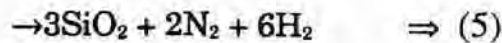
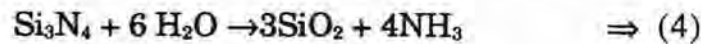


The compositional gradient, defined by the anion (oxygen ion) diffusion, sets up a reaction couple between the surface and the interior, which is a continuous phase containing Mg [Lange, 1979; Clarke and Lange, 1980]. If the initial phase of the material is the same as x.Mg<sub>2</sub>SiO<sub>4</sub> + (1-x) Si<sub>3</sub>N<sub>4</sub>, the reaction couple is SiO<sub>2</sub> (surface)/Mg<sub>2</sub>SiO<sub>4</sub> (interior); Mg<sub>2</sub>SiO<sub>3</sub> is the reaction product. Attainment of equilibrium in this type of reaction couple (Eqn. 3) requires the cation (MgO ion) diffusion. Since, Mg concentrates in the oxide scale, it is obvious that Mg is the principal diffusing cation species of such a couple. Mg will diffuse from the interior to the surface in an attempt to equilibrate the



reaction 3. Continuous depletion of Mg from the  $\text{Si}_3\text{N}_4$  -  $\text{SiO}_2$  interface would lower the concentration of Mg at the interface. This provides a gradient from bulk to interface for Mg transfer.

The corresponding reactions occurring in water are given in the following



The oxidized layer of the  $\text{Si}_3\text{N}_4$  consists of 3 parts. First, a layer of finite thickness containing 3 phases of  $\text{Si}_3\text{N}_4$ ,  $\text{Si}_2\text{ON}_2$ , and  $\text{Mg}_2\text{SiO}_4$  with a steadily decreasing content of  $\text{Si}_3\text{N}_4$ ; an interface of negligible width contains  $\text{Si}_2\text{ON}_2$  and  $\text{Mg}_2\text{SiO}_4$ . Second, a layer of finite thickness consisting of 3 phases  $\text{Si}_2\text{ON}_2$ ,  $\text{Mg}_2\text{SiO}_4$ , and  $\text{Mg}_2\text{SiO}_3$  with an increasing  $\text{Mg}_2\text{SiO}_3$  content; an interface of  $\text{Si}_2\text{ON}_2$  and  $\text{Mg}_2\text{SiO}_3$ . A third layer of finite thickness consisting of  $\text{Si}_2\text{ON}_2$ ,  $\text{SiO}_2$ , and  $\text{Mg}_2\text{SiO}_3$ , and finally, at the top of the oxide scale, a layer of  $\text{SiO}_2$  and  $\text{Mg}_2\text{SiO}_3$ . It is this cation diffusion which is the rate controlling step in the oxidation of silicon nitride.

Enstatite ( $\text{Mg}_2\text{SiO}_3$ ) forms in appreciable amounts beyond  $1100^\circ\text{C}$  and this increases with temperature. Above  $1375^\circ\text{C}$ , the surface is mostly covered with  $\text{SiO}_2$  (Cristobalite) and  $\text{Mg}_2\text{SiO}_3$ . The amount of  $\text{SiO}_2$  formation is appreciable around  $982^\circ\text{C}$  and increases to a maximum up to  $1200^\circ\text{C}$ . [Cubiccioni and Lau, 1978 and 1979]

The compositional change from the bulk to the surface can be represented by a combination of the ternary phase diagrams formed by  $\text{Si}_3\text{N}_4$ ,  $\text{Si}_2\text{ON}_2$ ,  $\text{Mg}_2\text{SiO}_4$ ,  $\text{Mg}_2\text{SiO}_3$ ,  $\text{SiO}_2$ , and  $\text{MgO}$ . The composition at each location in the scale shifts from one compatibility triangle to another. Each compatibility triangle will have its own eutectic composition and temperature. Should the oxidation temperature exceed one of these eutectics, a liquid will be formed, within the oxide scale, at a depth where the composition lies within that compatibility triangle. The amount of liquid will depend on how close the compositional curve is to the eutectic temperature and on the temperature in excess of the eutectic temperature. Formation of the liquid glassy phase has two effects. First, it provides

a diffusional path for the reacting species to the scale/subscale interface. Second, it accommodates the molar volume changes which accompany the reaction products. Therefore, the formation of a eutectic glassy phase is the key in obtaining a smooth, defect free surface.

Thus, the flash temperature (temperature generated at the real area of contact between the abrasive and the workmaterial) determines the nature of chemical reactions occurring within the oxide scale among the species of the oxidation products and also the constituents of polishing, such as the abrasive and the medium (magnetite particles). Measurement of the temperatures in the vicinity of the contact points during polishing is difficult and not practicable in most situations. Analytical work performed by previous authors, however, concentrates on metals in which plastic deformation and junction growth at the contact asperities are considered [Archard, 1959; and Ashby et al, 1991]. The same analysis can not be used in the case of ceramics owing to their brittle nature and lack of junction growth. Therefore, it was determined to adapt a suitable mathematical model to determine the flash temperatures generated at the contact interface.

A model combining the heat transfer principles with the moving heat source concept was applied to determine the flash temperatures. This model was developed by Hou and Komanduri [1994] and in the present work that model was applied to magnetic abrasive finishing to calculate the flash temperatures generated (an example calculation and other details are given in Appendix A). Material properties such as thermal conductivity and thermal diffusivity were used to determine the amount of heat input into the workmaterial and the abrasive. Experimental conditions, including the rotational speed and the polishing pressure, were taken into account to relate the elastic behavior of the materials in question. The flash temperatures were determined at the real areas of contact using the model. Hertzian stresses were determined and the real area of contact was calculated using the mechanical properties of the abrasive and workmaterial and their shape factors. The flash temperatures generated in the case of silicon nitride rods polished dry (i.e. in air) were in the range of 1200 to 2,000 °C, while in the case of balls polished in a water-based magnetic fluid, they were much lower and in the range of 400 to 800 °C.

Determination of the most favorable conditions for compound formation in a particular medium was analyzed using Gibb's free energy of formation. In the present work silicon nitride balls were polished in water and silicon nitride rods were polished in air (dry). Therefore, the determination of Gibb's free energy under the experimental

conditions taking the flash temperatures developed into consideration, would yield the exact determination of the action of the medium under which the polishing is in progress. The results indicated that water favoured the oxidation of silicon nitride up to a temperature of 700 °C and at higher temperatures, oxidation was more dominant in air. The possible reaction products between the workmaterial and the abrasive in question were determined from the phase diagram study. The surface chemistry primarily determines the nature of reactions under the conditions of polishing. Chromium oxide abrasive was found to react with silica layer to form chromium silicate. Boron carbide abrasive, which inherently has a thin oxide layer ( $B_2O_3$ ), was found to react with silica to give borosilicate glass. Silicon carbide however, does not differ in surface chemistry from silicon nitride as both have silica layers on the surface. Therefore, it was assumed that the reaction would be of no consequence in the chemo-mechanical polishing of silicon nitride with silicon carbide.

### 7.3 CORRELATION OF RESULTS

Results from the theoretical analysis and from the experimental work were correlated in this section and a plausible mechanism leading to the chemo-mechanical polishing of silicon nitride with chromium oxide abrasive has been proposed. SEM work showed smooth surfaces in the case of chromium oxide and somewhat rough surfaces, with cracks, pits, and other surface defects in the case of carbide abrasives. Surface finish measurements indicated that the roughness obtained by the boron carbide to be the maximum and by chromium oxide to be the minimum, with silicon carbide in between. This can be attributed mainly to the hardness of the abrasive. Boron carbide being the hardest abrasive, though it has some affinity towards silicon nitride, did not result in a good finish. Because of the extremely high contact stresses generated at the real area of contact at the interface, the workmaterial failed due to conchoidal fracture and cleavage. Silicon carbide abrasives, on the other hand, had a lower hardness compared to boron carbide abrasives. However, the energy utilized in the chemical reaction was minimal (the only possibility is the reaction of silica layer present on the abrasive to reaction with the species of magnesium). Therefore, the mechanism of material removal was mainly due to mechanical abrasion. Particles of silicon nitride were dislodged due to multigrain pullout and tearing modes.

EDX analyses were conducted on the wear debris obtained with all the three abrasives. The results showed that the carbide abrasives did not give any reaction products as predicted. Borosilicate formation could not be detected because boron is a light element

and the X-ray dispersive microanalyzer associated with the SEM is not capable of detecting light elements. However, chromium silicate could be detected in the wear debris obtained during polishing of silicon nitride balls in water. The particle size of the reaction product was about 150 nm. It could not be seen directly (other than the particles adhering to the surface of the silicon nitride particle) because of the magnification needed was about 50,000 X to 75, 000 X. However, in the case of silicon nitride rods polished with chromium oxide in air, the particles of chromium silicate could be directly observed owing to their larger size. This could be attributed to the higher flash temperatures generated at the contact interface. The particle would readily crystallize at this temperature owing to its high surface area compared to that obtained when polishing in water.

XRD results obtained from the wear debris confirmed the above findings. Silicon carbide wear debris could not give any peaks other than silica and boron carbide wear debris indicated the presence of Borosilicate and other silica phases.

However, chromium oxide wear debris, obtained from the polishing of silicon nitride ball, indicated the presence of chromium silicate in less proportion when compared to that of the peaks obtained from the wear debris of rod polished in air. This, again, confirms that the wear particles of the reaction product obtained in the previous case are either too fine a grain or amorphous in nature. Particles obtained in the second case were more crystalline, indicating stronger peaks.

The other reaction product found from the chromium oxide wear debris in both cases was particularly interesting in the sense that it has directly reacted with the parent material itself instead of the surface layers. Presence of chromium nitride was found in both the cases. The chemical behavior of the chromium oxide abrasive, along with its mechanical behavior, is evident from the above results. Therefore, a model was developed explaining the chemo-mechanical action of chromium oxide abrasive in generating a defect free polished surface on silicon nitride.

## 7.4 PROPOSED CHEMO-MECHANICAL POLISHING MODEL

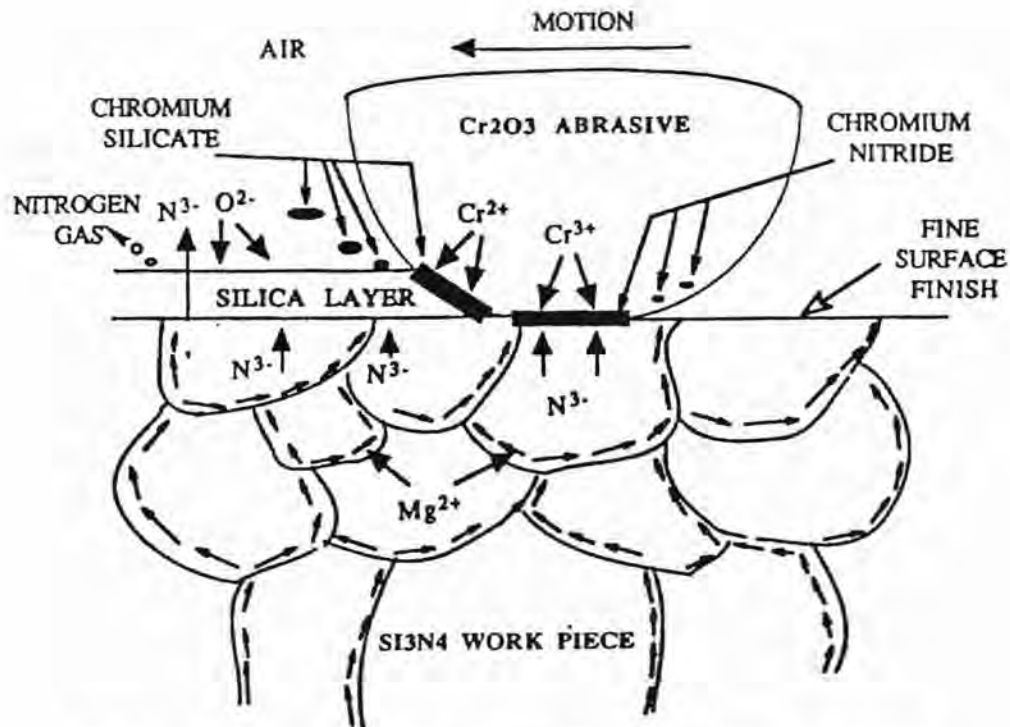
### 7.4.1 CHEMO-MECHANICAL ACTION OF CHROMIUM OXIDE IN AIR

Figure 7.4.1.1 is a schematic of the chemo-mechanical model for polishing silicon nitride with chromium oxide abrasive in air. During polishing, chromium oxide abrasive slides over the silicon nitride workmaterial with a relative velocity that can be calculated from the experimental conditions. It is well known that silicon nitride is generally covered with a thin layer of silica. During polishing, the abrasive makes contact with this layer. If the depth of cut of the abrasive is larger than the silica layer thickness, which is generally the case, then a part of the abrasive is in contact with the silica layer and another part is in contact with the silicon nitride parent material.

At the conditions of polishing (flash temperature and contact pressure), oxygen from the surrounding atmosphere can penetrate through the silicon nitride to form silica on the surface. This has to be balanced by the evolution of nitride ions through the bulk of the material and the migration of magnesium ions to the top surface along the path provided by the grain boundaries. When two nitride ions combine, a molecule of nitrogen gas is formed in the bulk of silicon nitride and is evolved from the silica layer, giving rise to porosity on the surface.

However, nitride ions can also react with the chromium ions provided by the chromium oxide abrasive to form chromium nitride [Earnshaw and Harrington, 1973]. Chromium is also comparatively stable in the  $2^+$  state when compared to the other states such as the  $6^+$ ,  $5^+$ , and  $4^+$  the last two states being the least stable. Chromium in its  $3^+$  state can form an enormous number of complexes, particularly when nitrogen is the donor atom, virtually all being six co-ordinate and octahedral [Earnshaw and Harrington, 1973].

The nitride ion, therefore, preferentially gets attached to a chromium ion. If it were to combine with another nitride ion, as already pointed out, it forms nitrogen gas which is subsequently released. Silicon nitride in the absence of chromium oxide in the vicinity, has to release nitride ions which combine to form nitrogen gas. But, in the presence of chromium oxide, nitride ions can react in two ways: 1. to combine with the chromium  $3^+$



REACTIONS OCCURRING IN THE CHEMOMECHANICAL POLISHING OF SILICON NITRIDE WITH CHROMIUM OXIDE ABRASIVES IN AIR

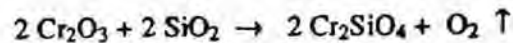
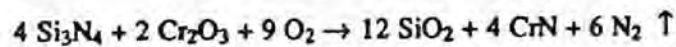
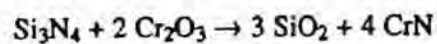
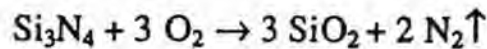
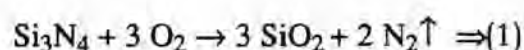


Figure 7.4.1.1 Schematic of the chemo-mechanical model for polishing silicon nitride in air using chromium oxide abrasives

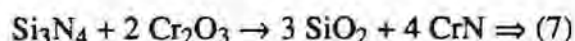
ions, 2. to combine with the neighboring nitride ion to achieve a stable state. Thus, in the first place, the residence time of nitride ions is increased which is advantageous from the polishing point of view. When nitride ions do not get an opportunity to form molecules, correspondingly, the amount of nitrogen gas evolved also gets reduced. This situation is preferred as there would be less number of pores and microcracks generated on the surface during polishing.

Furthermore, when nitride ions combine in two ways, correspondingly, the oxygen ion diffusion into the silicon nitride work material would increase. In other words, chromium oxide abrasive facilitates in further enhancing the oxidation of silicon nitride directly by forming chromium nitride. This hypothesis is somewhat different from the earlier models, where the role of chromium oxide is assumed to be a mere catalyst in the oxidation of silicon nitride [Vora et al, 1982]. The arguments developed here can be represented by the following equations.

The effect of air on the oxidation of silicon nitride can be represented by Eqn. 1. It is believed that flash temperatures in polishing of silicon nitride workmaterial can be in the range of 1200-2000 °C. At temperatures above 1000 °C, oxygen dissociates the Si - N bond to form silica on the surface. This action generates four nitride ions which combine to form two molecules of nitrogen gas. The nitrogen gas is evolved from the surface giving rise to pores and microcracks.

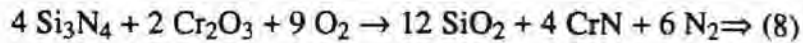


The effect of chromium oxide alone on the oxidation of silicon nitride can be represented by the following equation.



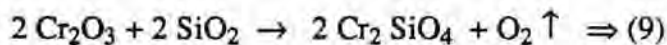
The attraction of chromium ions towards nitride ions and the presence of three oxygen molecules of gas in chromium oxide and high flash temperatures present in the vicinity, can provide enough energy to dissociate the Si - N bond from silicon nitride to form silica. All the four nitride ions released from this action are combined to form chromium nitride. Hence, there is no nitrogen gas formation in this case.

However, the combined effect of chromium oxide and oxygen can be obtained by adding and balancing Equations 1 and 7. This is represented by the following equation:



Here, it can be seen that the amount of nitrogen gas production is effectively reduced because of the chromium nitride compound formation. In the absence of chromium oxide, four silicon nitride atoms would have needed 12 oxygen molecules of gas to produce 8 molecules of nitrogen, giving rise to 12 molecules of silica. But, the presence of 2 molecules of chromium oxide will facilitate in all the 12 atoms of silica formation, even in the presence of only 9 oxygen molecules, while limiting the nitrogen gas generation to only 6 molecule. In other words, the activation energy required for silica formation is being reduced and nitrogen gas generation is not being favored. Both these issues are critical in the ultimate polishing characteristics of silicon nitride.

Further, the action of chromium oxide on the formation of silicate phase can be represented by the following equation:



Chromium in its 2<sup>+</sup> state reacts with the silica layer to form chromium silicate as the reaction product evolving oxygen as a by product. This oxygen in turn is made available for the subsequent oxidation of silicon nitride. As silica is abundantly available near the contact interface, naturally, the amount of silicate phase formation is favored at the point of contact because of the high flash temperatures generated. Chromium silicate is a brittle intermetallic compound that gets removed during subsequent mechanical action by the abrasive. The contact stresses generated at the interface are adequate to remove the reaction product without disturbing the parent material. Consequently, the function of chromium oxide is three fold. First, it enhances the oxidation kinetics by forming chromium nitride which facilitates the formation of silica layer. Second, it increases the nitrogen ion residence time, which ultimately reduces the formation of surface porosity, which is crucial in achieving a good surface without stress concentrations. Third, it reacts with the silica layer to form chromium silicate, which gets removed during the subsequent mechanical abrasion. Though, silica layer does not provide a protective layer, physical removal of the surface film increases the diffusional characteristics which again facilitates the oxidation process. This may be termed as an autocatalytic action of the abrasive, which removes



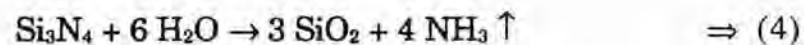
material from the workmaterial while reacting with it, and the mere action of material removal again forms the same material which will be removed in the next instant.

#### 7.4.2. CHEMO-MECHANICAL ACTION OF CHROMIUM OXIDE IN WATER

Figure 7.4.2.1 shows a schematic of the chemo-mechanical model for polishing silicon nitride with chromium oxide abrasive in water. Here, the reactions are essentially the adsorption of hydroxyl ions to the surface of silicon nitride and oxidizing the surface, which forms initially a silica layer which further gets oxidized to form hydrated silica layer. When the nitrogen ions get an opportunity to pair up with hydrogen ions present in water, it forms ammonia gas. Generation of ammonia gas was detected by the previous investigators that lending support to this hypothesis [Kanno et al, 1983].

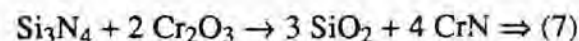
Chromium in its 2<sup>+</sup> state in chromium oxide can react with silica, as in the above case, to form chromium silicate. However, the reaction may be reduced by the action of water on silica itself.

The following sequence of reactions explain the chemo-mechanical behavior of polishing silicon nitride with chromium oxide in water. Oxidation of silicon nitride proceeds in water as represented by equation 4:

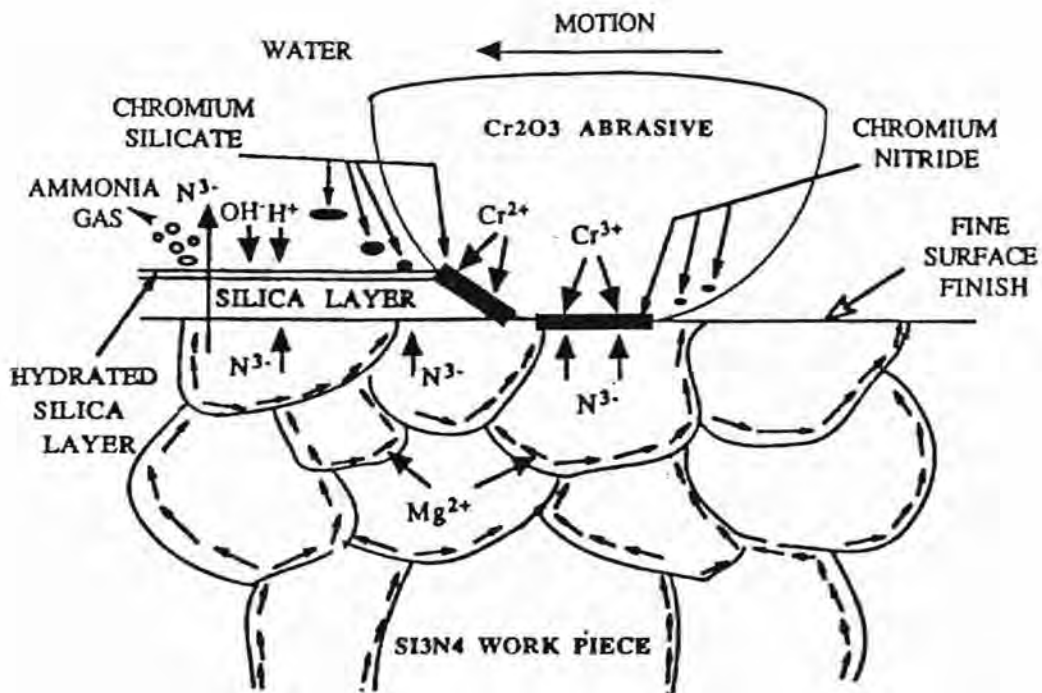


Each molecule of silicon nitride requires 6 molecules of water giving rise to 3 molecules of silica and 4 molecules of ammonia gas. Six hydroxyl ions present in water have again three equivalent molecules of oxygen gas to favour this reaction.

The action of chromium oxide alone in its 3<sup>+</sup> state on silicon nitride can be again represented by equation 7. The argument mentioned above is equally applicable here, except that instead of nitrogen gas, ammonia gas is produced.



The combined action of chromium oxide and water can be represented by the following equation:



REACTIONS OCCURRING IN THE CHEMOMECHANICAL POLISHING OF SILICON NITRIDE WITH CHROMIUM OXIDE ABRASIVES IN WATER

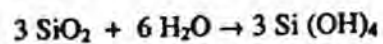
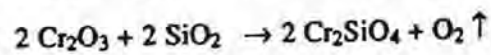
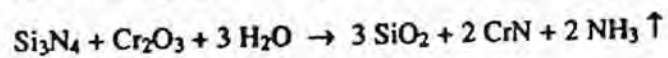
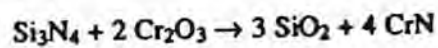
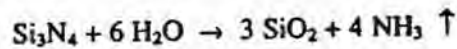
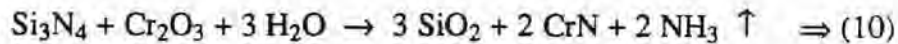
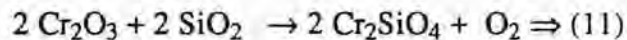


Figure 7.4.2.1 Schematic of the chemo-mechanical model for polishing silicon nitride in water using chromium oxide abrasives



Here, it can be seen that one molecule of silicon nitride, in the presence of one molecule of chromium oxide, needs only 3 molecules of water, instead of the regular 6 molecules in the absence of chromium oxide. Rest of the 3 oxygens atoms required for the reaction is provided by chromium oxide, which ultimately forms the same amount of silica. Also, in the usual situation there would have been 4 molecules of ammonia gas generated, but, in the present situation, there are only 2 molecules of gas produced, because the rest of the 4 nitride ions are reacting with the two chromium ions (again in its 3<sup>+</sup> oxidation state) to form two atoms of chromium nitride. Therefore, chromium oxide is enhancing the oxidation of silicon nitride in water, exactly in the same manner as in air. Here, too, the reduced ammonia gas generation is advantageous in the production of a defect free or pore free surface.

Further, chromium oxide, with chromium in its 2<sup>+</sup> oxidation state, can react with silica in the presence of water to form chromium silicate. As this reaction product is brittle it can be removed during subsequent mechanical action of the abrasive. This reaction can be represented by the following equation:



This equation is similar to the above case of air, chromium oxide in its 2+ oxidation state reacts with silica, forming chromium silicate as a reaction product. This reaction also evolved oxygen, partly replenishing to the amount that was spent during the previous reactions. Therefore, oxygen is made continuously available even in water for oxidation. Consequently, these reactions are almost identical. However, the important difference in polishing silicon nitride with chromium oxide in water and in air is that water has a separate reaction with silica which is represented by equation (6) and is repeated here for convenience.



This reaction produces a hydrated layer of silica forming silicic acid (H<sub>2</sub>SiO<sub>3</sub>) as the reaction product. This hydrated silica layer being amorphous, the reaction products such as chromium silicate and chromium nitride generated during the chemo-mechanical

polishing with chromium oxide could not be detected in higher amounts as was the case in polishing in air. Also, the flash temperatures generated during polishing of silicon nitride in water are in the range of 500 to 800 °C where as in the case of polishing in air are much higher, in the range of 1200 to 2000 °C. This enables chromium silicate (the reaction product) and chromium nitride (the oxidation product) to increase in their crystallinity and to achieve higher order arrangement of the lattices. XRD results obtained in both the cases indicate the same result supporting this argument.

In conclusion, it can be pointed out that the chemo-mechanical polishing mechanism is essentially the same in both air and in water, except that the intensities of the reaction products are lesser in the case of water.

## CHAPTER 8

### CONCLUSIONS

Based on a detailed study of the magnetic field assisted polishing of silicon nitride balls and rollers with chromium oxide abrasive the following conclusions can be drawn:

1. Chromium oxide abrasive provides a smooth surface in polishing of silicon nitride workmaterial
2. The mechanism of polishing of silicon nitride workmaterial with chromium oxide abrasive is due to chemo-mechanical polishing.
3. The flash temperatures generated at the real areas of contact in polishing of silicon nitride with chromium oxide abrasive are believed to be in the range of 1200 to 2000 °C.
4. Based on the analysis of the wear debris, as well as that of polished balls and rollers in polishing of silicon nitride with chromium oxide abrasive using SEM with X-ray analyzer and X-ray diffraction, a new chemo-mechanical polishing model is proposed. The role of chromium oxide is found to be more than a catalyst, as proposed by the earlier researchers.
5. Water enhances the oxidation of silicon nitride. It is an effective medium for oxidation up to 800 °K beyond which air becomes the effective medium.
6. Using the flash temperatures generated in polishing of silicon nitride workmaterial, various reaction products that can be formed are identified. They were used as a basis for the identification of the reaction products by X-ray diffraction.
7. SiC abrasives remove material entirely by mechanical abrasion. The surface chemistry being the same as that of silicon nitride, the possibility of chemical reaction

between them is negligible. Material removal mechanism in this case was found to be by multigrain pull out.

8. Boron carbide can form borosilicate as the reaction product during chemo-mechanical polishing of silicon nitride. This being a low temperature reaction (around 800 °C -1000 °C), most of the energy is utilized in mechanical material removal. Particle cleavage was the main material removal mechanism with boron carbide.

9. Carbide abrasives yielded higher material removal rates and are thus advantageous in the initial stages of polishing where the emphasis is on material removal rates.

10. Chromium oxide abrasives on the other hand proved to be the most effective abrasive in the chemo-mechanical polishing of silicon nitride. This abrasive perform three functions. 1. It promotes oxidation of silicon nitride by directly reacting with the nitride ions released during the initial oxidation to form chromium nitride. This reaction causes reduction in the release of nitride ions, 2. Oxidation in the presence of chromium oxide increases the residence time of the nitride ions, and promotes the release of nitride ions from the bulk material which would otherwise get released as nitrogen gas from the bulk of the material. The activation energy required for oxidation in the presence of chromium oxide is reduced considerably owing to the strong attraction of nitride ions towards chromium ions in their 3+ oxidation state. Thus, it reduces the generation of surface porosity during the oxidation of silicon nitride, and 3. Chromium oxide also takes part in the chemical reaction with the silica layer and forms Chromium silicate as the brittle reaction compound which is removed during the subsequent mechanical abrasion.

11. Being softer than silicon nitride, chromium oxide does not abrade the surface and generates smooth surfaces. The surface and subsurface defects are thus minimized.

12. Chromium oxide abrasive invokes forms an autocatalytic action involving formation and removal of the silica surface layer during chemo-mechanical polishing of silicon nitride.

13. The reaction mechanisms, in the case of magnetic abrasive finishing of rollers and magnetic float polishing of balls using chromium oxide abrasives are identical.

The main difference is the amount of crystallinity of the reaction products which increased in the case of magnetic abrasive finishing because of higher temperatures generated at the real areas of contact. Water causes hydrolyzation of silica layer, making it amorphous.

## CHAPTER 9

### SUGGESTIONS FOR FUTURE WORK

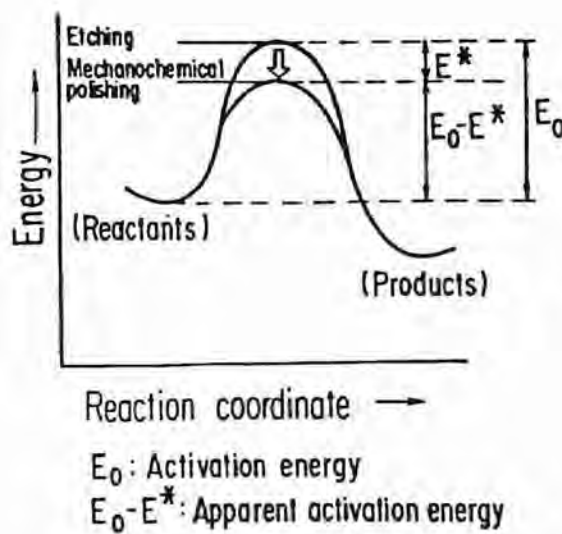
The present experimental investigation concentrated on the reaction mechanisms occurring at the contact interface between the silicon nitride material and three different abrasives, namely boron carbide, silicon carbide, and chromium oxide with emphasis on the last abrasive. It was concluded from the experimental results that chromium oxide is an important abrasive material for chemo-mechanical polishing of silicon nitride. It not only facilitates in the material removal process by the formation of reaction products (chromium silicate) but also influences the oxidation of the silicon nitride workmaterial directly. The present investigation mainly focussed on the issues involved in the determination of the chemical reactions occurring between silicon nitride and chromium oxide.

It would be valuable to consider the material removal mechanisms involved in polishing of silicon nitride workmaterial with other abrasives, including  $\text{Fe}_2\text{O}_3$ ,  $\text{CeO}_2$ ,  $\text{MgO}$ . Also, a more detailed analysis of the interactions between boron carbide abrasive and silicon nitride workmaterial would be helpful in identifying the micromechanisms of material removal. Also, more work is needed in the analysis of the wear debris using both SEM with X-ray microanalyzer and X-ray diffraction.

Gibb's free energy analysis carried out during this study has facilitated in the identification of possible reaction products but it alone can not provide the information required for the determination of the kinetics of the reactions involved. This has to be carried out in a separate study and then it would be possible to predict the rates of material removal in chemo-mechanical polishing. The material removal rates, measured in the present experimental work, are a result of the sum of the two modes of material removal, namely, mechanical removal and chemical removal. By conducting the reaction kinetics study, it would be possible to separate the two modes and control the process in order to yield the optimum material removal rates besides giving the best possible surface finish.



Figure 9.1 explains the activation energy concept from the mechanical polishing and chemo-mechanical polishing, where  $E^*$  represents the amount of energy lowered by the action of friction for the chemical reaction to proceed [Karaki-Doy, 1993]. The energy  $E_0$  is the energy which would be required if the process is mechanical removal alone. Thus, the difference in energies give the energy required for mechanical material removal coupled with chemical reaction.



$$V = V_0 \exp\left(-\frac{E_0}{RT}\right) \quad (1)$$

$V_0$ : Const.

$R$ : Gas const.

$T$ : Absolute temp.

$$V_c = V_0 \exp\left(-\frac{E_0 - E^*}{RT}\right) \quad (2)$$

$$E^* = E_1^* + E_2^*$$

$E_1^*$ : Thermal energy

$E_2^*$ : Strain energy

Figure 9.1 Relationship between chemo-mechanical polishing and activation energy

After performing these studies and Arrhenius plots can be developed for various situations. Controlled experiments must be carried out in order to validate the results obtained. The Arrhenius plots reported in the literature are mainly concerned with the determination of the activation energies required in the case of oxidation of silicon nitride in air and hydrothermal oxidation of silicon nitride. However, Xu et al [1994] attempted to determine the activation energies involved in the chemo-mechanical polishing of silicon nitride. They have conducted experiments in a high pressure autoclave which could generate pressures high enough to keep water in the liquid state up to temperatures of the order of 400 °C. The results obtained could predict a reduction in the activation energy in the case of chemo-mechanical polishing of silicon nitride. These experiments can not be conducted in air, as some of the experiments in the sequence proposed later would require the precise measurements of the reaction products. Collection of wear debris from the experiments would be more accurate in water than in air. Moreover, while Gibb's free energy analysis could not provide the information about the kinetics of the process, it did provide an important information in that the oxidation of silicon nitride is dominant in water up to a temperature of 700 °C beyond which oxidation is more dominant in air.

Silicon nitride samples were rubbed against each other in water at very low velocities (of the order of few centimeters per minute) and the temperatures were maintained high so as to account for the generation of flash temperatures in a real life situation where high relative velocities generate high flash temperatures. But, their study could not totally eliminate the effect of stresses exerted on the sample which would favour the oxidation. Further, the action of abrasives have not been studied in a detailed manner. Application of stresses on silicon nitride was found to increase the oxidation of silicon nitride material [Gogotsi and Grathwohl, 1993].

From the present experimental results chromium oxide was found to directly involve in the oxidation of silicon nitride by forming chromium nitride instead of acting as a catalyst as per the previous investigators. Therefore, if the experiments must consider these both effects in order to validate the experimental results from the following algorithm proposed. This algorithm is proposed to solve for the determination of the material removal rates from the chemical mode and the mechanical mode.

There are five sets of experiments required for providing the complete information about the various steps involved in the chemo-mechanical polishing of silicon nitride. Pin on disc experiments would be the most ideal experiments for this study as the set up can be

immersed in water and the temperature and pressure can be controlled with the help of an autoclave. The material of the pin can be changed to the abrasive in question to slide on the silicon nitride disc. The following assumptions are made for this study.

1. Temperatures under which the experiments conducted in all the five sets are identical.
2. The surface of the disc is assumed to be perfectly flat.
3. Thickness of silica layer on the samples prior to the start of the experiments is uniform. It should be determined from the XRD.
4. Depth of cut or the area of contact between the pin and the disc is maintained uniform irrespective of the hardness of the pin material chosen for the study. This depth of cut should never exceed the thickness of the silica layer as it would remove material from the parent substrate in which case the measurements would be redundant.
5. The depth of cut in each case could be determined prior to the experiment with the help of Hertzian stress approach. The load applied should be accordingly modified so as to yield the same amount of stress in each case.

The first set of experiments is the oxidation of silicon nitride in water. Silicon nitride sample should be heated in water up to temperatures of 500 °C in a high pressure autoclave. The sample is held stationary and the pressure and temperature of the autoclave are increased. The weight gains obtained from the measurements should be plotted against the reciprocal of temperature to yield the first plot. This result is already available in the literature from which it was determined that the activation energy required for the hydrothermal oxidation is about 108 KJ/mole. [Contet et al., 1987]. The slope of the plot gives the activation energy for the hydrothermal oxidation in the absence of stress.

The second set of experiments is to conduct mechanical polishing of silicon nitride using silicon carbide abrasives in water. Polishing should be conducted at various speeds that would generate the flash temperatures as in the first set. There are two rates involved in this measurement. They are 1) silica produced due to the application of stress 2) silica removed due to the mechanical action.

The third set of experiments is to polish silicon nitride with chromium oxide. The speeds of polishing are accordingly modified taking into consideration the thermal properties of the couple to yield the same flash temperatures as in the previous case. There are four rates involved in this case. They are 1) silica produced due to the enhanced oxidation because of chromium oxide. 2) silica produced due to the application of stress 3) silica removed due to the mechanical abrasion, and 4) chromium silicate removed due to the chemo-mechanical action.

The fourth set of experiments is to conduct experiments using Silicon nitride pin on silicon nitride disc at low velocities. Temperatures should be controlled using the pressure of the autoclave. Speeds should be selected in such a way that material does not get removed due to abrasion. There is only one rate involved in this case which is the formation of silica due to the application of stress alone.

The final set of experiments is conducted using chromium oxide pin on a silicon nitride disc in ESEM. The relative velocities should not be high enough to form chromium silicate. If the formation of chromium silicate is unavoidable at any speed, then it is preferred that experiment be conducted keeping the pin stationary (diffusion couple test). This set of experiments would yield two rates. 1) silica formation due to the application of stress 2) silica formation due to the action of chromium oxide.

The following calculations would yield correct results in separating all the terms involved.

- 1) Rates from SET 1 - Rates from SET 2 = Rate of silica formation due to the application of stress.
- 2) Rates from SET 4 - Rates from SET 2 = Rate of silica removal due to mechanical mode.
- 3) Rates from SET 5 - Rates from SET 4 = Rate of Silica formation due to the action of chromium oxide.
- 4) Rates from SET 4 - Rates from SET 3 = Rate of silica removal due to mechanical action + Rate of Chromium silicate removal due to mechanical action + Rate silica formation due to the action of chromium oxide.

- 5) STEP 4 - STEP 3 = Rate of silica removal due to mechanical action + Rate of chromium silicate removal due to mechanical action.
- 6) STEP 5 - STEP 2 = Rate of Chromium silicate removal due to chemo-mechanical action.

Thus, Steps 2 and 6 provide the most important information from which the activation energies can be back calculated and the problem can be effectively solved. The experiments must be complimented with the SEM and XRD studies which facilitate in determining the controlling parameters for the chemo-mechanical polishing process and thus, would facilitate in determining the optimum polishing conditions.

Using this approach, the action of other oxide abrasives such as magnesium oxide, cerium oxide and iron oxide could be found out and the optimum polishing conditions for them also could be determined.

However, caution must be exercised in providing the information as the experimental sequence requires high accuracy and there is bound to be some error from the experimental work. Therefore, error limits should be specified while providing the information. The tests should be conducted in an autoclave even if the speeds are higher as in real life situation. This provides an effective enclosure for the set up and erroneous measurements can be minimized.

## REFERENCES

Akazawa, M., and K. Kato, "Wear Properties of Silicon Nitride in Rolling Contact," *Wear*, 112, (1988), 123

Akazawa, M., Kato, K., and K. Umeya, "Wear Properties of Silicon Nitride in Rolling Contact," *Wear*, 110, (1986), 285

Archard, J. F., "The Temperature of Rubbing Surfaces," *Wear*, 2, (1959), 438

Ashby, M. F., Abulawi, J., and H.S. Kong, "Temperature Maps for Frictional Heating in Dry Sliding," *Trib. Trans.*, 34, (1991), 577

Babushkin, V., Matveyev, G.M., and O.P., Mchedlov-Petrovssyan, "Thermodynamics of Silicates," Ed. Mchedlov - Petrovssyan, O.P., Springer-Verlag, Berlin, (1985)

Chen, C. P., and W. J. Knapp, "Delayed Fracture of an Alumina Ceramic," *J. Am. Cer. Soc.*, 60, (1977), 87

Clarke, D. R. and, F. F. Lange, "Oxidation of  $\text{Si}_3\text{N}_4$  Alloys: Relation to Phase Equilibria in the System  $\text{Si}_3\text{N}_4\text{-SiO}_2\text{-MgO}$ ," *J. Am. Cer. Soc.*, 63, (1980), 586

Contet, C., Kase, Noma, J.I., Yoshimura, T. M., and S. Somiya, "Hydrothermal Oxidation of  $\text{Si}_3\text{N}_4$ ," *J. Mater. Sci. Lett*, 6, (1987), 963-964

Cranmer, D. N., "Wear Surface Analysis of Silicon Nitride," *STLE Lubrication Engg.*, 44, (1989), 975

Cubicciotti, D. and, K. H. Lau "Kinetics of Oxidation of Hot-Pressed Silicon Nitride Containing Magnesia," *J. Am. Cer. Soc.*, 61, (1978), 512

- Cubicciotti, D. and, K. H. Lau, "Kinetics of Oxidation of Yttria Hot -Pressed Silicon Nitride," J. Electrochem. Soc., 126, (October 1979), 1722
- Davis, H. M., and M. A. Knight, "The System MgO - B<sub>2</sub>O<sub>3</sub>," J. Elect. Chem. Soc., 4 , (1945), 100
- Dayson, C., "Surface Temperatures at Unlubricated Sliding Contacts," ASLE Trans., 10 , (1967), 169
- Dong, X., and S. Jahanmir, "Wear Transition Diagrams for Silicon Nitride," Wear, 165 , (1993), 169
- Echeberria, J. and, F. Castro "Oxidation of Silicon Nitride Sintered with ceria and Alumina," Matls. Sc. and Tech., 6, (1990), 497
- Ernest M. L., McMURdie, H. F., and F. P. Hall, "Phase Diagrams for Ceramists," The Am. Cer. Soc., 1956
- Falk, L. K., and E. U., Engstrom, "Elemental Concentrations Profiles in an Oxidized Silicon Nitride Material," J. Am. Cer. Soc., 74, (1991), 2286
- Fischer, T. E., Liang, H., and W. M. Mullins, "Tribochemical Lubricious Oxides on Silicon Nitride," Mat. Res. Symp. Proc., 140,(1989), 339
- Fischer, T.E. and H. Tomizawa, "Interaction of Tribochemistry and Microfracture in the Friction and Wear of Silicon Nitride," Wear, 105 , (1985), 29
- Fischer, T.E., "Tribochemistry," Annual Review of Materials Science., 18 (1988), 303
- Furrey, M. J., "Surface Temperatures in Sliding Contact," ASLE Trans., 7, (1964), 133
- Gardos, M. N., and R. G. Hardisty, "Fracture Toughness and Hardness Dependent Polishing Wear of Silicon Nitride Ceramics," Trib. Trans., 36, (1993), 652

Gates, R.S., Hsu, S. M., and E. E. Klaus, "Tribochemical Mechanism of Alumina with Water," STLE Trib. Trans., 32, (1989), 357

Gee, M. G., and D. B. Butterfield, "The Combined Effect of Speed and Humidity on Wear and Friction of Silicon Nitride," Wear, 162-164, (1993), 234

Gogotsi, Y. G., and Grathwohl, G., "Stress enhanced oxidation of silicon nitride ceramics," J. of Am.Cer.Soc., 76, (1993), 3093.

Hines, J. E., Jr., Bradt, R. C., and J. V. Biggers, "Delta Alumina Formation During Abrasive Wear of Polycrystalline Alumina," Wear of Materials, (1979), 540

Hockin, H., Xu, K., and S. Jahanmir, "Simple Technique for Observing Subsurface Damage in Machining Ceramics," J. Am. Cer. Soc., 77, (1994), 1388

Hou, Z. B., and R. Komanduri, "On the Calculation of Flash Temperatures Developed During Silicon Nitride Polishing," to be published (1994)

Hsu, S. M., Shen, M. C., Klaus, E. E., Cheng, H. S., and P. I. Lacey, "Mechano-Chemical Model: Reaction Temperatures in a Sliding Contact," Wear, 175, (1994), 209

Ikeda, M., Yamada, A., Kokaji, Y., and S. Kiryura, "Fine Polishing of Sapphire Crystals," Natl. Bue. Stds., 562, (1979), 325

Jahanmir, S., and T. E. Fisher, "Friction and Wear of Silicon Nitride Lubricated by Humid Air, Water, Hexadecane + 0.5 % Steric Acid," STLE Trans., 31, (1988), 32

Kanno, Y., et al., "NH<sub>3</sub> Formation Caused by the Presence of Water in the Wet Grinding of Silicon Nitride Powder," Yogyo-Kyokai-Shi, 91, (1983), 386

Karaki-Doy, T., Horio, K. I., Kasai, T., Horikawa, H., and M. Nomuya, "Mechanochemical Polishing of Compound Semiconductor Substrates," Proc. of 5th Int. Cong. on Tribology, held at Helsinki in 1989



Karaki-Doy, T., "Study on Mechanism of Mechanochemical Polishing and its Application - An Instance of Silicon Wafers," J. of Saitama Univ. Fac. of Edcn., 42, (1993), 33

Kato, K, "Tribology of Ceramics," Wear, 136, (1990), 117

Katz, R. N., and J. G. Hanoosh, "Ceramics for High Performance Rolling Element Bearings: A Review and Assessment," Int.J. High.Tech. Cer., 1, (1985), 69

Katz, R. N., "Opportunities and Prospects for the Application of Structural Ceramics in Nitrogen Ceramics," Ed. F. L. Riley, Publ. Martinus Nijheff, Boston, (1989) , 417

Katz, R. N., "Application of Silicon Based Ceramics," Presented at the 8<sup>th</sup> CIMTEC. Florance, Italy, June 30, 1994

Katz, R. N., "Nitrogen Ceramics 1976-1981," Progress in Nitrogen ceramics, (1983), Martinus Nijhoff Publishers, Boston.

Kiehle, A. J. , L. K. Heung, P. J. Gielisse, and T. J. Rockett, "Oxidation Behavior of Hot-Pressed Si<sub>3</sub>N<sub>4</sub>," J. Am. Cer. Soc., 58, (1975), 17

Kikuchi, M, Takahshi, Y., Suga, T., Suzuki, S., and Y. Bando, "Mechanochemical Polishing of SiC Single Crystal with the Chromium Oxide Abrasive," J. Am. Cer.Soc., 75, (1992), 189

Kim, S. S., and K. Kato et. al., "Wear Mechanisms of Ceramic Materials in Dry Rolling Friction," Trans. ASLE, 108, (1986), 522

Kubashevski, O. and C. B. Block, "Metallurgical Thermo Chemistry," 5th Edition., in Int. Series on Materials. Science and Technology, 24, 1979

Lancaster, J. K., Marshal, A. H., and A. T. Atkins, "The Role of Water in the Wear of Ceramics," J. Phy, D: Appl. Phy., 25, (1992) , A205

Lange, F. F. , "Eutectic Studies in the System  $\text{Si}_3\text{N}_4\text{-Si}_2\text{N}_2\text{O-Mg}_2\text{SiO}_4$ ," J. Am. Cer. Soc., 62, (1979), 617

Loffelbein, B., Waydt, M., and K. H. Habig, "Sliding Friction and Wear of Ceramics in Neutral, Acid and Basic Aqueous Solutions," Wear, 162-164, (1993), 220

Marshall, D.B., "The Nature of Machining Damage in Brittle Materials," Proc. Roy. Soc. Lond, 385,(1983), 461

McColm, I. J., "Ceramic Science for Materials Technologists," (1983), Leonard Hill Publication.,107

Mizutani, Y., Shimusa, Y., Yahagi, Y., and S. Hotta, "Friction and Wear of Ceramics in Various Environments," Proc. of Japan. Int. Trib. Conf., at Nagoya, 1990

Munro R. G., and S. J. Dapkunas "Corrosion Characteristics of Silicon Carbide and Silicon Nitride," J. Research of the Ntl. Ins. of Stds. and Tech., 98, (1993), 607

Namba, Y and H. Tsuwa, "A Chemomechanical Ultrafine Polishing of Polycrystalline Materials," Annals CIRP, 26, (1977), 325

Namba, Y and H. Tsuwa, "A Chemomechanical Ultrafine Polishing of Polycrystalline Materials," Annals CIRP, 28, (1979), 425

Sato, T., Murakami, T., Endo, T., Shimada, M., Komeya, K., Kameda, T. and M. Komatsu, "Corrosion of Silicon Nitride Ceramics under Hydrothermal Conditions." J. Material Sci. , (1991) , 1749-1754

Schnieder, S. J., "Handbook on Ceramics and Glasses," published by ASM Int. Volume 4 (1991 ) , 31

Singhal, S. C, "Thermodynamics and Kinetics of Hot Pressed Silicon Nitride." J. of Material Science., 11 , (1976 (a)), 500

Singhal, S. C., "Effect of Water Vapour on the Oxidation of Hot Pressed Silicon Nitride and Silicon Carbide," *J. Am. Cer. Soc.*, 59, (1976 (b)) , 81

Sugita, T., Kawakami, S., and O. Imanaka, "A New Ultrafine Polishing Technique for Sapphire," NBS Publication No. 562 , (1979) , 317

Sugita, T., Veda, K., and Y. Kanemura, "Material Removal Mechanism of Silicon Nitride During Rubbing in Water," *Wear*, 97, (1984), 1

Suzuki, K., Uematsu, T., Ohashi, H., Kitajima, K., Suga, T., and O. Imanaka, "Development of a New Mechano-Chemical Polishing Method with a Polishing Film for Ceramic Round Bars," *Annals of CIRP.*, 41/1, (1992) , 339

Tighe, N. J. "Analysis of Oxide and Oxide/Matrix Interfaces in Silicon Nitride", Technical report submitted to Dept of Energy, Washington D.C., in July 1982

Tomizawa, H and T.E. Fischer, "Friction and Wear of Silicon Nitride and Silicon Carbide in Water: Hydrodynamic Lubrication at Low Sliding Speed Obtained by Tribochemical Wear," *ASLE Trans.*, 30,1, (1987) , 41

Uematsu, T., Wu, M. H., Suzuki, K., and O. Imanaka, "Efficient Mechanochemical Polishing for Silicon Nitride Ceramics," *Machining of Advanced Ceramics*, NIST, Special Publications, No. 847, (Jan 1993), 409

Vora, H., Orent, T. W., and R.J. Stokes, "Mechanochemical Polishing of Silicon Nitride," *Commn. of Am. Cer. Soc.*, (1982) , C140

Wang, J.C., and S. M. Hsu, "Chemically Assisted Machining of Ceramics," *J. of Tribology*, 116, (1994) ,423

Xu, J. G. , K. Kato, and N. Umehara, "Tribo-activation of Silicon Nitride reacted with Water," Personal communication, 1994

Yasunaga, N., Obasa, A., and N. Taruni, "Study of Mechanomchemical Effect on Wear and its Application to Surface Grinding," (in Japanese), Researches of Electrotech Laboratory, 776, (1977), 73

Yasunaga, N., Tasuni, N., and Akira Ohara, "Mechanism and Application of the Mechanochemical Polishing Method Using Soft Powder," NBS Publication No. 562. (1979), 171

Yust, C. S., and F. J. Carigan, "Observations on the Sliding Wear of Ceramics," ASLE Trans., 28, (1984), 245

## APPENDIX A

### HEAT TRANSFER MODELING AND FLASH TEMPERATURE CALCULATION IN MAGNETIC ABRASIVE FINISHING

Temperature is the crucial parameter which determines the possibility and the rate of chemical reaction that occurs between the workmaterial and the abrasive during chemo-mechanical polishing. It is somewhat impractical to measure the temperatures at the point of contact experimentally, as it is not only cumbersome but also uneconomical solution. Therefore, heat transfer model developed by Hou and Komanduri (1994) utilizing the moving heat source approach and Jaeger's solutions was used to determine the flash temperatures generated at the point of contact between the abrasive and the work material. The theoretical background for the model developed by Hou and Komanduri is presented in this section.

#### A.1 HEAT TRANSFER MODELLING OF POLISHING

In the magnetic abrasive finishing of rollers, abrasives apply pressure on the cylindrical surface of the roller and due to the action of Hertzian stresses, a contact area is established at the point of contact which can be determined from calculations. During the rotation of the roller, abrasive slides on the surface of the roller making the contact area to slide along the roller surface. The real shape of the contact can be assumed to be a disc with a diameter of about 10~20 mm depending upon the hardness of the work piece and abrasive. The rod has a sliding velocity  $v$ , which generates heat at the rate of  $q$  at the real area of contact, which is given by,

$$q = p \cdot m \cdot v \cdot 2.342 \quad \text{cal/sec}$$

where

$p$  is the load in  $\text{Kg}_f$

$m$  is the coefficient of friction

$v$  is the resultant sliding velocity in  $\text{m/sec}$

The moving disc heat source problem can be solved by assuming the disc consisted of many concentric rings. Each ring moves on the surface of the rod with a resultant velocity  $v$  which is actually the vector sum of the surface velocity of the rod and the oscillating velocity of the abrasive sliding on the rod. Figure. A.1 shows the schematic of the moving ring heat source problem [Hou, Z. B., and R., Komanduri, 1994].

Consider a moving ring heat source continuously liberating heat  $q_{rg}$  (cal/sec) and moves along  $x$ -axis with velocity  $v$  (cm/sec). The problem is to determine the temperature rise at point  $M(x,y,z)$  after a time  $t$  (in seconds) after the heat source begins to move.

The solution to this problem is given by the following equation.

$$q_M = \frac{q_{rg} v}{16lap^{3/2}} \sum \exp(-XV) \int_0^{\frac{v^2 t}{4\alpha}} \frac{dw}{w^{3/2}} \sum \exp\left(-w - \frac{u^2}{4w}\right)$$

$$\sum I_0 \left[ \frac{r_0 V^2}{2w} \sqrt{\left(X + \frac{2w}{V}\right)^2 + y^2} \right] \Rightarrow (1)$$

where,

$q_{rg}$  is the heat generated at each ring, cal/sec.

$v$  = Sliding velocity in Cm/sec.

$l$  = Thermal conductivity of silicon nitride, Cal/Cm.sec. °C.

$a$  = Thermal diffusivity of silicon nitride, Cm<sup>2</sup>/Sec.

$X$  = Co-ordinate of the point of interest,

$V = v/2.a$

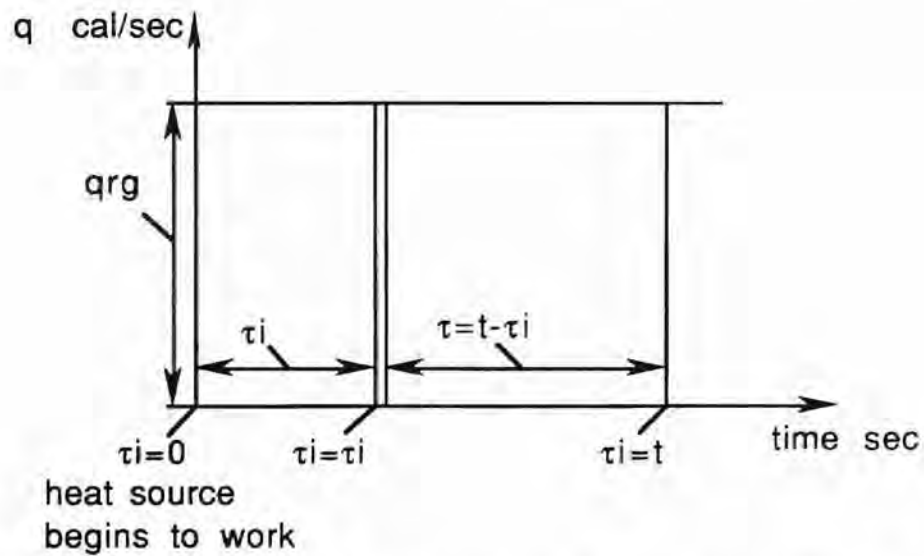
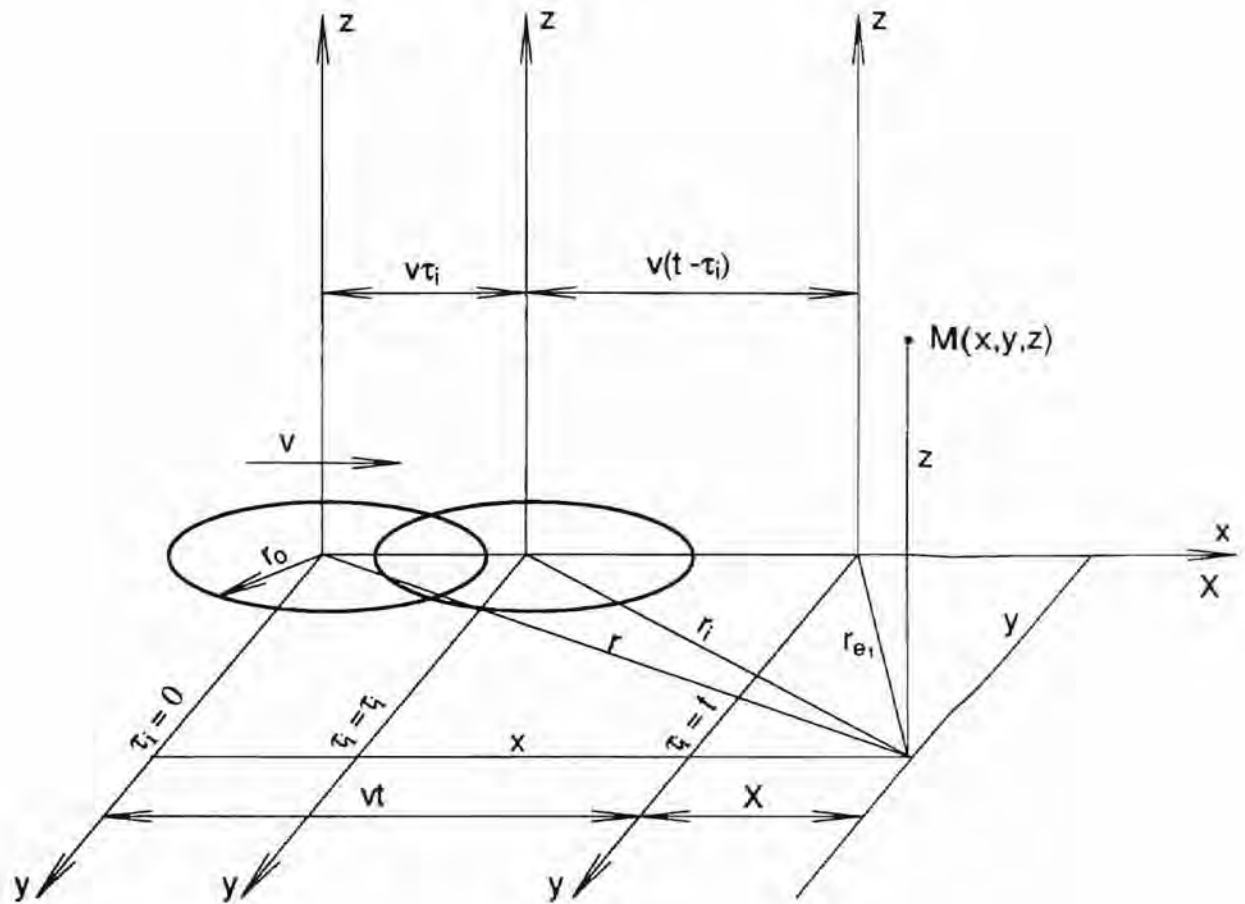


Figure. A.1 Schematic of the moving ring heat source problem [Hou and Komanduri, 1994]

$w =$  a dimensionless number in the limit equals the upper limit of the integral,  
 $r_0 =$  radius of the ring, Cm.

Each disc is now can be assumed to be a the assembly of number of such concentric rings placed one in another. The solution for this problem is simply the algebraic sum of the temperature rise determined by each ring using equation (1), which upon simplification is modified to yield the solution for an infinite body,

$$\theta_M = \frac{q_{rg} v}{16 \sum l \sum a \sum p^{3/2}} \sum \exp(-XV)$$

$$[0.1777KR_1(u) + 0.563KR_2(u) + 0.274KR_3(u)] \Rightarrow (2)$$

where,

$$KR_1(u) = \int_0^{\infty} \frac{dw}{w^{3/2}} \sum \exp\left(0.967p - w - \frac{u^2}{4w}\right)$$

$$KR_2(u) = \int_0^{\infty} \frac{dw}{w^{3/2}} \sum \exp\left(0.431p - w - \frac{u^2}{4w}\right)$$

$$KR_3(u) = \int_0^{\infty} \frac{dw}{w^{3/2}} \sum \exp\left(-2.245p - w - \frac{u^2}{4w}\right)$$

$$p = \frac{r_0 V^2}{2w} \sqrt{\left(X + \frac{2w}{V}\right)^2 + y^2}; \quad V = \frac{v}{2a}; \quad u = \frac{R_h v}{2a};$$

$$R_h^2 = r_0^2 + X^2 + y^2 + z^2$$



The solution for a semi-infinite body, as in the present case is given by the following equation.

$$\theta_M = \frac{q r g v}{8 \sum_{i=1}^n \frac{1}{a^i} \sum_{p=3/2}^{\infty} p^{3/2} \exp(-XV)} \sum_{i=0}^{i=n}$$

$$(0.1777KR_1(u) + 0.563KR_2(u) + 0.274KR_3(u)) \Rightarrow (3)$$

where ,

$n = 10$  (number of concentric rings)

$$KR_1(u) = \int_0^{\infty} \frac{dw}{w^{3/2}} \sum \exp\left(0.967p-w - \frac{u^2}{4w}\right)$$

$$KR_2(u) = \int_0^{\infty} \frac{dw}{w^{3/2}} \sum \exp\left(0.431p-w - \frac{u^2}{4w}\right)$$

$$KR_3(u) = \int_0^{\infty} \frac{dw}{w^{3/2}} \sum \exp\left(-2.245p-w - \frac{u^2}{4w}\right)$$

$$p = \frac{r_i V^2}{2w} \sqrt{\left(X + \frac{2w}{V}\right)^2 + y^2};$$

$$V = \frac{v}{2a^i}$$

$$u = R_h \sum V$$

$$R_h^2 = r_i^2 + X^2 + y^2 + z^2$$

$$i = 1 \text{ to } 10$$

## A. 2. Steps Taken for the Calculation of Flash Temperature Using Moving Disk Heat Source Model

1. Surface velocity is determined by obtaining the resultant of the rotational velocity of the rod and translational velocity of the abrasives sliding on the rod.
2. Number of abrasives taking part in the polishing were determined by ratio of the area of magnetic holder and the cross sectional area of the abrasive. The assumption used here was the abrasives are in the form of a mono layer on the surface of the rod.
3. Total force acting is the ratio of polishing pressure to the area of magnetic holder. Load per abrasive is the ratio of total force and the number of abrasives taking part in the polishing .
4. The radius of contact was determined from the Hertzian stress equation.

$$a = \left( \frac{1.5 * W * R'}{E'} \right)^{1/3}$$

where

W is the load per abrasive,

R' is the equivalent radius,

E' is the equivalent Young's modulus.

where

$$\frac{1}{R'} = \frac{1}{R_1} + \frac{1}{R_2}$$

R<sub>1</sub> is the radius of the sphere,

R<sub>2</sub> is the radius of the flat surface ( in our case,

R<sub>2</sub> = 0 since cylinder surface when compared to the abrasive radius is assumed to be flat.

$$\frac{1}{E'} = \frac{1 - \nu_1^2}{E_1} + \frac{1 - \nu_2^2}{E_2}$$

Where

- E' is the equivalent Young's modulus,
- $E_1$  is the Young's modulus of the work piece,
- $E_2$  is the Young's modulus of the abrasive,
- $\nu_1$  is the Poisson's ratio of work piece,
- $\nu_2$  is the Poisson's ratio of the abrasive.

6. Heat developed was determined by the product of the load and the sliding velocity and coefficient of friction.

7. Fraction of heat contributing to the temperature rise is a linear function of thermal conductivities of the Silicon Nitride work piece, Chromium oxide Abrasives and the Volume fraction of Iron powder used in the polishing.

8. Heat dissipated into the work piece is responsible for the temperatures (flash temperatures) generated in the work piece.

9. Flash time is calculated in the following manner :

i) calculate from the temperature plots, the total distance in the vicinity of the abrasive which exceeds 100 °C.

ii) divide this distance by the sliding velocity obtained in step 1 to yield the flash time.

10. To determine whether the abrasive adjacent to the present abrasive has any effect on the cumulative rise in the flash temperature , the time taken by the adjacent abrasive to reach the present abrasive position is calculated. This is simply the ratio between the center distance between the abrasives and the sliding velocity. If this time is higher, then, there is no cumulative effect.

### A.3. Sample Calculations Using the Moving Disk Heat Source Model

#### Polishing conditions:

1. Polishing pressure,  $p = 5$  PSI

2. Diameter of the silicon nitride rod,  $D = 25 \text{ mm}$
3. Rotational speed of the rod,  $N = 2000 \text{ rpm}$
4. Oscillational frequency of the magnetic head,  $f = 25 \text{ Hz}$
5. Amplitude of oscillation of the magnetic head,  $A = 0.25 \text{ Cm}$
6. Width of the magnetic head,  $L = 1.0 \text{ Cm}$
7. Size of the magnetic abrasives =  $400 \text{ mm}$
8. Volume fraction of Iron powder,  $v = 60\%$

Properties of materials:

1. Thermal conductivity of Silicon nitride,  $k_1 = 0.026 \text{ W/m. } ^\circ\text{K}$
2. Thermal conductivity of Chromium oxide,  $k_2 = 0.076 \text{ W/m. } ^\circ\text{K}$
3. Thermal conductivity of Iron powder,  $= 0.2 \text{ W/m. } ^\circ\text{K}$
4. Thermal diffusivity of silicon nitride,  $a = 0.039 \text{ Cm}^2/\text{Sec.}$
5. Heat capacity of silicon nitride,  $C = 0.202 \text{ Cal/gm. } ^\circ\text{K}$
6. Density of silicon nitride,  $\rho = 3.3 \text{ gm/cc}$
7. Elastic modulus of silicon nitride,  $E_1 = 304 \text{ GPa}$
8. Elastic modulus of Chromium oxide,  $E_2 = 103 \text{ GPa}$
9. Poisson's ratio of silicon nitride,  $\nu_1 = 0.25$
10. Poisson's ratio of chromium oxide,  $\nu_2 = 0.24$

**SPECIMEN CALCULATIONS:**

1. Surface velocity of the abrasives,  $V_1 = \pi D N / 60 \text{ 00}$   
 $= 3.14 \times 25 \times 2000 / 60000$   
 $= 1.57 \text{ m/sec.}$
2. Oscillational speed of the magnetic head,  $V_1 = 2 \times \text{Amp} \times \text{Freq} / 100$   
 $2 \times 0.25 \times 25 / 100 = 0.125 \text{ m/sec}$
3. Relative velocity between the abrasive and work piece,  
 $V = [V_1^2 + V_2^2]^{1/2}$   
 $V = 1.575 \text{ m/sec.}$

4. Number of abrasives =  $p \cdot 0.5 \cdot D \cdot L / \text{abr. size}^2$ .

$$= 3.14 \times 0.5 \times 25 \times 10 / 400 \times 400 \times 10^{-6}$$

$$= 2455.$$

5. Effective young's modulus,  $E'$  is given by,

$$E' = \frac{1}{\frac{1 - \nu_1^2}{E_1} + \frac{1 - \nu_2^2}{E_2}}$$

$$E' = \frac{1}{\frac{1 - 0.24^2}{103 \times 10^9} + \frac{1 - 0.25^2}{304 \times 10^9}}$$

$$E' = 8.17 \times 10^{10}$$

6. Effective radius of contact,  $R'$  is given by,

$$R' = \frac{1}{\frac{1}{R_1} + \frac{1}{R_2}}$$

Where  $R_1$  is the radius of the abrasive, and  $R_2$  is the radius of the roller at the point of contact.  $R_2$  is actually, infinity when compared to  $R_1$ , as the radius of the cylindrical surface which is assumed to be a straight line compared to the radius of the abrasive.

$$R' = \frac{1}{\frac{1}{0.5 \times 400 \times 10^{-3}}}$$

$$R' = 0.2 \text{ mm.}$$

7. Total load on the rod = polishing pressure  $\cdot 0.5 \cdot p \cdot \text{rod. dia} \cdot 10 \cdot$   
length of heat source/ 25.4  $\cdot 25.4$

$$= 5 \cdot 0.5 \cdot p \cdot 25 \cdot 10 / 25.4 \cdot 25.4$$

$$= 3.04 \text{ lb.}$$

8. Load per abrasive,  $w = \text{Total load} / \text{number of abrasives}$

$$= 3.04 / 2455$$

$$= 0.0012 \text{ lb.}$$

9. Radius of contact,  $a'$  is given by,

$$a' = \left[ \frac{1.5 \cdot w \cdot R'}{E'} \right]^{1/3}$$

$$a' = \left[ \frac{1.5 \cdot 0.0012 \cdot (9.81/2.2) \cdot 0.2 \cdot (10^{-4})}{8.17 \cdot 10^{10}} \right]^{1/3}$$

$$= 0.0000014 \text{ m.}$$

$$= 1.4 \text{ mm.}$$

10. Total amount of heat produced during polishing at the plane heat source,  $Q$  is given by,

$$Q = (w \cdot m \cdot v \cdot 2.342) \cdot 2$$

(For semi-infinite body, heat produced will be twice that of infinite body)

$$= (0.0012 \cdot (4.448/9.81) \cdot 0.1 \cdot 1.57 \cdot 2.342) \cdot 2$$

$$= 0.0004 \text{ Cal/ Sec.}$$

11. Fraction of heat that goes to the work piece,  $x$  is given by,

$$x = \frac{\lambda_{\text{Si}_3\text{N}_4}}{\lambda_{\text{Si}_3\text{N}_4} + \left[ \frac{100 - \% \text{ of Iron content}}{100} \right] \cdot \lambda_{\text{Cr}_2\text{O}_3} + [0.01 \cdot \% \text{ of Iron content} \cdot \lambda_{\text{Fe}}]}$$

$$x = \frac{0.026}{0.026 + \left[ \left( \frac{100 - 60}{100} \right) \cdot 0.078 + [0.01 \cdot 60 \cdot 0.2] \right]}$$

$$x = 0.147 \approx 0.15$$

12. Amount of heat that goes to Silicon nitride work piece,  $Q_{wp}$  is given by,

$$\begin{aligned} Q_{wp} &= Q \cdot x = 4.02 \times 10^{-4} \cdot 0.15 \\ &= 6.03 \times 10^{-6} \text{ Cal/Sec.} \end{aligned}$$

Temperature rise from the above model is shown in Figures A.2 and A.3. As the polishing pressure increases, the flash temperatures produced also increase. As the rotational speed of the rod increases, the flash temperatures also increase. Thus, the flash temperatures produced during the polishing of silicon nitride rods in air varied from 1200 to 2000 °C.

#### FLASH TIME DETERMINATION

Flash time can be calculated by measuring the distance on the plot which is above a certain temperature, and dividing by the velocity of the abrasives. In other words, the time taken by the point below the abrasive (say  $T_1$ ), to cool from a certain temperature to the temperature selected. If this time is more than the time taken (say  $T_2$ ), for the next abrasive to reach this present location, there would be a cumulative effect of the abrasives on the rise of flash temperatures on the rod, otherwise, there would be no cumulative effect. Considering the Temperature rise plot of Figure A.2, for 5 p.s.i. polishing pressure, the flash time for 200 °C rise can be found by,

13. (a) Flash time for 200 °C rise  $T_1$  is given by,

$$T_1 = \frac{-25 - (-80) \cdot 10^{-6}}{1.57} = 35.0 \text{ m Sec.}$$

(b) Time taken by the next abrasive to travel from 400 mm (center to center distance between the abrasives) to -25 mm (the point after which the flash temperature is more than 200 °C,  $T_2$  is given by,

$$T_2 = 400 + (-80) \cdot 10^{-6} / 1.57 = 204 \text{ m Sec.}$$

Since  $T_1 < T_2$ , there would be no cumulative effect of the abrasive on the flash temperature rise of the rod.



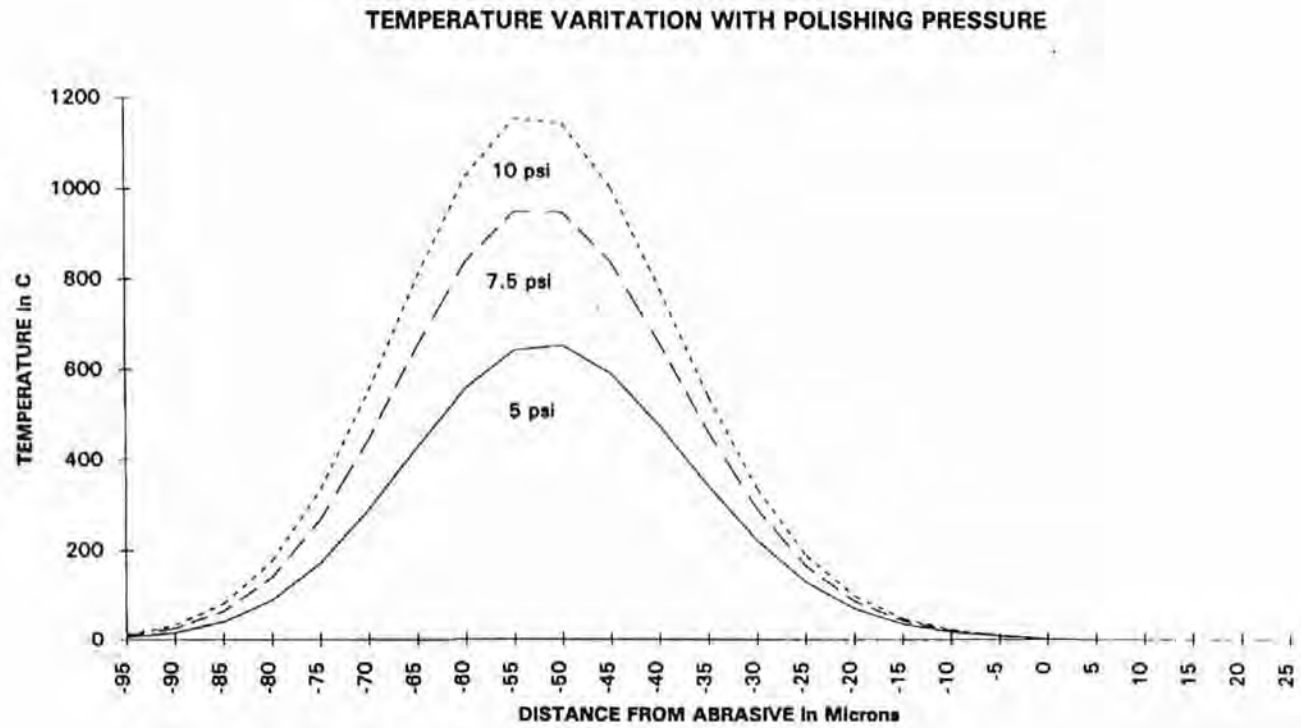


Figure A.2 Flash Temperature Raise with polishing pressure

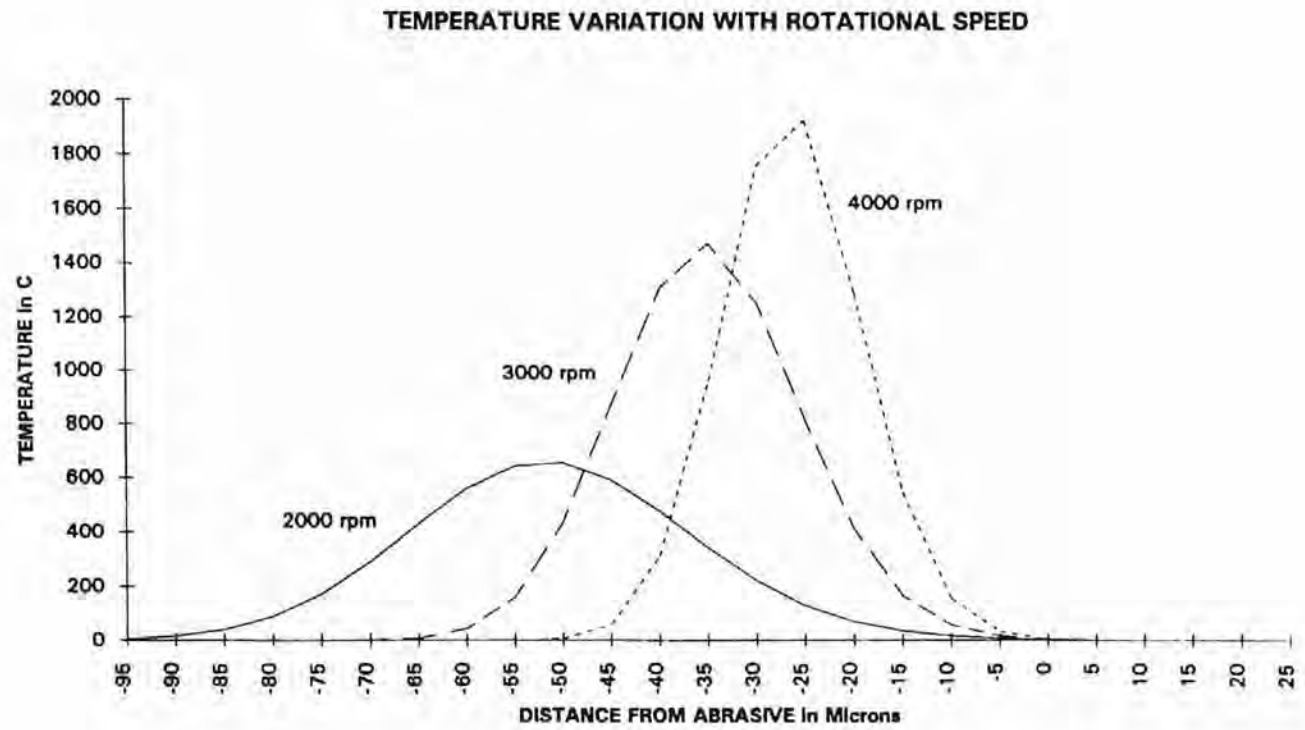


Figure A.3 Flash Temperature Raise with Rotational speed of the rod<sub>d</sub>

## VITA

SEKHAR .R. BHAGAVATULA

Candidate for the degree of

Master of Science

Thesis: CHEMO-MECHANICAL POLISHING OF SILICON NITRIDE WITH  
CHROMIUM OXIDE ABRASIVE

Major Field: Mechanical Engineering

### Biographical:

Personal data: Born in Kollur, India, on August 12, 1964, the native son of Savithri and Madhusudana Sharma and the adopted son of Saradamba and Radha Krishna Murthy.

Education: Received Bachelor of Engineering degree in Mechanical Engineering from Manipal Institute of Technology, Manipal, India in May 1987; received Master of Technology degree from Indian Institute of Technology, Bombay, India, in May 1991 with a major in Mechanical Engineering. Completed the requirements for the Master of Science degree with a major in Mechanical Engineering at Oklahoma State University, Stillwater, in July 1995.

Experience: Worked as a Research Scientist in Ceramics Laboratory, Department of Metallurgical Engineering at IIT, Bombay, India, during June 1987 till May 1989; worked as Graduate Research Assistant in Metallurgical Engineering Department, IIT, Bombay, India, during Masters study (from June 1989 till May 1991); worked as a Senior Research Fellow from June 1991 till August

1992 in Metallurgical Engineering Department, IIT, Bombay, India; worked as a Graduate Research Assistant in Mechanical Engineering Department, Oklahoma State University, Stillwater, From Jan 1993 till July, 1995.